DISSERTATIONES CHIMICAE UNIVERSITATIS TARTUENSIS

66

# ELECTROREDUCTION OF HEXACYANOFERRATE(III) ANION ON CADMIUM (0001) SINGLE CRYSTAL ELECTRODE

## JAAK NERUT

Department of Chemistry, Institute of Physical Chemistry, University of Tartu, Estonia

Dissertation in physical and electrochemistry

Dissertation is accepted for the commencement of the degree of Doctor of Philosophy in Chemistry on April 27, 2007, by the Doctoral Committee of the Department of Chemistry, University of Tartu.

Doctoral advisor:     Prof. Enn Lust, University of Tartu

Opponents:     Prof. Renat R. Nazmutdinov (Kazan State Technological University, 420015 Kazan, Republic Tatarstan, Russia)
Prof. Emer. Vello Past (University of Tartu, Estonia)

Commencement:     $12^{00}$ June 29 2007, in Tartu, 2  Jakobi Str., room 154

# CONTENTS

2

# 1. LIST OF ORIGINAL PUBLICATIONS

**I**  **J. Nerut**, P. Möller, E. Lust, Electroreduction of hexacyanoferrate(III) anions on electrochemically polished Cd(0001) plane, Electrochim. Acta 49 (2004) 1597.

**II**  T. Thomberg, **J. Nerut**, K. Lust, E. Lust, The kinetics of electroreduction of peroxodisulfate anion on electrochemically polished Cd(0001) plane, Electrochim acta 49 (2004) 1271.

**III**  T. Thomberg, **J. Nerut**, E. Lust, Impedance spectroscopy data for $S_2O_8^{2-}$ anions electroreduction kinetics at Cd(0001) plane electrode, J. Electroanal. Chem. 586 (2006) 237.

**IV**  E. Lust, **J. Nerut**, E. Härk, R. Jäger, K. Lust, K. Tähnas, Electroreduction of Complex Ions at Bismuth and Cadmium Single Crystal Plane Electrodes, ECS Trans. 1 (17) (2006) 9.

**V**  **J. Nerut**, K. Lust, E. Lust, Adsorption of hexacyanoferrate(II) and hexacyanoferrate(III) anions on electrochemically polished Cd(0001) plane, J. Electroanal. Chem. Submitted (JELECHEM-D-06-00250R2).

**VI**  **J. Nerut**, K. Lust, E. Lust, Impedance spectroscopy study of hexacyano-ferrate(III) anion electroreduction kinetics at electrochemically polished Cd(0001) plane, J. Electrochem. Soc. Submitted (JES-07-0695).


**Author's contribution**

Performed the electrochemical measurements, modelling, interpretation and writing the article [I, IV–VI].

Participated in the modelling and interpretation of the cyclic voltammetry and impedance spectroscopy data [II–III].

# 2. ABBREVATIONS AND SYMBOLS

| | |
|---|---|
| $a_{Ox}^0$ | – activity of the oxidant in the bulk solution |
| ac | – alternating current |
| $B_v$, $B_{02}$ | – second virial coefficients |
| $c_i$, $c_{Ox}^0$, $c_{A*}$ | – concentration of the particle (ion, oxidant, anion) in the bulk solution |
| cTp | – corrected Tafel plots |
| $C$ | – differential capacitance |
| $C_s$ | – series differential capacitance |
| $C_0$ | – equilibrium differential capacitance |
| $C_{02}^0$ | – inner layer differential capacitance |
| $C_2^0$ | – differential capacitance of the diffuse layer |
| $C_{01}^0$ | – capacitance of the volume between the metal surface and the plane of localisation of the charge of specifically adsorbed ions |
| $C_{ad}$ | – adsorption capacitance |
| CPE | – constant phase element |
| $D_i$ | – diffusion coefficient of the particle $i$ |
| $E$ | – electrode potential |
| $E^0$ | – equilibrium potential in the standard conditions; – formal potential |
| $E_1^0$, $E_2^0$ | – standard redox potentials of the reaction |
| $E_{min}$ | – potential of the minimum in the $C$, $E$-curve of the base electrolyte |
| $E_{min}^*$ | – potential of the $C$, $E$-curve diffuse layer minimum with the addition of $K_3[Fe(CN)_6]$ |
| $E_r$ | – equilibrium potential |
| $E_{q=0}$ | – zero charge potential |
| EC | – equivalent circuit |
| edl | – electrical double layer |
| Eq. | – equation |
| EP | – electrochemically polished |
| F | – Faraday constant |
| $f$ | – frequency of the alternating current |
| $f_{max}$ | – frequency of maximum in low-frequency semicircle |
| Fig. | – figure |
| $g_{Ox}$; $g_{Red}$ | – absolute values of the specific adsorption energies of the oxidant and reductant |
| j | – imaginary unit (j = $\sqrt{-1}$ ) |

| | |
|---|---|
| $\vec{j}$ | – current density of the forward reaction |
| $j_F$ | – current density of the Faradaic reaction |
| $j_k$ | – kinetic current density |
| $j_0$ | – exchange current density |
| $j_d$ | – limiting current density |
| k | – Boltzmann constant |
| $k_s^0$; $k_s^{(ex)}$ | – absolute and measurable rate constants of the electrochemical reaction |
| $k_{het}$ | – apparent rate constant for the heterogeneous charge transfer process |
| $k_f$, $k_b$, $\overrightarrow{k_1}$, $\overleftarrow{k_{-1}}$, $\overrightarrow{k_2}$, $\overleftarrow{k_{-2}}$ | – forward and reverse reaction rate constants |
| $k_0$, $k_1^0$, $k_2^0$ | – standard rate constant at the formal electrode potential $E^0$ |
| M | – metal |
| $m$, $m1$ | – number of alkaline metal cations |
| $n$ | – number of transferred electrons |
| $N_A$ | – Avogadro number |
| Ox | – oxidized form of the standard system Ox + $n$e⁻ = Red |
| $q$ | – surface charge density |
| $q_0$ | – surface charge density in the base electrolyte solution |
| $q_1$ | – charge density of the specifically adsorbed ions |
| $q_d$ | – charge density of the diffuse layer |
| $Q$ | – CPE constant |
| R | – universal gas constant |
| Red | – reduced form of the standard system Ox + $n$e⁻ = Red |
| $R_{ad}$ | – adsorption resistance |
| $R_{ct}$ | – charge transfer resistance |
| $R_p$ | – total polarisation resistance |
| $R_{el}$ | – electrolyte resistance |
| $r^2$ | – determination coefficient |
| sol, ads | – particles in solution and adsorbed state |
| $T$ | – absolute temperature |
| $v_1$, $v_2$ | – rates of the reactions 1 and 2 |
| $w$, ($w_{Ox}$, $w_{Red}$) | – electrostatic work term of the particle (oxidant, reductant) |
| zcp | – zero charge potential |
| $z_i$, $z_{Ox}$, $z_{Red}$ | – charge number of the particle (ion, oxidant, reductant) |
| $z_i$ | – point charge at site $i$ |
| $z_{eff}$ | – effective charge number of the specifically adsorbed ions |
| $Z_F$ | – Faradaic impedance |
| $Z_{CPE}$ | – impedance of CPE |
| $Z'$, $Z''$ | – active and imaginary parts of the complex impedance |
| $Z$ | – magnitude of the complex impedance |

| | |
|---|---|
| $x, y$ | – molar concentration of a surface-inactive component and a surface-active electrolyte |
| $x_1, x_2$ | – distances of the inner and outer Helmholtz planes from an electrode surface |
| $\alpha, \alpha_1, \alpha_2$ | – transfer coefficients |
| $\alpha_{app}$ | – apparent transfer coefficient |
| $\alpha$ | – CPE fractional exponent |
| $\beta_v, \beta_{02}, \beta$ | – adsorption equilibrium constants obtained from various isotherms |
| $\gamma_{\neq}$ | – activity coefficient of the activated complex |
| $\gamma_\theta, \gamma_{\theta=0}$ | – surface tension in the presence and absence of the surface-active ions in the electrolyte |
| $\Gamma_i$ | – surface concentration |
| $\Gamma_{A*}$ | – relative surface concentration of the specifically adsorbed anions (Gibbs excess) |
| $\Gamma_B, \Gamma_s$ | – surface concentrations of the species B and of free adsorption sites $S$ |
| $\Gamma_{max}$ | – maximal surface concentration |
| $\Delta c_{Ox}, \Delta c_{Red}$ | – concentration fluctuations of the reacting particles in response to the ac voltage perturbation $\Delta E$ |
| $\Delta E$ | – amplitude of the ac potential |
| $\Delta E_{min}$ | – shift of the minimum potential in the $C, E$-curves |
| $\Delta\phi^{m-2}$ | – potential drop across in the inner layer |
| $\Delta G_A^0$ | – Gibbs adsorption energy |
| $\Delta j_F$ | – response of the Faradaic current density to the ac voltage perturbation $\Delta E$ |
| $\varepsilon_r$ | – dielectric constant of the solvent |
| $\varepsilon_0$ | – permittivity of vacuum |
| $\theta, (\theta_0, \theta_i)$ | – surface coverage (in base electrolyte and with addition of $i$, respectively) |
| $\sigma$ | – conductivity |
| $\tau_{max}$ | – characteristic time constant of the process |
| $\phi$ | – surface pressure |
| | – phase angle |
| $\psi_1$ | – potential at the reaction site |
| $\psi_{eff,i}$ | – potential at site $i$ |
| $\psi_0$ | – potential drop in the diffuse layer (outer Helmholtz plane potential) |
| $\omega$ | – angular frequency ($\omega = 2\pi f$) |
| $\omega_{rot}$ | – angular velocity of the electrode |

# 3. INTRODUCTION

The complex ions of the transition metals constitute the interesting systems for examining the ''simple'' heterogeneous electron transfer reactions [1–6]. The double layer effect observed may be varied significantly by varying the chemical nature and structure of the surrounding ligands [1–3]. When the redox reaction occurs by an outer-sphere mechanism (i.e. the redox reaction is ''simple''), the kinetic parameters, usually the experimental transfer coefficient, provide very useful information about the location of the reaction centre [1–3]. During some years, there has been considerable interest in fundamental studies of electron transfer kinetics at the well-defined single crystal plane electrodes [4–10]. It was found that the kinetics of electroreduction of the various complex ions depend considerably on the crystallographic structure of the electrode surface as well as on the chemical characteristics of the electrode studied.

The electrochemical behaviour of the $[Fe(CN)_6]^{3-}/[Fe(CN)_6]^{4-}$ redox couple has been extensively studied as a model redox reference system [1, 2, 11–26]. In early studies the reaction was regarded to proceed via the simple outer-sphere electron transfer mechanism, but it became clear that the process is actually quite complex [1, 2, 11–26]. The kinetic parameters were reported for systems of various combinations of electrode materials and supporting electrolytes. The heterogeneous electron transfer rates calculated depend strongly upon the electrolytes, especially on the cations nature. This so called ''cation effect'' has been ascribed mainly to the ion association with the $[Fe(CN)_6]^{3-}$ or $[Fe(CN)_6]^{4-}$ anions. On the other hand, strong adsorption of reactants or intermediates on platinum electrode surfaces is also recognized [12, 14–19], which has been discussed in correlation with the surface blocking effect [1]. However the detailed nature and the structure of the adsorbates at the electrode surface is unknown.

The main aim of this work was to study the charge-transfer mechanism and the electroreduction kinetics of the $[Fe(CN)_6]^{3-}$ anion on the electrochemically polished (EP) Cd(0001) electrode because there is no experimental data on the influence of the crystallographic structure of the so called mercury-like metals on the electroreduction kinetics of the $[Fe(CN)_6]^{3-}$ anion. The cyclic voltam-metry, rotating disc electrode voltammetry and impedance spectroscopy methods have been used. The kinetic current densities at constant electrode potential have been obtained by the Koutecký–Levich method and used for the determination of the rate constant values for the heterogeneous electroreduction reaction of the $[Fe(CN)_6]^{3-}$ anion on the Cd(0001) plane. The kinetic analysis was performed using the kinetic current values calculated: the charge of the reacting particle has been calculated and the corrected Tafel plots have been constructed using different theoretical approximations. The method of constant ionic strength has been employed to study the strength of adsorption of the $[Fe(CN)_6]^{3-}$ and $[Fe(CN)_6]^{4-}$ anions. For the more detailed analysis of the

reduction mechanism of the $[Fe(CN)_6]^{3-}$ anion on the Cd(0001) plane the impedance spectra have been measured. The parameters of the $[Fe(CN)_6]^{3-}$ electroreduction has been compared with the corresponding data for the $S_2O_8^{2-}$ anion electroreduction on the electrochemically polished Cd(0001) plane electrode.

# 4. LITERATURE OVERVIEW

## 4.1. The classical model of the reduction kinetics of the anions

The slow charge transfer process is caused by the difficulties in the transport of the reacting particles through the metal-solution interface and there upon the redox system shifts away from the electrochemical equilibrium. At the conditions where the diffusion process is affected only by the concentration gradient of the reactants or products in the surface layer then the charge transfer is directly influenced by electrode surface charge density, i.e. by the potential distribution near the electrode surface.

The study of the electrical double layer (edl) effects dates back from the early works of Frumkin [25, 27–29], who noted that the current due to the reduction of the hydrogen ions from solutions of a dilute acid at a mercury electrode is independent of the acid concentration at the constant over-potential. This result was attributed to a change in the concentration of the $H^+$ ion at the reaction site in the double layer, together with a shift in the equilibrium potential for the reaction with the change in acid concentration in the bulk of the solution [29].

The reaction

$$Ox + ne^- (M) = Red \qquad (I)$$

is quantitatively described by the main equation of the Frumkin slow charge transfer theory for reduction:

$$\vec{j} = nFk_s^{(ex)} \frac{a_{Ox}^0}{\gamma_{\neq}} \exp\left[ -\frac{\alpha nF(E - E^0)}{RT} \right] \text{ and} \qquad (4.1.1)$$

$$k_s^{(ex)} = k_s^0 \exp\left[ \frac{(1-\alpha)g_{Ox} + \alpha g_{Red}}{RT} \right] exp\left[ \frac{(\alpha n - z_{Ox})F\psi_1}{RT} \right], \qquad (4.1.2)$$

where $k_s^0$ and $k_s^{(ex)}$ are the on absolute and measurable rate constants of the electrochemical reaction, respectively; $\alpha$ is the transfer coefficient; $g_{Ox}$ and $g_{Red}$ are the absolute values of the specific adsorption energies of the oxidant and reductant; $a_{Ox}^0$ is the activity of the oxidant in the bulk solution; $z_{Ox}$ is the charge number of the oxidant; $\gamma_{\neq}$ is the activity coefficient of the activated complex; and $E^0$ is the equilibrium potential at the standard conditions; R and $T$ have their conventional meanings. In Eq. (4.1.1) the effects of the edl are characterized by the $\psi_1$-potential, i.e. by the potential at the reaction site [30, 31].

Pronounced edl effects are easily observed, when the kinetics of anion electroreduction is studied at the ideally polarizable electrodes for potentials negative of the zero charge potential (zcp) $E_{q=0}$. A deep minimum is observed

in a plot of the rate of electroreduction of $S_2O_8^{2-}$ in a region, where the diffusion limited current densities is expected, if the background electrolyte concentration is relatively low. Results of the early works showed that the dependence of the kinetic data on the concentration of the supporting electrolyte could be explained on the basis of the Frumkin model i.e. with the help of the Eq. (4.1.1) [1]. From the Eq. (4.1.1) it is evident that when $\psi_1 = 0$ all the curves should coincide and the current density is independent of the base electrolyte concentration. The potential value at this point is equal to the zcp, but there is not enough experimental data verifying this theoretical assumption [26].

Fedorovich et al. [1, 32] demonstrated that we can distinguish two groups of the anionic reactants. Anions of the so-called first group, including peroxodi-sulfate ($S_2O_8^{2-}$), tetrathionate ($S_4O_6^{2-}$) and hexacyanoferrate(III) ($[Fe(CN)_6]^{3-}$), are reduced without involvement of the solvent molecules into the elementary steps of the reaction. From this point of view the reduction of the hexacyanoferrate(III) is a simple electron transfer reaction, but the anions involved are highly charged, so the ion pairing effect is expected to play a very important role. In the case of $S_2O_8^{2-}$ and $S_4O_6^{2-}$, the electrode reaction is irreversible due to the breaking of the O-O and S-S bonds in these anions, respectively. Anions of the second group include very many complex ions, like $ClO_4^-$, $BrO_4^-$, $IO_4^-$, $ClO_3^-$, $BrO_3^-$, $BF_4^-$, $PF_6^-$ etc. For these systems, the solvent molecules are involved in the total electrode reaction, so the kinetics of the electroreduction of these anions depend on the activity of the solvent at the interface and thus on the hydrophilicity of the metal electrode studied.

A very important observation is that the rate of the electroreduction of the $S_2O_8^{2-}$ and $S_4O_6^{2-}$ anions increases with the increasing of the radius of the cation of the electrolyte in the series $Li^+ < Na^+ < K^+ < Rb^+ < Cs^+$ and $Ca^{2+} < Sr^{2+} < Ba^{2+}$ [24–31, 33, 34]. This can be partly attributed to the specific adsorption of these cations on metal at large negative surface charge densities. However, the specific adsorption effect of these cations cannot explain for the cation effect observed near the zcp. Thus, a major portion of this effect is due to the local ion pairing between the reacting particle and the cations located on the outer Helmholtz. Another important point is, that the position of the outer Helmholtz plane depends on the nature of the cation in the solution at negative charge densities [1].

The relationship (4.1.1) can be linearized taking the logarithm from both sides of equation:

$$\ln j_k + \frac{z_{Ox}F}{RT}\psi_1 = \ln\left(nFk_s^0 c_{Ox}^0\right) - \frac{\alpha nF}{RT}\left(E - E_{q=0} - \psi_1\right), \text{[30, 31, 33]} \quad (4.1.3)$$

4

where $j_k$ is the kinetic current density and $c_{Ox}^0$ is the concentration of the oxidant in the bulk solution. Linear dependences $\ln j_k + \dfrac{z_{Ox}F}{RT}\psi_1 = f(E - \psi_1)$, based on Eq. (4.1.3), are called corrected Tafel plots (cTp) [35]. From the slope of the cTp-s it is possible to calculate the transfer coefficient and from the intercept we can calculate the rate constant for the heterogeneous reaction. The best proof of the Frumkin model is the experimental result, that the cTp-s for the $S_2O_8^{2-}$ anion electroreduction at different polycrystalline Hg-like (Cd, Zn, Bi, Sb etc) and Hg electrode coincide [25–29]. According to the experimental results cTp-s are linear and they coincide also if the base electrolyte concentration is varied, but the $S_2O_8^{2-}$ ion concentration is held constant.

The Eq. (4.1.3) is correct only, if the following assumptions are fulfilled: the reacting particle in the transition state of the reaction is in equilibrium with the particles in the bulk of the solution in accordance with the Boltzmann equation; the edl structure can be described by the Gouy-Stern-Grahame theory; noncoulombic interactions of the reacting particles and of the reaction products, both with the electrode surface and with the other edl ions, do not depend on $E$ (thus the Gibbs adsorption energy of reactant and products is independent of $E$); the dependence of the rate of the electrochemical reaction, in which the adsorbed particles participate, on the effective potential difference is expressed by the classical Tafel equation with a constant transfer coefficient $\alpha$; the discreteness-of-charge effects in edl are not important. As shown in Refs. [1–8, 13, 21, 23, 36–40], this picture is oversimplified even for the ideally flat and very inactive Hg electrode.

## 4.2. The electroreduction kinetics of the hexacyanoferrate(III) anion

The electroreduction kinetics of the hexacyanoferrate(III) anion
$$[Fe(CN)_6]^{3-} + e^- = [Fe(CN)_6]^{4-}. \tag{II}$$
has been an object of many studies [1, 2, 11–26]. However the influence of chemical nature of the electrode material on the kinetic parameters of electroreduction for various anions is an open question, because there is no quantitative data for the various metals, except Hg, Pt, Ag, Cd, Bi and Au [1–29, 32, 41–43]. It should be noted that there is only very few data discussed about the influence of the crystallographic structure of the electrode surface on electroreduction of the $[Fe(CN)_6]^{3-}$ anion [12].

Systematic analysis of the experimental data shows that for the so-called simple redox reactions ($[Co(NH_3)_6]^{3+}$ and other Co(III) and Cr(III) complexes
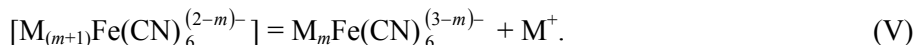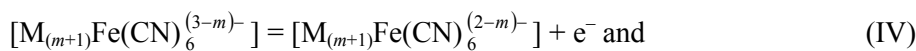
[1–11], where the redox transfer probably occurs by an outer-sphere mechanism) the kinetic parameters depend noticeably on the chemical nature of the electrode metal and on the crystallographic structure of the electrode surface [1, 8, 10, 12]. However only for some limited number of systems this dependence can be explained by the so-called edl effect, i.e. simply by the electrostatic work terms, $w$, associated with bringing the reductant and product to their reaction sites in edl [1]. The usual way of estimating the work terms: $w_{Ox}$ and $w_{Red}$ is to assume that the reactant and the product can be represented as the point charges and accordingly $w_{Ox} = z_{Ox} F \psi_1$ and $w_{Red} = z_{Red} F \psi_1$ [2, 27–29, 32, 41–43]. If the charge is distributed to a number of discrete sites within the reactant such that $z_{Ox} = \sum_i z_i$ ($z_i$ is the point charge at site $i$), then the expression for $w_{Ox}$ becomes $w_{Ox} = \sum_i z_i F \psi_{\mathrm{eff},i}$, where $\psi_{\mathrm{eff},i}$ is the potential at site $i$ [1, 2, 44–48].

In recent works Fawcett et al. have calculated theoretically the charge distribution for the various complex ions: $[Fe(CN)_6]^{3-}$, $[Co(NH_3)_6]^{3+}$ and $[Fe(H_2O)_6]^{3+}$, but the results are somewhat disputable and a bit surprising, because for example the charge number of the $[Fe(CN)_6]^{3-}$ approaches "-5" at far negative potentials and it is explained by the fact, that the charge distribution of the reactant is highly disturbed by the charge on the electrode surface. On the other hand it might indicate, that the charge number of the reacting particle differs from the stoichiometrical one and this effect should be taken into account.

Rate constant $k_{het}$ for the heterogeneous charge transfer reaction of the couple $[Fe(CN)_6]^{3-}$/$[Fe(CN)_6]^{4-}$ at the platinum (111), (100) and (110) single crystal electrodes in the aqueous 1.0 M $KClO_4$ solution was obtained by ac impedance spectroscopy [12]. It was found that the apparent rate constant values $k_{het}$ depend largely on the surface structure of the Pt electrode and $k_{het}$ increases along the series (110) < (100) < (111), i.e. with increasing the reticular density of the Pt(hkl) plane [12]. The in situ IR spectroscopy data indicate the presence of adsorbates ascribable to the cyanide group on every Pt(hkl) surface and the spectral features on the Pt(111) surface were found to be different from Pt(110) and Pt(100) planes [12]. For a polycrystalline Pt electrode the heterogeneous reaction rate constant depends strongly on the electrolyte, especially on the cation nature, increasing with the decrease of the hydration energy in the order of cations $Li^+ < Na^+ < K^+$ [12–21, 48]. It was concluded that the electron transfer process for this redox couple would not obey a simple outer-sphere mechanism [12]. Strong adsorption of reactants and intermediates on the Pt electrode surface is also recognized in other works [12–16], which has been explained simultaneously with the surface blocking effect. It has been pointed out that the "true" rate constant of this couple should be obtained in the

very dilute solutions of the $[Fe(CN)_6]^{3-}$ or $[Fe(CN)_6]^{4-}$ ions, when the surface coverage of the adsorbates is very low [14, 17–20].

Peter et al. proposed a mechanism for Au electrode, which explains the first-order dependence on the cation concentration in solution, $c_{K^+}$, in terms of a catalytic effect of the potassium cation:

$$M_mFe(CN)_6^{(4-m)-} + M^+ = [M_{(m+1)}Fe(CN)_6^{(3-m)-}], \qquad (III)$$

$$[M_{(m+1)}Fe(CN)_6^{(3-m)-}] = [M_{(m+1)}Fe(CN)_6^{(2-m)-}] + e^- \text{ and} \qquad (IV)$$

$$[M_{(m+1)}Fe(CN)_6^{(2-m)-}] = M_mFe(CN)_6^{(3-m)-} + M^+. \qquad (V)$$

where $m$ is the number of alkali metal atoms. It has been shown that at high concentrations the anion is associated with at least one cation [13]. Therefore the formation of the activated complex requires the addition of one cation to the species, which are already associated at least with one cation. In recent works of Petrii et al. this effect has been attempted to take it into account using the classical Frumkin's model [45, 46, 48]. However, this model introduces some new variables, the physical values of which are difficult to experimentally estimate and explain.

In addition to the theoretical complications the kinetic data for electroreduction of $S_2O_8^{2-}$ on the Au, Bi and Cd single crystal plane electrodes demonstrate the noticeable dependence of $k_{het}$ and apparent transfer coefficient, $\alpha_{app}$, on the chemical nature and crystallographic structure of the electrode surface studied [36, 49, 50]. Thus the metal electrode surface has noticeable influence on the reaction mechanism and rate of the reaction of the so-called first group anions.


## 4.3. The method of constant ionic strength for studying adsorption of anions

Usually the specific adsorption of different inorganic ions at the metal electrodes in a system with constant ionic strength: $x$ M $K_2SO_4 + y$ M $K_mA^*$, where A* denotes the surface-active anion; $x$ and $y$ are the molar concentrations of a surface-inactive component and a surface-active electrolyte, respectively. The method of mixed electrolyte with constant ionic strength was originally proposed more than 40 years ago [51, 52] and thereafter used in many papers [51–55]. For many years the model description of these data was based only on the Grahame-Parsons theory [56, 57]. Some new approaches simulating the reversible specific adsorption of ions on the ideally polarizable electrodes have been developed [58–65]. In the contemporary theories of specific adsorption on the electrodes, different electrical variables are used: the electrode surface charge $q$ in the Grahame-Parsons model [51, 52, 56, 57]; potential drop across in the

inner layer $\Delta\phi^{m-2}$ in the Alekseyev-Popov-Kolotyrkin model [58] future developed by Damaskin et al. [59–61]; and electrode potential $E$ in the Vorotyntsev model [62–65].

The more simple standard procedure for finding the adsorption parameters is to fit the charge density of the specifically adsorbed ions ($q_1$) with the charge number $z_i$ to the simple virial isotherm

$$\ln\left(\Gamma_{A*}/c_{A*}\right) = \ln\beta_v + 2B_v\Gamma_{A*} \tag{4.3.1}$$

where $\ln\beta_v = -\Delta G_A^0/RT$ is the adsorption equilibrium constant and $B_v$ is the second virial coefficient, characterizing the mutual repulsion of the ions adsorbed and $\Gamma_{A*} = q_1 N_A/z_i F$ is the Gibbs excess (relative surface concentration) of the specifically adsorbed anions. It should be noted that the standard state is an 'ideal' $\Gamma_{A*} = 1$ ion cm$^2$ for the adsorbed species and an 'ideal' $c_{A*} = 1$ mol dm$^{-3}$ for the bulk solution.

It is generally accepted [56, 57, 66–69] that in the case of ion adsorption the isotherm must include the diffuse layer potential term $\psi_0$ to give the real values of the Gibbs adsorption energy $\Delta G_A^0$ at $q \neq 0$. If we assume according to Grahame [56, 70] that the cations do not enter into the inner layer, then the outer Helmholtz plane potential $\psi_0$ can be obtained as

$$q + q_1 = A\sqrt{\sum_i c_i\left(exp\left(-\frac{z_i F\psi_0}{RT}\right) - 1\right)} \tag{4.3.2}$$

where $A = \sqrt{2\varepsilon_r\varepsilon_0 RT}$ ($\varepsilon_r$ is the dielectric constant of the solvent and $\varepsilon_0 = 8.854\times10^{-12}$ F m$^{-1}$ is the permittivity of vacuum) and $c_i$ is the bulk concentration of the $i$-th ion. As shown by Grahame and Parsons [56, 57] the following corrected virial isotherm is valid

$$\ln\left(\Gamma_{A*}/c_{A*}\right) + \frac{z_i F}{RT}\psi_0 = \ln\beta_{02} + 2B_{02}\Gamma_{A*} \tag{4.3.3}$$

where $\beta_{02}$ and $B_{02}$ may be arbitrary functions of $q$. In Eq. (4.3.3) $\beta_{02}$ is the corrected (by $\psi_0$ effect) adsorption equilibrium constant and $B_{02}$ is the corrected second virial coefficient characterising the mutual repulsion of anions adsorbed.

According to Eqs. (4.3.1) and (4.3.3), for the condition $\Gamma_{A*} = 0$, the $\beta_{02}$ can be calculated as

$$\ln\beta_{02} = \ln\beta_v + \frac{z_i F}{RT}\psi_0. \tag{4.3.4}$$

The calculation of the Gibbs excess involves a comparatively inexact differentiation step. To avoid this step, the adsorption equilibrium constant can be calculated by fitting the surface pressure data $\phi = \gamma_{\theta=0} - \gamma_\theta$ to an equation of a "square root" isotherm [71–74]

5

$$\ln(kTc_{A*}) + \ln\beta = \ln\phi + B\sqrt{\phi} \qquad (4.3.5)$$

where $\gamma_\theta$ and $\gamma_{\theta=0}$ are the surface tension values in the presence and absence of the surface-active ions in the electrolyte, respectively; $\beta$ is the adsorption equilibrium constant. The square root isotherm is an empirical isotherm and would be used only as a convenient procedure for linearising the experimental data, and the value of the isotherm slope $B$ has no physical meaning.

According to the Vorotyntsev model [62–65] for solutions with constant ionic strength at $E$ = const the specific adsorption of anions is described by the simple virial isotherm

$$\ln\beta_E + \ln c_{A*} = \ln\left(\frac{q_1}{z_i}\right) + 2B_E\frac{q_1}{z_i} \qquad (4.3.6)$$

where $B_E$ is the second virial coefficient expressed as

$$B_E = \frac{z_i^2\Delta^2}{2RT/F(C_{02}^0 + C_2^0)} \qquad (4.3.7)$$

$$C_2^0 = \frac{2RT|z_i|}{F}\sqrt{4A^2c + q_0^2} \qquad (4.3.8)$$

where $C_{02}^0$ is the inner layer differential capacitance and $C_2^0$ is the capacitance of the diffuse layer calculated according to the classical Gouy-Chapman theory (at $q_1 = 0$), and $q_0$ is the surface charge density in the base electrolyte solution at $x = 0$, the value $\Delta = z_{eff}C_{02}^0/z_iC_{01}^0$ characterises the effective charge number of the specifically adsorbed ions $z_{eff}$ and the structure of the surface layer, where the term $C_{01}^0$ describes the capacitance of the volume between the metal surface and the plane of localisation of the charge of specifically adsorbed ions [62–65].

The thermodynamic parameters obtained before tell very little about the structure and charge distribution of the Cd | electrolyte interface. The most frequently used inner layer model for estimation of the inner layer structure has been the classical Grahame-Parsons model [53, 56, 57]. According to this model, the potential drop in the inner layer $\Delta\phi^{m-2} = E - E_{q=0} - \psi_1$, to a first approximation, can be considered to depend on the charge of the metal ($q$) and on the amount of specifically adsorbed ions ($\Gamma$) per unit area [53, 56, 57, 62, 73–75]

$$\Delta\phi^{m-2} = f(q,\Gamma) \qquad (4.3.9)$$

because the interface as a whole is electrically neutral, and if the charge in the diffuse layer $q_d$ is kept constant, then

$$\left(\frac{\partial(\Delta\phi^{m-2})}{\partial\Gamma_{A*}}\right)_{q_d} = -z_ie\left(\frac{\partial(\Delta\phi^{m-2})}{\partial q}\right)_{\Gamma_{A*}} + \left(\frac{\partial(\Delta\phi^{m-2})}{\partial\Gamma_{A*}}\right)_q = z_ie\left(\frac{1}{_\Gamma C} - \frac{1}{_q C}\right) \quad (4.3.10)$$

where

$$_qC = \left( \frac{\partial q}{\partial \left( \Delta \phi^{m-2} \right)} \right)_{\Gamma_{A*}} \tag{4.3.11}$$

is the capacitance of the inner layer at constant amount of adsorption ($\Gamma_{A*}$) and

$$_\Gamma C = \left( \frac{ze\partial \Gamma_{A*}}{\partial \left( \Delta \phi^{m-2} \right)} \right)_q \tag{4.3.12}$$

is the capacitance of the inner layer at constant electrode charge ($q$). If the inner layer capacities are regarded as constant, i.e. as integral capacities, they may be expressed as

$$_\Gamma C = \frac{\varepsilon}{x_2 - x_1} \tag{4.3.13}$$

$$_qC = \frac{\varepsilon}{x_2} \tag{4.3.14}$$

where $\varepsilon$ is the permittivity in the inner layer, $x_1$ and $x_2$ are the distances of the inner and outer Helmholtz planes from an electrode surface, respectively [53, 56, 57, 75].

## 4.4. Impedance spectroscopy and modelling the charge transfer processes

Rate of the heterogeneous charge transfer reaction $\mathrm{Ox} + ne^- \underset{k_{-b}}{\overset{k_f}{\longleftrightarrow}} \mathrm{Red}$ is given by the expression

$$-j_F = nF\left( k_f c_{Ox} - k_b c_{Red} \right) \tag{4.4.1}$$

where $k_f$ and $k_b$ are the forward and reverse reaction rate constants [6, 13, 14, 42, 76–86]. Using impedance spectroscopy method, the current is composed of a steady-state (or direct) part (determined by the mean dc potential and the mean dc concentrations at the interface, $c_{Ox}$ and $c_{Red}$) and an ac part $\Delta j_F$ (determined by the ac perturbing signal $\Delta E$ and concentration fluctuations, $\Delta c_{Ox}$ and $\Delta c_{Red}$). The Faradaic impedance is given by the ratio of the Laplace transform of the ac parts of the voltage and current density respectively [6, 13, 14, 76–86]

$$Z_F = \{\Delta E\}/\{\Delta j_F\} \tag{4.4.2}$$

The presence of an electric field at the interface affects differently the energies of the variously charged species as they approach the interfacial region [28, 42, 76–78, 87–89]. Therefore, the activation energy barriers for the reaction depend on the potential difference across the interface. It is convenient to express the

potential dependence of the rate constants of the reaction in the following manner [42, 76–79, 81, 87–89]

$$k_f = k_0 \exp\left[-\alpha(E - E^0)\frac{nF}{RT}\right],$$ (4.4.3)

$$k_b = k_0 \exp\left[(1-\alpha)(E - E^0)\frac{nF}{RT}\right],$$ (4.4.4)

where $k_0$ is the rate constant at the formal electrode potential $E^0$.

Generally $\Delta j_F$ is expressed as an expansion of the ac parts of the concentrations and electrode potential [6, 13, 14, 76–85] as follows

$$\Delta j_F = \sum_{Ox, Red}\left(\frac{\partial j_F}{\partial c_i}\right)\Delta c_i + \left(\frac{\partial j_F}{\partial E}\right)\Delta E + \text{higher order terms}$$ (4.4.5)

Neglecting all but the first-order terms (linearisation) and solving for $\Delta E$

$$-\Delta E = \frac{1}{(\partial j_F / \partial E)}\left[\sum_{Ox, Red}\left(\frac{\partial j_F}{\partial c_i}\right)\Delta c_i - \Delta j_F\right]$$ (4.4.6)

the Faradaic impedance has a form

$$Z_F = \frac{1}{(\partial j_F / \partial E)}\left[1 - \sum_{Ox, Red}\left(\frac{\partial j_F}{\partial c_i}\right)\frac{\{\Delta c_i\}}{\{\Delta j_F\}}\right].$$ (4.4.7)

The first term is the so-called charge transfer resistance ($(\partial j_F / \partial E)^{-1} = R_{ct}$), the second term contains the influence of the ac part of the mass transfer step on the impedance. The value $\{\Delta c_i\}/\{\Delta j_F\}$ can be expressed as a solution of the diffusion equation and under condition of semi-infinite diffusion to a planar electrode [6, 13, 76–81]

$$\frac{\{\Delta c_i\}}{\{\Delta j_F\}} = \frac{1}{nF\sqrt{pD_i}},$$ (4.4.8)

where $p$ is the complex frequency variable ($p = \sigma + j\omega$, where $\sigma$ is conductivity, j is imaginary unit, and $\omega = 2\pi f$ is angular frequency, where $f$ is ac frequency) and $D_i$ is the diffusion coefficient of the particle $i$. Under equilibrium conditions the charge transfer resistance

$$R_{ct} = \frac{RT}{nFj_0},$$ (4.4.9)

where the exchange current density is expressed as

$$j_0 = nFk_0c_{Ox}\exp\left[-\alpha(E_r - E^0)\frac{nF}{RT}\right] = nFk_0\left(c_{Ox}^*\right)^{1-\alpha}\left(c_{Red}^*\right)^{\alpha}.$$ (4.4.10)

For heterogeneous charge transfer (Faradaic) reaction, involving one adsorbed particle [81, 85, 86], the following stages can be separated:

$$A_{sol} + e^- \underset{k_{-1}}{\overset{\vec{k_1}}{\longleftrightarrow}} B_{ads} \qquad (4.4.11)$$

$$B_{ads} + e^- \underset{k_{-2}}{\overset{\vec{k_2}}{\longleftrightarrow}} C_{sol} \qquad (4.4.12)$$

where the indexes sol and ads denote the particles in solution and adsorbed state, respectively. The rates of these reactions may be written, assuming a Langmuir adsorption isotherm for B [81, 86], as

$$v_1 = k_1^0 \Gamma_s c_A \, exp\left[-\alpha_1\left(E - E_1^0\right)\frac{F}{RT}\right] - k_1^0 \Gamma_B \, exp\left[\left(1-\alpha_1\right)\left(E - E_1^0\right)\frac{F}{RT}\right], \qquad (4.4.13)$$

$$v_2 = k_2^0 \Gamma_B \, exp\left[-\alpha_2\left(E - E_2^0\right)\frac{F}{RT}\right] - k_2^0 \Gamma_s c_C \, exp\left[\left(1-\alpha_2\right)\left(E - E_2^0\right)\frac{F}{RT}\right], \qquad (4.4.14)$$

where $k_1^0$ and $k_2^0$ are the standard rate constants of these reactions; $\alpha_1$ and $\alpha_2$ are the transfer coefficients; $\Gamma_B$ and $\Gamma_s$ are the surface concentrations of the species B and of free adsorption sites $S$, respectively; $c_A$ and $c_C$ are the surface concentrations of A and C (assumed as equal to the bulk concentrations), respectively; and $E_1^0$ and $E_2^0$ are the standard redox potentials of the reactions 1 and 2, respectively. At equilibrium potential, $E_r$, the net rates of both reactions are zero and the following relations are obtained:

$$exp\left[\left(E_r - E_1^0\right)\frac{F}{RT}\right] = \frac{\Gamma_s^0 c_A}{\Gamma_B^0} = \frac{\left(1-\theta_0\right)c_A}{\theta_0}, \qquad (4.4.15)$$

$$exp\left[\left(E_r - E_2^0\right)\frac{F}{RT}\right] = \frac{\Gamma_B^0}{\Gamma_s^0 c_C} = \frac{\theta_0}{\left(1-\theta_0\right)c_A}, \qquad (4.4.16)$$

where the index 0 indicates equilibrium conditions, and a following relation is introduced: $\Gamma_i = \theta_i \Gamma_{max}$ (where $\Gamma_{max}$ is the maximal surface concentration [81, 86]).

The total current density observed is given as $j = F\left(v_1 + v_2\right)$ and the Faradaic admittance is given by

$$\hat{Y}_t = A + \frac{B}{j\omega + G}, \qquad (4.4.17)$$

where the inverse charge transfer resistance is obtained as [81]

$$A = \frac{1}{R_{ct}} = \frac{1}{RT}\left[\alpha_1 \vec{k_1}(1-\theta) + (1-\alpha_1)\overleftarrow{k_{-1}}\theta + \alpha_2 \vec{k_2}\theta + (1-\alpha_2)\overleftarrow{k_{-2}}(1-\theta)\right] \qquad (4.4.18)$$

and

$$B = -\frac{1}{C_{ad}R_{ct}^2} = \frac{1}{RT\Gamma_{max}}\left(-\overrightarrow{k_1} - \overleftarrow{k_{-1}} + \overrightarrow{k_2} + \overleftarrow{k_{-2}}\right) \times$$

$$\times\left[\alpha_1\overrightarrow{k_1}(1-\theta) + (1-\alpha_1)\overleftarrow{k_{-1}}\theta - \alpha_2\overrightarrow{k_2}\theta - (1-\alpha_2)\overleftarrow{k_{-2}}(1-\theta)\right] \qquad (4.4.19)$$

and

$$G = \frac{1}{R_{ad}C_{ad}} + R_{ct}|B| = \frac{1}{\Gamma_{max}}\left(\overrightarrow{k_1} + \overleftarrow{k_{-1}} + \overrightarrow{k_2} + \overleftarrow{k_{-2}}\right) \qquad (4.4.20)$$

The more complicated cases, taking into account the slow diffusion step to the fractal and disc electrodes, have been discussed by Lasia [81].

The main aim of this work was to study the processes taking place at the Cd(0001) | $K_3[Fe(CN)_6]$ + aqueous base electrolyte interface and to analyse the processes obtaining the rate of the $[Fe(CN)_6]^{3-}$ electroreduction process. Comparison with the Cd(0001) | $Na_2S_2O_8$ + aqueous base electrolyte interface will be given, where the electroreduction of the $S_2O_8^{2-}$ anion occurs.

# 5. EXPERIMENTAL DETAILS

Distilled water for preparing the solutions was treated with the Milli-Q+ purification system (resistance $> 18.2$ MΩ cm). $K_2SO_4$ was purified by triple recrystallisation from water and calcined at 798 K immediately prior to the experiments. $K_3[Fe(CN)_6]$ ($\geq 99.9$ %) and KF ($\geq 99.5$ %) from Fluka were used as delivered. $K_4[Fe(CN)_6]\cdot 3H_2O$ was purified by triple recrystallisation from water and treated in vacuum to dryness. Air was removed from the solution by bubbling argon (Ar: 99.999 %) through or over the solution prior to / or during measurement, respectively.

Electrochemically polished Cd(0001) single-crystal plane electrodes were prepared according to the method described in works [90–93]. After electrochemical polishing the Cd(0001) plane was rinsed with Milli-Q+ water and submerged into a deaerated surface-inactive solution at potential $E = -1.2$ V (Ag|AgCl|sat. KCl). Thus in this paper all the potentials are given against Ag|AgCl|sat. KCl in $H_2O$ reference electrode. Electrochemical measurements were performed at $T = 298$ K and the long Luggin capillary was used for the reference electrode.

Conventional electrochemical equipment (Pine Company) was used for stationary and rotating disc voltammetry studies. The impedance spectra and capacitance values at fixed ac frequency were measured by the Autolab PGSTAT 30 with a FRA 2 system, using ac voltage amplitude 5 mV [90–93].

# 6. RESULTS AND DISCUSSION

## 6.1. Cyclic and rotating disc electrode voltammetry data for electroreduction of hexacyanoferrate(III) anions at Cd(0001)

The voltammograms of the hexacyanoferrate(III) anion reduction (uncorrected for the current density in the base electrolyte solution) on the Cd(0001) electrode in the KF solutions (from $1 \cdot 10^{-3}$ M to $1 \cdot 10^{-1}$ M) are displayed in Fig. 1. According to these data the noticeable increase of current density takes place at $E < -1.35$ V. It is probably caused by the cathodic hydrogen evolution reaction, because the current density is practically independent of the rotation velocity of the EP Cd(0001) electrode. For that reason the current densities for the base electrolyte solution were subtracted from the data for systems with addition of $[Fe(CN)_6]^{3-}$ in the base electrolyte to study the electroreduction kinetics of the $[Fe(CN)_6]^{3-}$ anion on Cd(0001) plane. According to the data in Figs. 1 and 2, the rate of electroreduction of $[Fe(CN)_6]^{3-}$ to $[Fe(CN)_6]^{4-}$ depends noticeably on the electrode potential, as well as on the base electrolyte and $[Fe(CN)_6]^{3-}$ concentrations. Unlike Pt electrodes [12] no hysteresis of current density between the negative and positive scans of potential in the region of mixed kinetics was observed if $5 \cdot 10^{-5} \leq c_{K_3[Fe(CN)_6]} \leq 7 \cdot 10^{-4}$ M. In the region of potentials $-1.05 \leq E \leq -0.95$ V, the very clear current plateaus were found. The limiting current density $j_d$ at constant potential measured at the rotating EP Cd(0001) disc electrode was found to fit very well to the Levich ($j$, $\omega^{1/2}$) plot ($0.997 \leq r^2 \leq 0.999$):

$$j_d = 0.620 n F v^{-1/6} D^{2/3} \omega_{rot}^{1/2} c_i \tag{6.1.1}$$

where $v$ is the kinematic viscosity and $\omega_{rot}$ is the angular velocity of the electrode. Taking the number of electrons transferred $n = 1$ and $v = 0.01$ cm$^2$ s$^{-1}$ [1, 2, 11], the values of the diffusion coefficient for the $[Fe(CN)_6]^{3-}$ anion have been calculated ($D = 7 \cdot 10^{-6}$ cm$^2$s$^{-1}$ for a $1 \cdot 10^{-2}$ M KF solution), which are in a good agreement with the literature data [4, 16, 43]. Thus, in this region of potentials, the electroreduction of the $[Fe(CN)_6]^{3-}$ anion on the EP Cd(0001) plane is mainly limited by the rate of diffusion of the $[Fe(CN)_6]^{3-}$ anions to the electrode surface.

According to the data in Figs 1, with increasingly negative potential ($q \leq -2.0$ μC cm$^{-2}$; $E < -1.05$ V), the inhibition of $[Fe(CN)_6]^{3-}$ electroreduction begins, caused by the increase of the negative value of the $\psi_1$ potential, and a minimum of current density at $-1.4 \leq E \leq -1.25$ V was found in the dilute KF solutions. At constant concentration of $c_{K_3[Fe(CN)_6]}$ potential of the minimum is practically independent of the concentration of base electrolyte.
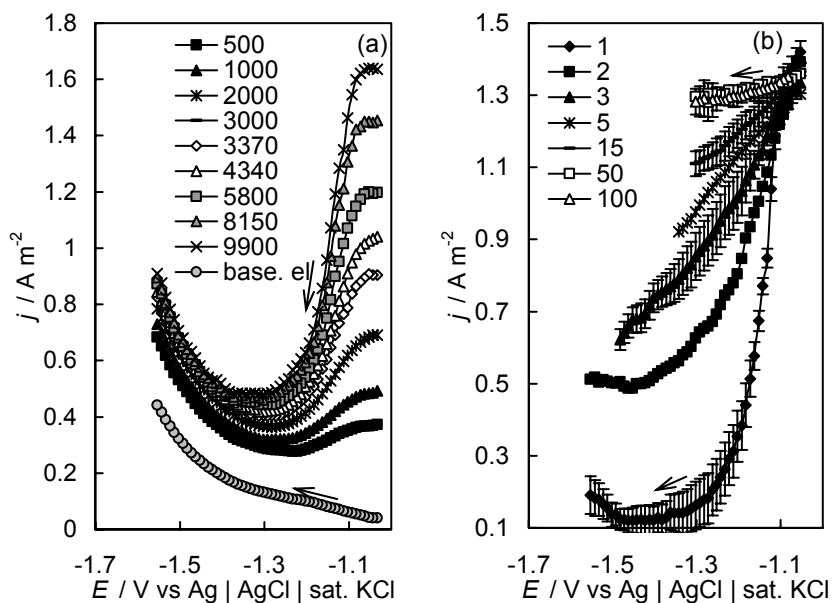
**Figure 1.** Rotating disc voltammetry $(j, E)$ curves (scan rate $v = 10 \text{ mV s}^{-1}$) for EP Cd(0001) electrode (a) (not corrected for the base electrolyte current density) in $1 \cdot 10^{-4}$ M $K_3[Fe(CN)_6] + 1 \cdot 10^{-3}$ M KF solution at different rotation velocities (rev min$^{-1}$), noted in figure, and base. el – $(j, E)$ curve for pure $1 \cdot 10^{-3}$ M KF solution at 0 rev min$^{-1}$. (b) (corrected for the base electrolyte current density) at 9000 rev min$^{-1}$ in $1 \cdot 10^{-4}$ M $K_3[Fe(CN)_6]$ solution with different additions of base electrolyte (KF, mM), noted in figure. (Here and further arrows represent the direction of the potential scan.)

According to the data in Fig. 2 the current density (corrected for the base electrolyte current density) at fixed constant potential systematically increases with the rise of reactant concentration in the solution. The results of the systematic kinetic analysis show that the current values are stable and very well reproducible if the electrode potential has been cycled in the region $-1.55 \leq E \leq -0.95$ V. The attempts to study the $[Fe(CN)_6]^{3-}$ electroreduction process on the Cd(0001) plane at more positive potentials than $E \geq -0.90$ V caused a very quick decrease of the current density values in the all region and, thus similarly to the Pt electrodes [12, 15–17], experimental data indicate to the surface "blocking effect". The surface "blocking effect" could be caused by irreversible adsorption of the $[Fe(CN)_6]^{3-}$, reaction intermediates or $[Fe(CN)_6]^{4-}$ on the electrode surface. But the situation might be more complex and the oxidation of the cadmium electrode to cadmium hexacyanoferrate could take place. This oxidation current partly counter-balances the electroreduction current of $[Fe(CN)_6]^{3-/4-}$ and, as a result, one observes the decrease of the resulting current. In addition cadmium ferrocyanide, which is formed on the electrode,

presumably inhibits the studied process. However, differently from Pt electrodes [12, 15–17] there is no hysteresis in the current density potential curves as well as no dependence of $j$ on time (i.e. on the cycle number) if $E \leq$ -0.95 V. The data in inset of Fig. 2 show that there is a really linear dependence of the limiting diffusion current density $j_d$ (corrected for the base electrolyte current density) on $c_{K_3[Fe(CN)_6]}$ if $c_{K_3[Fe(CN)_6]} < 8 \cdot 10^{-4}$ M. At higher $c_{K_3[Fe(CN)_6]}$ the surface blocking i.e. the irreversible adsorption of solution components or intermediates is possible. In the experiments where the influence of the base electrolyte on the reaction rate was investigated the concentration of $K_3[Fe(CN)_6]$ was $1 \cdot 10^{-4}$ M and the potential interval was $-1.55 \leq E \leq -1.05$ V. Choosing these experimental conditions ensures that the reduction is not influenced by the adsorbed cadmium hexacyanoferrate because there is no deviation of the limiting diffusion current density from linear in Levich plot (inset in Fig. 2) so the cadmium hexacyanoferrate has not formed on the electrode surface. Otherwise there must be decrease of the limiting diffusion current density from the straight line.
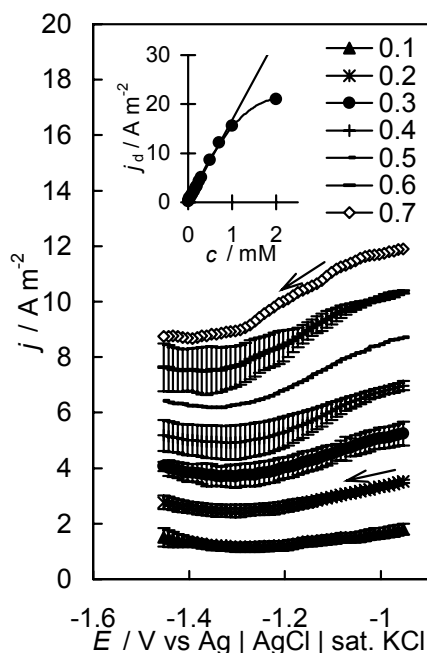


**Figure 2.** ($j$, $E$) curves ($v = 10$ mV s$^{-1}$, corrected for the base electrolyte current density) for EP Cd(0001) electrode at 9000 rev min$^{-1}$ in 0.01 M KF solution with different additions of $K_3[Fe(CN)_6]$ (mM): noted in figure. Inset: dependence of the limiting diffusion current density (based on data on main figure) on $K_3[Fe(CN)_6]$ concentration.

At more negative surface charge densities ($q \leq -10\ \mu C\ cm^{-2}$), acceleration of the $[Fe(CN)_6]^{3-}$ anion electroreduction in the region of potentials, where the value of $d\psi_1/dE$ is approximately constant, takes place. Acceleration of the reaction is mainly caused by the increase of negative electrode potential, i.e. by the dependence of activation energy on $E$ as the overpotential increases [27–29]. On the other hand, the increase of $j_k$ at $E < -1.35$ V can be explained by the beginning of the weak specific adsorption of the base electrolyte cations at the negatively charged Cd(0001) electrode surface ($q \leq -13\ \mu C\ cm^{-2}$) and thus by the charge transfer through the adsorbed ion-pair [24, 26–29]. This result is in a good agreement with the impedance data as in this region of potential ($E \leq -1.35$ V) a weak rise in the differential capacitance $C$ values with $c_{KF}$ was observed [94]. It should be noted that the capacitance values in the 0.1 M KF solution are somewhat higher than those in the 0.1 M NaF solution ($\Delta C \sim 1.0\ \mu F\ cm^{-2}$) demonstrating that weak adsorption of the $K^+$ ions is possible on the Cd(0001) plane at $q \leq -14\ \mu C\ cm^{-2}$ [91]. The same dependences are valid for the Cd(0001) | $Na_2S_2O_8 + Na_2SO_4$ interface [49, 90, 95].
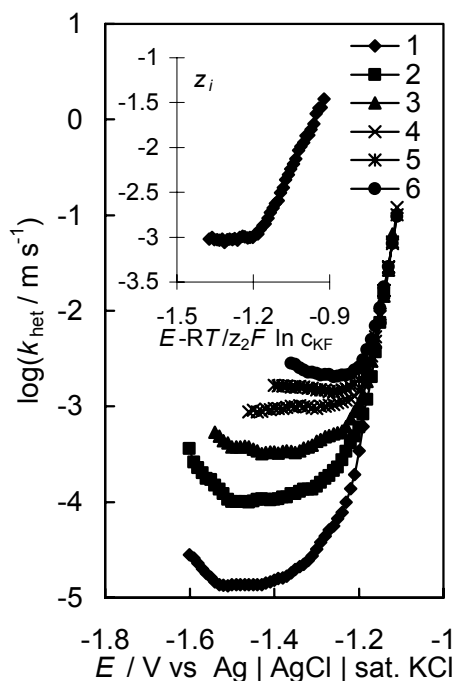


**Figure 3.** log $k_{het}$, $E$ curves for EP Cd(0001) electrode in $1 \cdot 10^{-4}$ M $K_3[Fe(CN)_6]$ with different additions of base electrolyte solution (KF, mM): noted in figure. Inset: Calculated charge of the reacting particle $z_i$ at various surface charge densities.

The apparent rate constant for the heterogeneous electroreduction reaction of the $[Fe(CN)_6]^{3-}$ anions, $k_{het}$, is defined by Eq.:

$$j_k = nFk_{het}c_i \tag{6.1.2}$$

The values of kinetic current density at constant potential were obtained from the linear Koutecký–Levich plots according to Frumkin, Aikazian, Tedoradze and Koutecky method [28, 39, 42, 87–89] ($0.997 \leq r^2 \leq 0.999$) according to Eq.:

$$1/j = 1/j_k + 1/j_d \tag{6.1.3}$$

The logarithmic dependences of the apparent rate constant (calculated from the current densities, which were corrected to the base electrolyte effects), on the electrode potential at different base electrolyte concentrations are presented in Fig. 3. At constant potential, $\log k_{het}$ increases with $c_{KF}$ in the solution, but at constant concentration of $c_{KF}$ it is practically independent of $c_{K_3[Fe(CN)_6]}$, if

$$c_{K_3[Fe(CN)_6]} \leq 8 \cdot 10^{-4} \text{ M}.$$

Analysis of the experimental data shows that there is a good linear dependence of $\ln j_k$ on $\ln c_{KF}$ ($0.995 \leq r^2 \leq 0.999$) if $c_{KF} \leq 0.01$ M and at $q \leq$ -5 µC cm$^{-2}$. Using these data the effective charge number of the reacting particle $z_i$ was obtained according to the Frumkin–Petrii method (described in more detail in Ref. [87]) according to Eq.:

$$\left( \frac{\partial \ln j_k}{\partial \ln c_{KF}} \right)_{E-\frac{RT}{z_2 F}\ln c_{KF}, c_i} = -\frac{z_i}{z_2}, \tag{6.1.4}$$

where $z_2$ is the charge number of the base electrolyte cations (i.e. $z_2 = +1$) According to the data in the inset of Fig. 3 the values of $z_i$ obtained depend on the electrode charge density and $z_i$ increases with the charge density if $q \leq$ -5 µC cm$^{-2}$. The comparatively low values of $|z_i|$ at $q \geq$ -5 µC cm$^{-2}$ indicate that there are noticeable deviations from the classical Frumkin model and the condition $\Gamma_{A^-} \ll \Gamma_{C^+}$ at $q \geq$ -5 µC cm$^{-2}$ is not satisfied for the Cd(0001)|$[Fe(CN)_6]^{3-}$ + KF + H$_2$O interface ($\Gamma_{A^-}$ and $\Gamma_{C^-}$ are the Gibbs adsorption of the anions and cations, respectively). The value of $z_i \approx$ -3 obtained at the negative values of the surface charge densities indicates that the ion-pairing effect might not be so important in determination of the reacting particle charge at the Cd(0001)| K$_3$[Fe(CN)$_6$] + KF + H$_2$O interface. However, the charge number of the $S_2O_8^{2-}$ ion at cathodic potentials is different from –2. The value of $z_i \approx$ -0.6 for the Cd(0001)|Na$_2$S$_2$O$_8$ + NaF + H$_2$O interface obtained indicate that the ion-pairing is important.
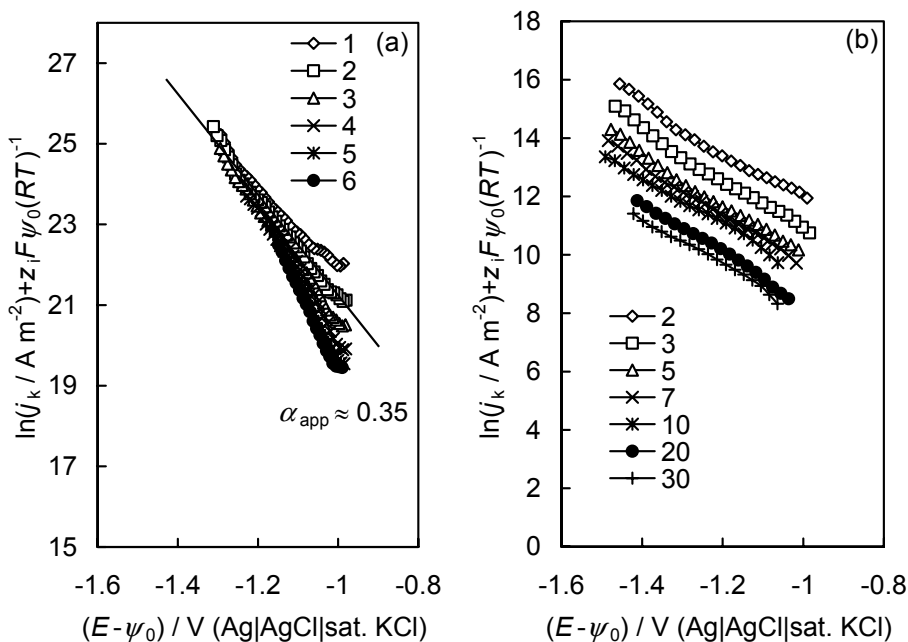
**Figure 4.** Corrected Tafel plots ($\psi_0$-potential obtained according to Gouy-Chapman-Stern-Grahame model) for EP Cd(0001) electrode in (a) $1 \cdot 10^{-4}$ M $K_3[Fe(CN)_6]$ ($z_i = -3$) solution with different additions of base electrolyte (KF, mM), noted in figure, and (b) $2 \cdot 10^{-5}$ $Na_2S_2O_8$ ($z_i = -2$) solution with different additions of base electrolyte (NaF, mM), noted in figure

The corrected Tafel plots [25, 26, 29] for the $[Fe(CN)_6]^{3-}$ anion electroreduction on the EP Cd(0001) have been calculated according to $j_k$ values using the $\psi_0$ values calculated from the impedance data for the pure base electrolyte solutions [91, 96, 97]. Thus, to a first approximation, the value of the $\psi_0$-potential has been taken equal to the value of the $\psi_1$ potential, i.e. to the mean potential of the plane at which are located the centres of the charges of reacting particles in the transition state of the reaction. As can be seen in Fig. 4a cTps for EP Cd(0001) interface in the less concentrated base electrolyte with addition of $[Fe(CN)_6]^{3-}$ are linear at $E - \psi_0 \leq -1.15$ V, if we assume that $z_i = -3$. The apparent transfer coefficient $\alpha_{app} \approx 0.35$ can be obtained. For more concentrated base electrolyte with addition of $[Fe(CN)_6]^{3-}$ at $E - \psi_0 > -1.15$ V these plots are non-linear, which is probably caused by the dependence of the adsorption energies of the reactant and product on the electrode potential. The attempts to use various new approximations, discussed in works [1, 2, 11, 44–48], did not give better fitting of the experimental data in the region of $E - \psi_0 >$

–1.1 V and therefore the more correct adsorption data of $K^+$ as well as $[Fe(CN)_6]^{3-}$ and $[Fe(CN)_6]^{4-}$ ions on the EP Cd(0001) plane was needed.

The more detailed analysis of ctp data (Fig. 4b) for Cd(0001)|Na$_2$S$_2$O$_8$ + Na$_2$SO$_4$ interface [49, 90, 95] demonstrates that for $S_2O_8^{2-}$ electroreduction there is very noticeable dependence of corrected current density values on the base electrolyte addition concentration. Differently from Cd(0001)|[Fe(CN)$_6$]$^{3-}$ electroreduction data very low $\alpha_{app} < 0.1$ have been calculated, indicating the activationless charge transfer process at Cd(0001)$|S_2O_8^{2-}$ interface. This is not surprising taking into account the totally different reaction mechanisms, i.e. for the $[Fe(CN)_6]^{3-}$ electoreduction there is no chemical bond dissociation taking place in comparison with the $S_2O_8^{2-}$ electoreduction.

## 6.2. Adsorption of hexacyanoferrate(II) and hexacyanoferrate(III) anions at Cd(0001)

The differential capacitance $C$ versus electrode potential plots at fixed different ac frequencies $f$ (5 Hz $< f <$ 750 Hz) have been measured for solutions with different base electrolyte and K$_3$[Fe(CN)$_6$] (Fig. 5a) concentrations, where the adsorption step is the main rate determining step. Thus, the $C, E$-curves measured at $f = 8$ Hz (Fig. 5a) demonstrate the total series capacitance $C_s$ including mainly edl $C_{edl}$ and adsorption $C_{ad}$ capacitance components. According to the data in Fig. 5a there is a diffuse layer minimum in the $C, E$-dependences and in case of KF the potential of this minimum $E_{min} = -0.94$ V is independent of $c_{KF}$ as well as of ac frequency. Thus, this minimum corresponds to the zcp for the Cd(0001) electrode in the aqueous KF solution [91–93, 96, 97]. In the K$_2$SO$_4$ solution the $E_{min}$ potential is shifted ~30 mV towards more negative potentials, caused by the asymmetric nature of the 1 : 2 – base electrolyte [21, 42, 91–93, 96–98]. The capacitance values in the diffuse layer minimum increase as $c_{base.el}$ increases, i.e. as the diffuseness of the edl decreases in good agreement with Gouy-Chapman theory.
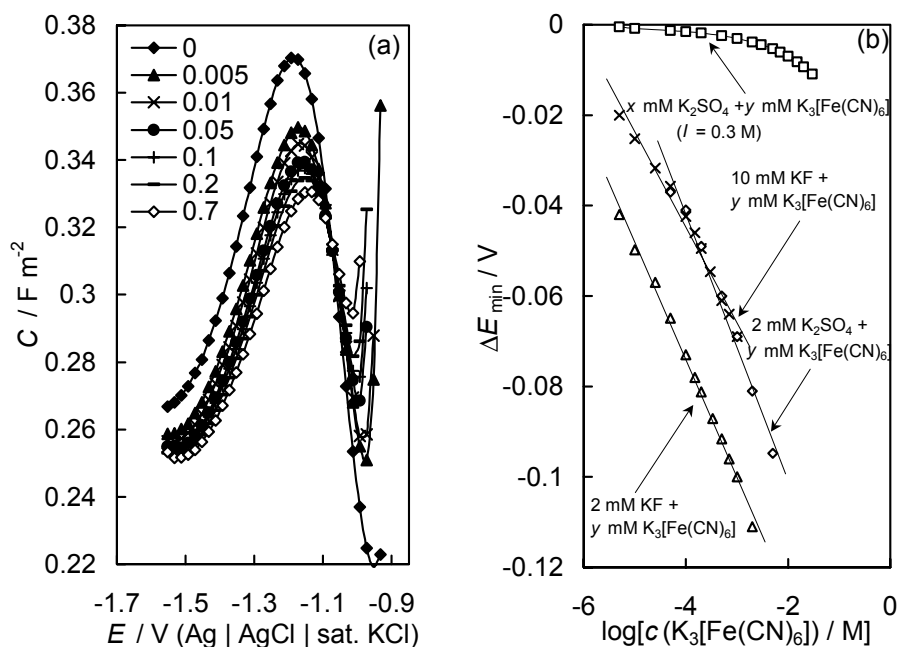
**Figure 5.** (a) The dependence of the differential capacitance $C$ ($f$ = 8 Hz) on the electrode potential for the EP Cd(0001) electrode in the 2 mM KF + $y$ mM $K_3[Fe(CN)_6]$ solution with different additions of $K_3[Fe(CN)_6]$ (mM), noted in figure.
(b) The dependence of the shift of the minimum in the $C, E$ – curves on the concentration of $K_3[Fe(CN)_6]$ for the EP Cd(0001) electrode in different base electrolyte solutions, noted in figure.

The addition the $[Fe(CN)_6]^{3-}$ anions cause the increase of the capacitance at $E \approx E_{min}$ (Fig 5a), i.e. the diffuseness of the edl decreases as the ionic strength $I$ increases and at the same time the $E_{min}$ potential shifts noticeably towards the more negative values (Fig. 5b). The capacitance minimum is symmetrical if $c_{K_3[Fe(CN)_6]}$ is very low, but in the more concentrated solutions the capacitance starts to increase faster at $E > E_{min}$ caused by the asymmetrical structure of the $K_3[Fe(CN)_6]$ (1 : 3–electrolyte) and by the specific adsorption of the $[Fe(CN)_6]^{3-}$ anion at the Cd(0001) surface [93, 96, 97]. In the more concentrated solutions of $K_3[Fe(CN)_6]$ there is an inflection point in the $C, E$-curves at -1.0 < $E$ < -0.9 V. Probably in this potential region the character of the adsorptive-bond between the electrode surface and adsorbed $[Fe(CN)_6]^{3-}$ anion changes, i.e. the partial charge transfer or formation of covalent bond is probable at $E > –0.9$ V in a good agreement with the cyclic voltammetry and rotating disc electrode data [49, 90–97, 99].

According to the data in Fig. 5 there is a very sudden change in $E_{min}$ values at very small $[Fe(CN)_6]^{3-}$ additions and the diffuse layer minimum is clearly asymmetric. At $E < -1.4$ V the capacitance starts to increase and this is caused by the weak adsorption of the $K^+$ cations or by the pseudocapacitive behaviour of the system (i.e. by the charge transfer process(es) at cathodic potentials) [91–93, 96, 97]. The increase in the capacitance is proportional to $c_{base.el}$ and $c_{K_3[Fe(CN)_6]}$, i.e. to the Gibbs adsorption of cations at $E < -1.4$ V [91–93, 96, 97]. However in addition to $K^+$ adsorption and electroreduction of $[Fe(CN)_6]^{3-}$ the hydrogen evolution could occur. Visual analysis shows that there are small bubbles of hydrogen at the electrode surface at $E < -1.6$ V in the concentrated $KF + K_3[Fe(CN)_6]$ solutions.

As noted before the specific character of the $[Fe(CN)_6]^{3-}$ anion adsorption can be characterized by the shift of $E_{min}$ potential in the $C, E$-curves: $\Delta E_{min} = E_{min} - E_{min}^*$, where $E_{min}$ and $E_{min}^*$ are the potentials of the $C, E$-curve diffuse layer minimum without and with the addition of $K_3[Fe(CN)_6]$, respectively. The $\Delta E_{min}$, $\log c_{K_3[Fe(CN)_6]}$-dependences for different base electrolytes are presented in Fig. 5b. This shift is more pronounced in the solution with addition of KF and could be explained mainly by the different negative charges and degrees of solvation of the base electrolyte anions ($F^-$ is more strongly solvated than $SO_4^{2-}$ or $[Fe(CN)_6]^{3-}$). There is a bigger shift of $E_{min}$ in the solutions with the lower ionic strength, i.e. the diffuseness of edl also affects the specific adsorption of the $[Fe(CN)_6]^{3-}$ anions. Quantitative analysis demonstrates that the shift of the minimum potential could not be caused only by the asymmetry of the electrolyte [21, 89, 97], because the corresponding shift of $E_{min}$ if $c_{K_3[Fe(CN)_6]} < 1 \cdot 10^{-4}$ M is smaller than 14 mV [99, 100]. Therefore the strong adsorption of anions at $E \approx E_{min}$ takes place at Cd(0001) plane. The slope of the $\Delta E_{min}$, $\log c_{K_3[Fe(CN)_6]}$-dependences in the dilute base electrolyte solutions (KF or $K_2SO_4$) is approximately the same ($\sim -0.0255$ V). If we assume that the discreteness effect in edl are unimportant, i.e. $\lambda = 1$, then from the Esin-Markov formula [91–93, 96, 97]: $d\Delta E_{min}/d\log c_{K_3[Fe(CN)_6]} \approx 0.058/(z_i \lambda)$ where $z_i$ is the charge number of the adsorbing particle and the parameter $\lambda$ describes the discreteness of the charge distribution, the effective charge number of the ionic complex calculated is equal to -2.3 but not -3. Therefore the $[Fe(CN)_6]^{3-}$ anion is presented mainly as an ion pair, $K^+-[Fe(CN)_6]^{3-}$, in the base electrolyte + $K_3[Fe(CN)_6]$ solution | Cd(0001) interface.

For quantitative study of the adsorption of the $[Fe(CN)_6]^{3-}$ and $[Fe(CN)_6]^{4-}$ anions the differential capacitance measurements in the system with constant ionic strength, varying the mole fraction of the surface-active anion in a system with constant ionic strength ($I = 0.3$, $x = 0 \ldots 0.1$ M, $y = 0 \ldots 0.03$ M), have been conducted. The dependences of the series capacitance $C_s$ on the square root of

the angular frequency $\omega$ ($\omega = 2\pi f$) at constant concentration of the surface-active anion and at various fixed electrode potentials are linear with the determination coefficient $0.994 \leq r^2 \leq 0.999$ if $100 < f < 750$ Hz. However in the wide ac frequency $\omega$ region $C$ is a non linear function of $\omega$ and only in the limited region where diffusion is the rate limiting step for specific adsorption there is a linear dependence of $C$ on $\sqrt{\omega}$. At lower frequencies $f < 5$ Hz, the $C, \sqrt{\omega}$-dependences deviate from the linearity and the increase in the differential capacitance is pronounced, which is caused by the slow Faradaic or partial charge transfer processes taking place at lower frequencies. The slope of the $C_s, \sqrt{\omega}$-dependences is independent of the concentration of the surface-active anion if it is less than 0.015 M. The increase of the slope can be mentioned starting from the 0.03 M solution of the surface-active anion. Thus, in the more concentrated solutions the charge or partial charge transfer process [21, 36, 49, 59, 60, 65, 73, 74, 90, 92, 94, 95, 99–103] involving surface-active component is probable (i.e. the formation of weak bond between the surface-active particle and the Cd(0001) surface). The influence of concentration is more pronounced for the $[Fe(CN)_6]^{3-}$ anion than for $[Fe(CN)_6]^{4-}$. The electroreduction of the $[Fe(CN)_6]^{3-}$ anion and electrooxidization of the $[Fe(CN)_6]^{4-}$ anion are both probable in the region of potentials studied [94, 95, 102, 103].

The linear regions of the $C_s, \sqrt{\omega}$-dependences ($97 \leq f \leq 752$ Hz) were extrapolated to the zero frequency ($\omega \to 0$) to achieve the equilibrium differential capacitance values $C_0$ [27, 30, 31]. $C_0$, $E$-dependences for the solutions containing the $[Fe(CN)_6]^{4-}$ and $[Fe(CN)_6]^{3-}$ anions are given in Fig. 6. In the case of both anions the differential capacitance increases as the potential shifts towards less negative values. The adsorption of $[Fe(CN)_6]^{4-}$-anion starts at potentials less negative than -1.06 V. This potential is shifted 20 mV towards more positive values in comparison with the $[Fe(CN)_6]^{3-}$-anion. The increase in the concentration of the surface-active anion causes the increase of the differential capacitance, which is caused by the specific adsorption of the $[Fe(CN)_6]^{4-}$ and $[Fe(CN)_6]^{3-}$ anions [102]. The remarkable adsorption of the $[Fe(CN)_6]^{3-}$ anion starts at lower concentrations compared with $[Fe(CN)_6]^{4-}$. The increase of the differential capacitance is sharper in the case of the $[Fe(CN)_6]^{3-}$ anions, which indicates that $[Fe(CN)_6]^{3-}$ adsorbs more strongly on the Cd(0001) plane than $[Fe(CN)_6]^{4-}$. It can be explained by the stronger electrostatic repulsion of the $[Fe(CN)_6]^{4-}$ anions from the surface at potentials more negative than the zcp.
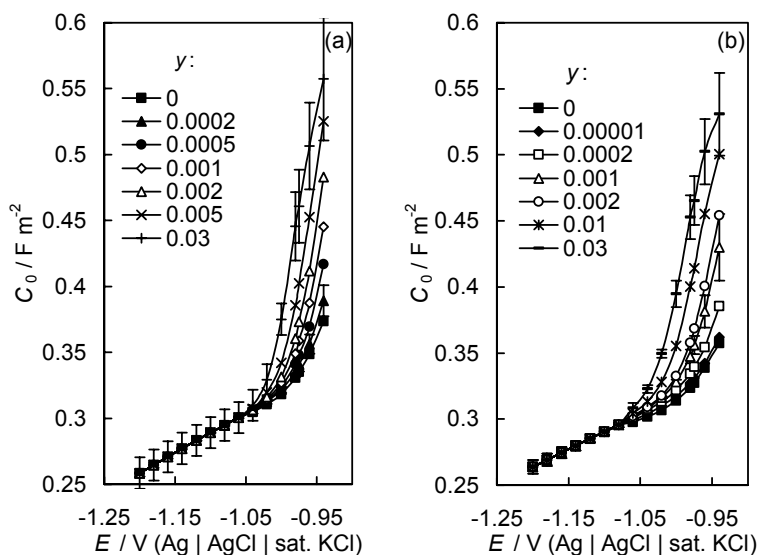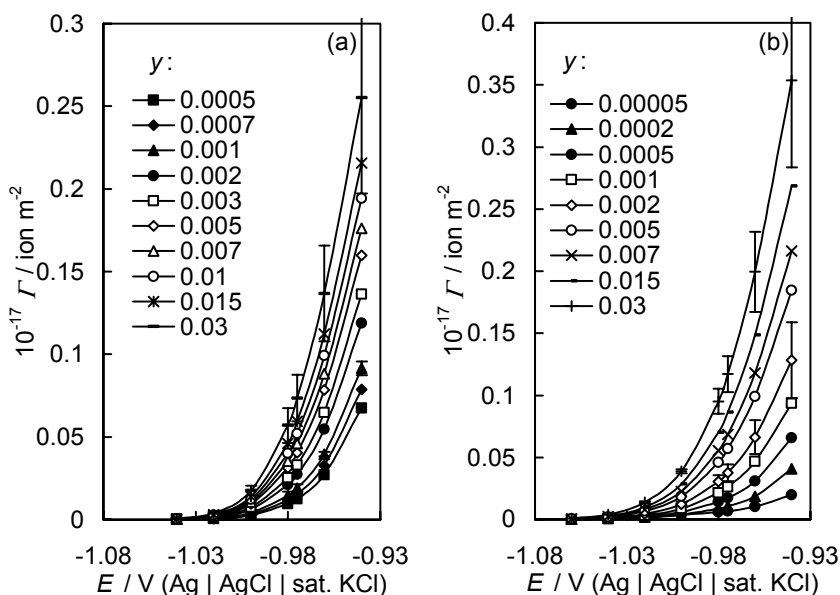
**Figure 6.** Dependence of the equilibrium differential capacitance $C_0$ on the electrode potential for the EP Cd(0001) electrode in the $x$ $K_2SO_4 + y$ $K_4[Fe(CN)_6]$ (a) and $x$ $K_2SO_4 + y$ $K_3[Fe(CN)_6]$ (b) solutions with constant ionic strength $I = 0.3$ M at different amounts of the surface-active anion (M), noted in figure.

The electrochemical impedance measurements in solution with addition of the $[Fe(CN)_6]^{3-}$ anion are more complicated at potentials less negative than -0.88 V because the formation of the surface compounds causes the irreversible surface blocking at higher concentrations of the $[Fe(CN)_6]^{3-}$ anion. In this region of potentials $E > $ -0.88 V the electrode surface is blocked and the sharp decrease of the differential capacitance can be observed. Therefore, high care must be taken at higher concentrations and potentials positive than zcp. The increase of the capacitance is in the same order as for the iodide ion on the Cd(0001) electrode, but the adsorption of the iodide ions begins at ~200 mV more negative potentials compared with hexacyanoferrate anions [93]. This could also be explained by the more pronounced electrostatic repulsion of hexacyanoferrate anions from the negatively charged electrode surface. At positive surface charges the hexacyanoferrate anions adsorb probably better than the halide ions. At potentials less negative than -0.9 V the maximum and also the hysteresis appears in the differential capacitance versus electrode potential dependences for both anions studied. This capacitance maximum is caused by the noticeable specific adsorption of anions as well as by the probable strengthening of the covalent nature of the adsorption bond due to the partial or "true" charge transfer [71, 100, 102–104], or by the onset of cadmium oxidation at $E > $ -0.9 V. At less negative potentials than -0.84 V the adsorption becomes irreversible: the capacitance peaks established in

*C*, *E*-curves at $E > -0.95$ V disappear and the values of the capacitance decrease from two to three times, i.e. the strong chemisorption of the anions and surface blocking takes place. Therefore, only the capacitance data obtained at more negative potentials than -0.94 V have been used for calculation of the adsorption data in this work [102, 103]. Similar behaviour for Ni270 [105] and Pt [106] electrodes has been discussed.

The equilibrium $C_0$, $E$-curves for various additions of $[Fe(CN)_6]^{4-}$ and $[Fe(CN)_6]^{3-}$ anions were back integrated [69, 107] (starting from -1.10 V where the specific adsorption of the anions is absent) in order to obtain the equilibrium surface charge density, $q$, vs. electrode potential, $E$, curves. At potentials less negative than -1.06 V the slope of the $q$, $E$-curves starts to increase as the concentration of the anions increases. Comparison of the $q$, $E$-curves for the anions investigated shows that the adsorption activity increases in the order of anions $[Fe(CN)_6]^{4-}$ < $[Fe(CN)_6]^{3-}$ as the negative charge number and the solvatation energy of anion decreases [103].

The $q$, $E$-curves were back integrated to obtain the relative specific surface work vs. potential curves. The relative specific surface work at constant potential was plotted versus $\ln c_{K_m A^*}$ and the resulting curves were differentiated to establish the Gibbs excess versus $E$ dependences at $c_{K_m A^*} = \text{const}$, given in Fig. 7. Independently, the Gibbs excess at the fixed values of the equilibrium surface charge density was calculated, using the Parsons function $\xi = qE + \gamma$ [51, 52, 56, 57, 67–71] and differentiating the relative $\xi$, $\ln c_{K_n A^*}$-curves at constant electrode charge. According to the analysis of data there are no big differences between the Gibbs excess values calculated at constant electrode potential or at constant electrode charge at more negative potentials than -0.94 V. However, the Vorotyntsev method [65] gives us the possibility to investigate the specific adsorption of the anions in the wider region of the surface charge densities. According to the data in Fig. 7, an almost exponential dependence of the Gibbs excess on the electrode potential has been observed at potentials more positive than zcp [102, 103]. The slope of the $\Gamma_{A^*}$, $E$-curve for the $[Fe(CN)_6]^{4-}$ anion is lower compared with that for $[Fe(CN)_6]^{3-}$. The dependences of the Gibbs excess on the electrode charge density at constant electrode potential are practically quasi-linear and parallel to each other at small negative and positive surface charge densities. At the same potential the Gibbs excess of the $[Fe(CN)_6]^{3-}$ anion is higher than that for $[Fe(CN)_6]^{4-}$ at the Cd(0001) electrode. However the values of the Gibbs excess for the halide ions (Br⁻ and J⁻) at Cd(0001) are noticeably higher i.e. the adsorption of halide ions from (0.1 - *y*) KF + *y* M KA* is much stronger at the same potentials [93] but the increase of the Gibbs excess with the concentration of the surface active ion is more pronounced for the $[Fe(CN)_6]^{3-}$ and $[Fe(CN)_6]^{4-}$ anions [102, 103].

**Figure 7.** Dependence of the Gibbs excess on the electrode potential for the EP Cd(0001) electrode in the $x$ K$_2$SO$_4$ + $y$ K$_4$[Fe(CN)$_6$] (a) and $x$ K$_2$SO$_4$ + $y$ K$_3$[Fe(CN)$_6$] (b) solutions with constant ionic strength $I = 0.3$ M at different additions of the surface-active anion (M), noted in figure.

*Adsorption isotherms.* In order to determine the Gibbs adsorption energy, the surface pressure data were fitted to the square root isotherm Eq. 4.3.5, which are quite linear to obtain the adsorption equilibrium constant for the anions studied. The charge density values of specifically adsorbed ions at fixed potentials were recalculated to the condition of constant charge and fitted to the simple virial isotherm Eq. 4.3.1. Like for the Hg | [Fe(CN)$_6$]$^{4-}$ interface [101] the simple virial isotherms at constant surface charge density are linear if the concentration of the surface-active anions is higher than 0.5 mM and at fixed surface charge density the intercept of isotherms increases (and the slope decreases) from [Fe(CN)$_6$]$^{4-}$ to [Fe(CN)$_6$]$^{3-}$ [102, 103]. To get the real values of the Gibbs adsorption energy at $E \neq E_{q_0=0}$ the simple virial isotherm were corrected for the $\psi_0$-potential term [56, 57, 66–69, 93]. The value of the $\psi_0$-potential, calculated according to Eq. (4.3.2), decreases as the concentration of the surface-active ion increases, i.e. the electrostatic work decreases. In the case of the [Fe(CN)$_6$]$^{3-}$ anions the $\psi_0$-potential is independent of the concentration of the anions at more negative surface charge densities than -0.01 C m$^{-2}$. However, as the charge type of K$_4$[Fe(CN)$_6$] is higher, the $\psi_0$-potential starts to decrease more steeply with the concentration of the [Fe(CN)$_6$]$^{4-}$ anion in solution.
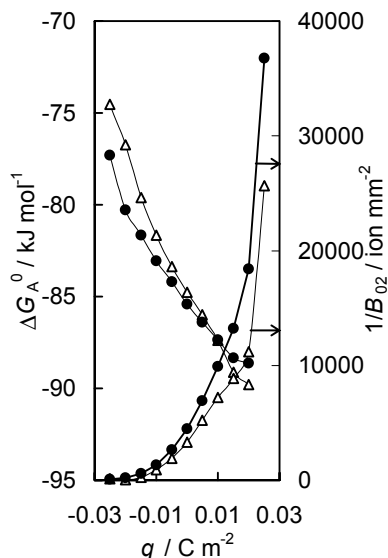
**Figure 8.** Gibbs energy of adsorption and the second virial coefficient versus electrode charge density dependences for the EP Cd(0001) electrode in the $x$ $K_2SO_4$ + $y$ $K_4[Fe(CN)_6]$ (triangles) and $x$ $K_2SO_4$ + $y$ $K_3[Fe(CN)_6]$ (circles) solutions with constant ionic strength $I = 0.3$ M calculated from the corrected virial isotherms.

The values of Gibbs adsorption energy obtained according to the 'square root', virial and corrected virial isotherm [51–65] are coincidental within the experimental errors ($\Delta\left(\Delta G_A^0\right) \leq 5$ kJ mol$^{-1}$) at zcp (Fig. 8) and at zcp the value of Gibbs adsorption energy is approximately the same as for the Bi(001)|Br$^-$ interface, but the Gibbs excess is many times lower for the Cd(0001)| $[Fe(CN)_6]^{3-}$ and Cd(0001)|$[Fe(CN)_6]^{4-}$ systems than for Bi(001)|Br$^-$ interface [92, 107]. The comparison of the data reveals that $[Fe(CN)_6]^{3-}$ has slightly more negative value of Gibbs adsorption energy i.e. the $[Fe(CN)_6]^{4-}$ anion is to the greater extent repelled from the slightly negatively charged Cd(0001) surface [102, 103].

As can be seen in Fig. 8, the inverse value of the second virial coefficient, $1/B_{02}$ (i.e. the number of ions engaged with the unit surface area) increases with the electrode surface charge density and from $[Fe(CN)_6]^{4-}$ to $[Fe(CN)_6]^{3-}$, which is caused by the decrease of the charge number of the anion in the adsorption layer. The value of the corrected virial coefficient is practically the same for $[Fe(CN)_6]^{3-}$ and $[Fe(CN)_6]^{4-}$ ions and there is about 20 times more ions on the surface in the case of the Bi(001)|Br$^-$ interface [92, 107] and 10 times more Br$^-$ anions at the Cd(0001) plane [93] than at the Cd(0001) | $[Fe(CN)_6]^{4-}$ or Cd(0001) | $[Fe(CN)_6]^{3-}$ interface [102, 103]. The $1/B_{02}$ values for the Hg | $[Fe(CN)_6]^{4-}$ interface [101] are somewhat higher near the zcp compared with Cd(0001) | $[Fe(CN)_6]^{4-}$ interface.

*Inner layer parameters*. The thermodynamic parameters obtained before reveal only somewhat about the structure and charge distribution on the Cd(0001) | surface active electrolyte interface. The $\Delta\phi^{m-2}, q_1$-dependences were constructed (Fig. 9a) to obtain some inner layer parameters. The $\Delta\phi^{m-2}, q_1$-plots are linear with the slope slightly decreasing with the rise of the electrode charge density. To a first very rough approximation, the data for $[Fe(CN)_6]^{4-}$ and $[Fe(CN)_6]^{3-}$ anions lie in the common plot at constant charge density. However, more detailed analysis shows that the $\Delta\phi^{m-2}, q_1$-plots for the $[Fe(CN)_6]^{4-}$ anions at higher values of electrode charge density have higher values of slope and intercept compared with the $[Fe(CN)_6]^{4-}$ anions. Extrapolation of the $\Delta\phi^{m-2}, q_1$-plots to the condition $q_1 = 0$ gives the values of $_qC$ (Fig. 9b) and the slope values give the values of $_\Gamma C$ (Fig. 9b inset). According to the experimental results the values of $_qC$ for the $[Fe(CN)_6]^{4-}$ and $[Fe(CN)_6]^{3-}$ ions at fixed electrode charge density are in a good agreement with the data for $F^-$ anions at positively charged surface but there are differences at negatively charged electrode surface. The values of $_qC$ for $[Fe(CN)_6]^{4-}$ are lower than those for the $[Fe(CN)_6]^{3-}$ anions at positively charged electrode surface. Assuming to a first approximation that the dielectric constant
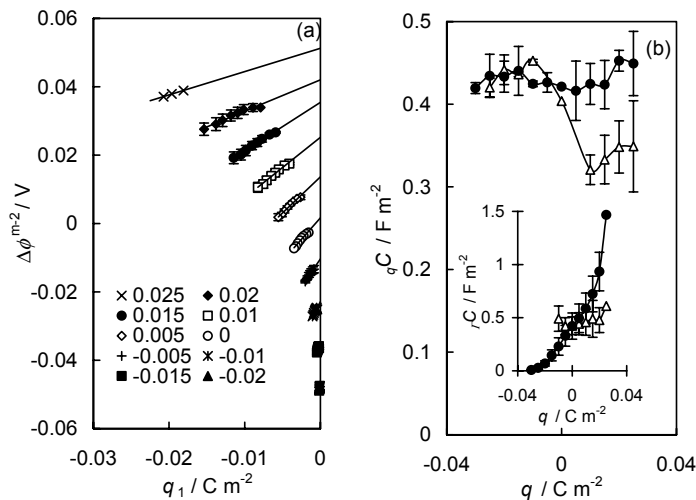


**Figure 9.** (a) Dependences of the potential drop across the inner layer on the charge density of the specifically adsorbed ions for the EP Cd(0001) electrode in the $x$ K$_2$SO$_4$ + $y$ K$_4$[Fe(CN)$_6$] solutions with constant ionic strength $I = 0.3\,\text{M}$ at fixed electrode charge densities $q$ (C m$^{-2}$), noted in figure.
(b) Inner layer capacitance at constant amounts of constant electrode charge density (main figure) and specifically adsorbed anions (inset) versus electrode charge density at curves for the EP Cd(0001) electrode in the $x$ K$_4$[Fe(CN)$_6$] + $y$ K$_2$SO$_4$ (triangles) and $x$ K$_3$[Fe(CN)$_6$] + $y$ K$_2$SO$_4$ (circles) solutions with constant ionic strength $I = 0.3\,\text{M}$.

of the inner layer is independent of the anion adsorbed then according to Eq. 4.3.14 and Fig. 9b the values of $x_2$ for $[Fe(CN)_6]^{4-}$ have to be higher than those for $[Fe(CN)_6]^{3-}$, i.e. the compact layer is thicker in case of the $[Fe(CN)_6]^{3-}$ anions adsorption at Cd(0001). The different behaviour of $_qC$ on the electrode charge density curves for $[Fe(CN)_6]^{3-}$ and $[Fe(CN)_6]^{4-}$ ions (Fig. 9b) can be explained by the higher surface activity of the $[Fe(CN)_6]^{3-}$ anions on Cd(0001) in comparison with the $[Fe(CN)_6]^{4-}$ anions at $E_{q=0} > 0$, which is probably caused by the different dependence of the distance of the outer Helmholtz plane $x_2$ on the surface charge density (smaller values of $x_2$ at constant electrode charge density) compared with corresponding dependences for the $[Fe(CN)_6]^{4-}$ anions [103].

The $_\Gamma C, q$-plots (Fig. 9b inset) show that the values of $_\Gamma C$ depend on the charge and electrical distribution of the surface-active anions. In the potential region of intensive specific adsorption the values of $_\Gamma C$ for the $[Fe(CN)_6]^{3-}$ anions are higher than those for the $[Fe(CN)_6]^{4-}$ anions adsorption at Cd(0001). Thus, according to Eq. 4.3.13 the value of $(x_2 - x_1)$ depends on the charge number of the anions adsorbed (if we assume that the dielectric constant of the inner layer is independent of the anion adsorbed, i.e. independent of $\Gamma_{A*}$). So, the relative position of the $[Fe(CN)_6]^{4-}$ anion in the compact Helmholtz layer is practically independent of the electrode surface charge density. The position of the $[Fe(CN)_6]^{3-}$ anion changes as the electrode charge density becomes from negative to positive, i.e. the $[Fe(CN)_6]^{3-}$ anion shifts towards electrode surface but, at the same time, the position of the outer plane remains the same [103].

## 6.3. Impedance spectroscopy data for electroreduction of hexacyanoferrate(III) anions at Cd(0001)

To establish the more detailed information about the reaction mechanism the complex impedance spectra were measured at ac frequency from $5 \cdot 10^{-2}$ to $1 \cdot 10^5$ Hz (14 frequencies per decade) within the region of the electrode potential from $-1.6$ to $-1.0$ V vs. Ag | AgCl | sat. KCl [102, 108]. At given base electrolyte concentration $c_{KF}$ the active $Z'$ and imaginary $Z''$ parts of the impedance depend noticeably on $c_{K_3[Fe(CN)_6]}$ and at fixed $c_{K_3[Fe(CN)_6]}$ on $c_{base.el}$ as well as on the electrode potential applied (Figs. 10–12). The so-called total polarization resistance $R_p$ (obtained from the difference between the high-frequency series resistance and low-frequency resistance) and $|Z''|$ have also complicated dependence on $E$, $c_{K_3[Fe(CN)_6]}$ and $c_{KF}$ [102, 108]. The similar behaviour of Au | $[Fe(CN)_6]^{3-}$/$[Fe(CN)_6]^{4-}$ + base electrolyte [13, 14] and Pt | $[Fe(CN)_6]^{3-}$/$[Fe(CN)_6]^{4-}$ + base electrolyte [109] system has been observed.

In a high frequency region ($f > 1000$ Hz) there are very small semicircles in the Nyquist plots (Fig. 10), however very well detectable at all potentials only in the dilute base electrolyte solutions $I < 0.03$ M. The shape of these high frequency semicircles is very well reproducible, depends on the total high frequency series resistance (i.e. electrolyte concentration) but does not depend on the electrode potential (Figs. 10–12). These high frequency semicircles are unimportant and undetectable if the ionic strength is higher than $I > 0.03$ M. It should be noted that the values of capacitance $C_{edl}$ or constant phase element (CPE) constant $Q$ obtained from this semicircle are very low ~$10^{-3}$ F m$^{-2}$, characterizing mainly the so-called geometrical capacitance because the auxiliary electrode surface area is extremely large compared with the Cd(0001) electrode studied [81, 90].

The Kramers-Kroning relations and corresponding error analysis [81] have been used [102, 108] for the selection out of the ac frequency region, where the impedance data can be used for the analysis of edl structure in base electrolyte and for the detailed analysis of reaction mechanism of the electroreduction of the $[Fe(CN)_6]^{3-}$ anions at Cd(0001) plane. It was found that mainly the ac frequency region $5 \cdot 10^{-2} < f < 2 \cdot 10^4$ Hz is free from noticeable $Z''$ and $Z'$ errors (Fig. 10b) ($|Z''$ error$| < 0.5$ % and $Z'$ error $< 0.6$ % with the random distribution of errors) and can be used for more detailed analysis, using least squared minimization fitting and other methods [6, 76–81, 102, 108, 109]. However, more detailed analysis at fixed electrolyte composition shows that at $f > 2 \cdot 10^3$ Hz there is no dependence of $Z''$, $Z'$-; $\log Z$, $\log f$-; $\phi$, $\log f$-; $Z''$, $\log f$- and $Z'$, $\log f$-plots on the electrode potential applied, but $Z$ and $Z'$ values systematically depend on the electrolyte concentration and can be used for obtaining the high-frequency series resistance, i.e. so-called electrolyte resistance $R_{el}$ values. It should be noted that the high-frequency resistance is proportional to the ionic strength of the solution (Fig. 10e) and thus it has been identified with the solution resistance [6, 76–81, 90, 108, 109].

The complex impedance plane plots show complicated behaviour at low frequencies, deviation to lower or higher values of the real part of the impedance (Figs. 10a-12a). These effects were found to be independent of time. The shape of the low-frequency part of $Z''$, $Z'$- and Bode plots depends noticeably on potential as well as on $c_{K_3[Fe(CN)_6]}$ (Figs. 10 and 11) explained by the adsorption of the electroactive species at Cd(0001), depending strongly on $E$ as well as on $c_{K_3[Fe(CN)_6]}$ [108].
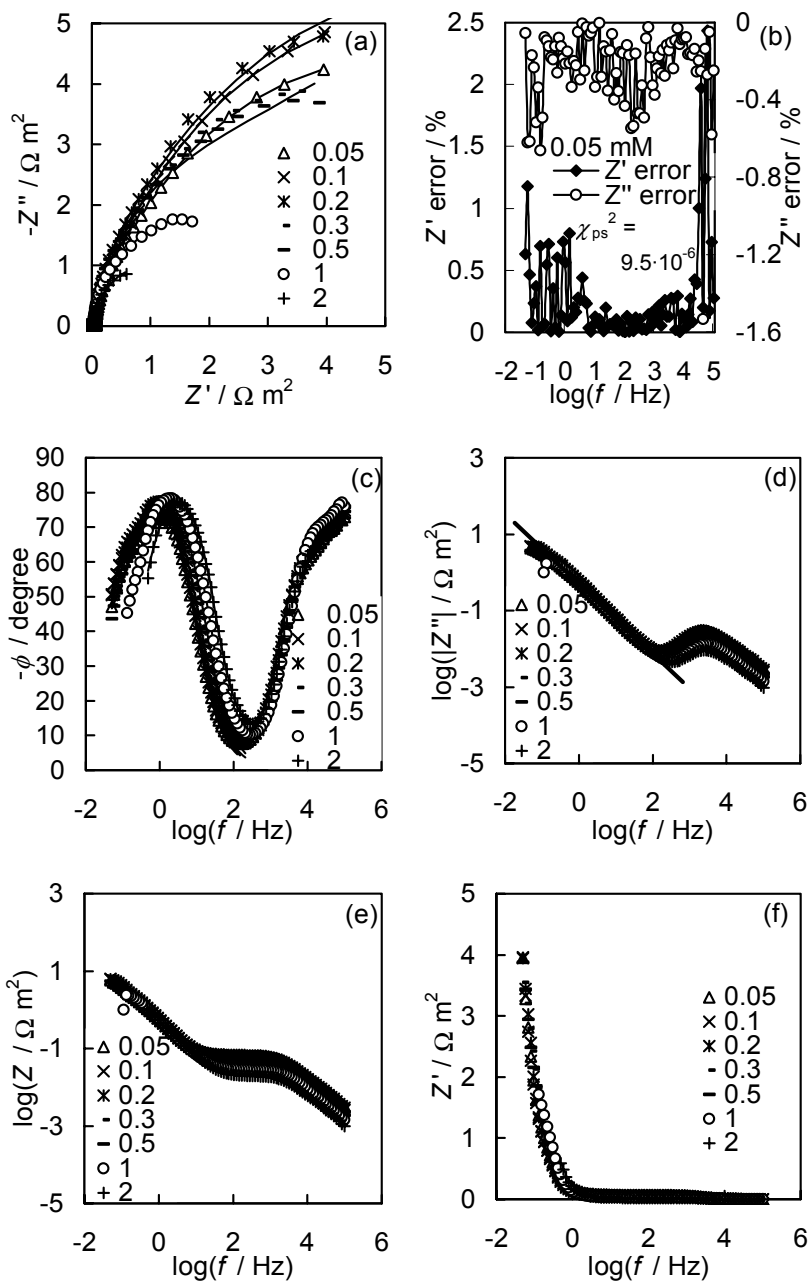
**Figure 10.** $Z'$, $Z''$- (a), residual (b), $-\phi$, $f$- (c), $\log|Z''|$, $f$- (d), $\log Z$, $f$- (e) and $Z'$, $f$- (f) plots for the EP Cd(0001) plane in 0.002 M KF aqueous solution with different additions of $K_3[Fe(CN)_6]$ (mM, noted in figure) at the electrode potential $E = -1.2$ V (marks – experimental data, solid lines – calculated data, see text).

11

The experimental data show that the low frequency parts of complex impedance plane plots depend noticeably on the concentrations of base electrolyte (Fig. 12) and $[Fe(CN)_6]^{3-}$ anions in solution (Fig. 10). The phase angle values obtained are somewhat higher than -90°, indicating to the presence of the so-called constant phase element behaviour (with the CPE impedance $Z_{CPE} = Q^{-1}(j\omega)^{-\alpha}$, where $Q$ is the CPE constant and $\alpha$ is CPE fractional exponent of the capacitive element (if $\alpha = 1$, then $Q = C_{edl}$), obtained from the slope of the $\log|Z''|$, $\log f$-plots (slope $\approx -\alpha$) [110]. Fractional exponent $\alpha$ values different from unity can be explained by the surface roughness, some distribution of energetic inhomogenity of surface causing the dependence of adsorption energy variations, as well as by distribution of the charge transfer process characteristic time on the surface structure of Cd(0001) electrode [6, 76, 80, 81, 91–93, 97, 109–112]. The same CPE behaviour can be obtained from Fig. 10d. The comparatively high values of $\alpha = 0.93$ for $2 \cdot 10^{-3}$ M and $\alpha = 0.95$ for $5 \cdot 10^{-2}$ M KF solutions [102, 108] indicate that there is only weak deviation of Cd(0001) interface from the ideally polarizable electrode (classical) conception [6, 76–81, 91, 92, 96]. Near the $E \approx E_{q=0}$ there is a small decrease of $\alpha$ values as $c_{KF}$ decreases.
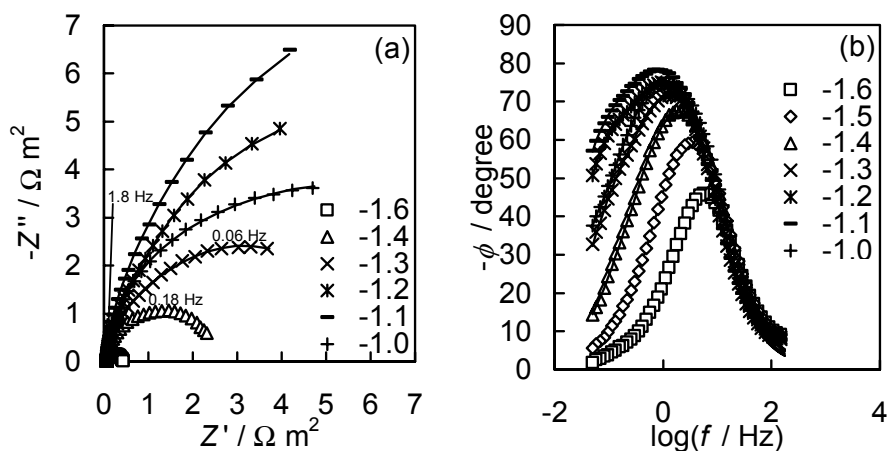


**Figure 11.** $Z'$, $Z''$- (a) and -$\phi$, $f$- (b) plots for the EP Cd(0001) plane in 0.002 M KF + 0.1 M $K_3[Fe(CN)_6]$ aqueous solution at different electrode potentials (V, noted in figure) (marks – experimental data, solid lines – calculated data, see text).

According to the data in Fig. 10, the frequency of the main low frequency maximum, $f_{max}$, in the $Z''$, $Z'$- as well as $\log|Z''|$, $\log f$-plots shifts toward lower values at first and the values of $|Z''|$ increase with increase of $c_{K_3[Fe(CN)_6]}$ at given base electrolyte concentration. Thus, the characteristic time constant obtained from experimental data increases with the rise of $c_{K_3[Fe(CN)_6]}$ from $5 \cdot 10^{-6}$ M to

$1 \cdot 10^{-4}$ M. However for more concentrated $K_3[Fe(CN)_6]$ solutions $\tau_{max} = (2\pi f_{max})^{-1}$ decreases with the rise of $c_{K_3[Fe(CN)_6]}$ in solution. This maximum in $\tau_{max}$, $c_{K_3[Fe(CN)_6]}$-dependences can be explained by the suggestion that for more concentrated reactant solutions, in addition to the adsorption limited charge transfer process, the classical Frumkin long-range charge transfer process starts [89, 102, 108]. It should be noted that $j, E$-dependences (Figs. 1 and 2) change in the analogous manner as $\tau_{max}$, i.e. the decrease of $\tau_{max}$ is related to the increase of the current density $j$ at the cathodic potentials. However, it is impossible to determine $\tau_{max}$ for the cathodic process in more concentrated $[Fe(CN)_6]^{3-}$ solutions (Figs. 10a and 10d) at $E \geq -1.2$ V, because there is no maximum in the $\log|Z''|$, $\log f$-plot. However, the data obtained at different $E$ for less concentrated solutions indicate that the time constant has maximum at $-1.15$ V and at potentials close to the diffuse layer minimum potential $E_{min}$ the time constant decreases again, because the electrostatic work term for $[Fe(CN)_6]^{3-}$ transition to the reaction centre depends on the charge density at the Cd(0001) plane [24, 28, 42, 89, 90, 94, 95, 97, 99, 102, 108]. The noticeable dependence of $\tau_{max}$ on the concentration of $[Fe(CN)_6]^{3-}$ anion in solution and the depressed shape of the low frequency region of the $Z''$, $Z'$-semicircles indicate the complicated mixed kinetic behaviour of $[Fe(CN)_6]^{3-}$ electroreduction at the Cd(0001) electrode. Thus, similarly to the KF | Cd(0001) [49] and $Na_2SO_4$| Cd(0001) interface, the characteristic time constant $\tau_{max}$ obtained is not a simple valued quantity [81, 113], but is distributed continuously or discretely around a mean $\tau_{max}$ value and shows that the balance of the various rate-determining processes changes with $c_{K_3[Fe(CN)_6]}$, $c_{KF}$ and electrode potential applied.

The plateaus in $\log Z$, $\log f$-plots (Figs. 10e and 11) indicate that similarly to the base electrolyte system at $E \leq -1.4$ V, there is a slow Faradaic process, however, more quick for more concentrated $[Fe(CN)_6]^{3-}$ solutions (Fig. 10e) compared with dilute reactant + the base electrolyte system. Thus, in addition to the slow cathodic hydrogen evolution process the simultaneous comparatively quick electoreduction of the $[Fe(CN)_6]^{3-}$ as well as $K^+$-$[Fe(CN)_6]^{3-}$ ionpairs takes place and the total polarization resistance decreases with $c_{K_3[Fe(CN)_6]} \geq 1 \cdot 10^{-4}$ M (Fig. 10).

The values of $|Z''|$ at fixed ac frequency and potential are systematically higher (capacitance $C_{edl}$ or CPE constant value $Q$ are lower) compared with the Cd(0001) | base electrolyte system in a good agreement with the data in Fig.5a, where the series capacitance at $E < -1.1$ V systematically decreases with the rise of $c_{K_3[Fe(CN)_6]}$. The constant phase exponent $\alpha \geq 0.92$ obtained from the slope of $\log|Z''|$, $\log f$-plots is practically independent of $c_{K_3[Fe(CN)_6]}$ and nearly the so-called ideal capacitive behaviour can be seen in Figs. 10 and 11, i.e. in the wide potential region $-1.4$ V $< E < -0.95$ V (where the current and potential are out of phase (so-called blocking electrode), and the high frequency asymptote is expressed as $\phi(\infty) = -90°\alpha$ [110]. However, at $E < -1.4$ V (Fig. 11) the phase

angle, $Z$, $Z'$ and $Z''$ values indicate the occurrence of the "true" Faradaic or partial charge transfer process at the Cd(0001) | base el. + $K_3[Fe(CN)_6]$ solution interface in a good agreement with the decrease of the total polarization resistance with the rise of negative polarization and $c_{K_3[Fe(CN)_6]}$. This $R_p$ is maximal at $E = $ -1.15 V in a good agreement with minimal $dj/dE$ values calculated at $E = $ -1.2 V (Fig. 1) [94, 102, 108].

The total experimental series differential capacitance [6, 76–81, 109, 110] can be obtained from the $Z''$, $Z'$-plots, using the relation $Z'' = (j\omega C)^{-1}$. At $f <$ 5 Hz, there is a noticeable increase in Faradaic or adsorption pseudocapacitance with increasing of $c_{K_3[Fe(CN)_6]}$ or $c_{base.el}$ at $E < -1.4$ V, which is caused by electroreduction of the $[Fe(CN)_6]^{3-}$ or $K^+$-$[Fe(CN)_6]^{3-}$ ions, $K^+$ adsorption followed by the partial charge transfer as well as by the slow cathodic hydrogen evolution reactions [36, 49, 90–97, 99, 102, 107, 108]. However, at $E \leq $ -1.1 V the systematic decrease of $C$ at $f \geq 10$ Hz with the rise of $c_{K_3[Fe(CN)_6]}$ in solution has been established, indicating the following strong blocking adsorption of $[Fe(CN)_6]^{3-}$ or reaction intermediates at the Cd(0001) surface [102, 108].
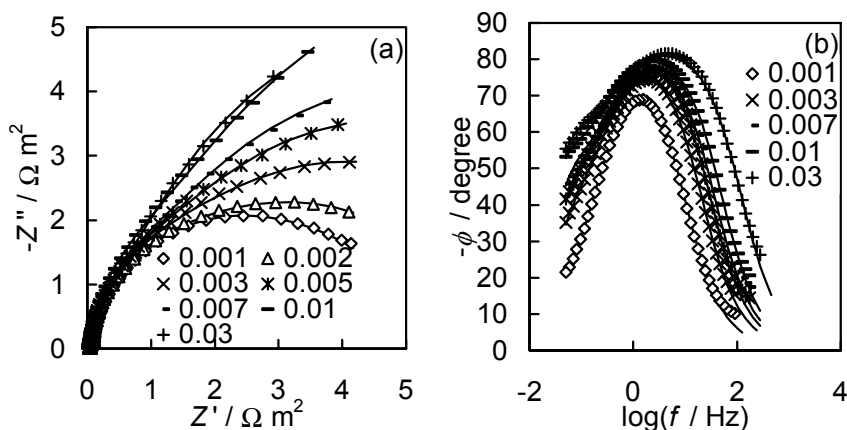


**Figure 12.** $Z'$, $Z''$- (a) and -$\phi$, $f$- (b) plots for the EP Cd(0001) plane in 0.1 mM $K_3[Fe(CN)_6]$ solutions with different additions of KF (M, noted in figure) at $E = -1.0$ V (marks – experimental data, solid lines –calculated data, see text).
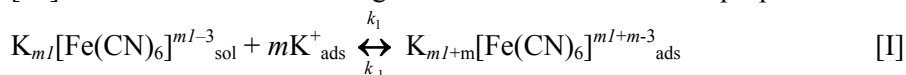
The data in Fig. 12 show the noticeable influence of the base electrolyte concentration, i.e. the electrostatic Frumkin $\psi_1$-effect [24–31, 33, 34, 36, 87–90, 94, 95, 99], on the $[Fe(CN)_6]^{3-}$ electroreduction rate. It is clear that with the increase of KF or $K_2SO_4$ concentration the more pronounced capacitive (i.e. surface blocking) behaviour of the Cd(0001) | base electrolyte + reactant interface can be observed in the region of -1.4 V $< E <$ -0.95 V, caused by the more compact structure of edl (decrease of Debye screening length) and by the decrease of the electrostatic work term needed to transport the reactant anions
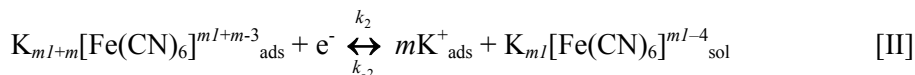
through the diffuse layer into the reaction zone [28, 36, 87–90, 94, 95, 99]. $\tau_{max}$ for the kinetically mixed limited process decreases with the rise of KF at $c_{K_3[Fe(CN)_6]}$ = const, but at $E \geq$ -1.2 V for more concentrated KF solutions it is impossible to obtain the values of $\tau_{max}$ in the region of ac frequencies studied. $\tau_{max}$ is maximal at -1.3 < $E$ < -1.1 V, where the maximal inhibition of electroreduction reaction takes place [94, 102, 108]. At $E$ = -1.2 V it is impossible to obtain $\tau_{max}$ values because $f_{max}$ is lower than ac frequency applied in this study indicating to very slow rate determining process.

Noticeably different behaviour of Cd(0001) surface at $E = -1.6$ V occurs, where the shape of $\phi$, log $f$-plots depends noticeably on $c_{K_3[Fe(CN)_6]}$ and there is a plateau in the $\phi$, log $f$-plots with comparatively low $|\phi|$ values($|\phi|$ < 62°) in the ac frequency region from 3 to 20 Hz. The $|\phi|$ values decrease with the increase of $c_{K_3[Fe(CN)_6]}$, indicating the deviation of mixed kinetic process toward the mainly charge transfer limited process at higher concentrations of the reactant [102, 108]. The phase angle values near zero at low ac frequency ($f$ < $5 \cdot 10^{-2}$ Hz) indicate that the current and the potential are in phase and thus the heterogeneous charge transfer step is a main rate-limiting stage.[6, 76–81, 113, 114] Total polarization resistance $R_p$ decreases as $c_{K_3[Fe(CN)_6]}$ rises if $c_{K_3[Fe(CN)_6]} \geq$ $1 \cdot 10^{-4}$ M in accordance with $j$, $E$-data. Only at very low reactant concentrations $c_{K_3[Fe(CN)_6]}$ < $5 \cdot 10^{-5}$ M the very weak increase of the total polarization resistance at $E \geq$ -1.4 V takes place, caused by the adsorption of the reactant or intermediate species at the Cd(0001) surface [102, 108]. Thus, in comparison with $E$ > -1.4 V the more quick simultaneous electroreduction of $[Fe(CN)_6]^{3-}$, ion-pairs $K^+$-$[Fe(CN)_6]^{3-}$, slow cathodic hydrogen evolution as well as adsorption of the $K^+$ cations with the following partial charge transfer are possible.

The nearly similar dependences of $Z''$, $Z'$-; log $Z$, log $f$-; $\phi$, log $f$-; $Z''$, log $f$- and $Z'$, log $f$-plots have been observed for Cd(0001) | $Na_2S_2O_8$ + $Na_2SO_4$ interface [90], however the surface blocking effect has smaller influence than that for Cd(0001) | $K_3[Fe(CN)_6]$ + KF interface.

*Analysis of fitting data.* – The data is Figs. 5 and 10–12 indicate that the electro-reduction of $[Fe(CN)_6]^{3-}$ is occurring probably through the adsorbed state [12–14, 21, 102, 105, 106, 108, 109, 115, 116] and probably the cationic catalysis at $E$ < -1.4 V is possible [28, 36, 49, 88–90, 94, 95, 99], i.e. the formation of the $K_{ml}[Fe(CN)_6]^{ml-3}$ ion pairs or cationic bridges at the Cd(0001) surface is essential at more negative potentials [13, 14, 21, 89, 94, 102, 108]. Thus, the $K_{ml}[Fe(CN)_6]^{ml-3}$ complex could be viewed as an adsorbed intermediate particle [14] and therefore the following reaction mechanism can be proposed:

$$K_{ml}[Fe(CN)_6]^{ml-3}{}_{sol} + mK^+{}_{ads} \underset{k_{-1}}{\overset{k_1}{\longleftrightarrow}} K_{ml+m}[Fe(CN)_6]^{ml+m-3}{}_{ads} \qquad [I]$$

$$K_{m1+m}[Fe(CN)_6]^{m1+m-3}{}_{ads} + e^- \overset{k_2}{\underset{k_{-2}}{\leftrightarrow}} mK^+{}_{ads} + K_{m1}[Fe(CN)_6]^{m1-4}{}_{sol} \qquad [II]$$

As the negative charge number of the reduced anion is higher than for the reactant, after formation the reaction product is electrostatically repelled from the electrode surface into the solution phase. The $Cd(0001) \mid KF + K_3[Fe(CN)_6]$ interface could be approximated to the here given equivalent circuit (EC) where the resistance of the electrolyte and CPE element have been added to the model of one adsorbing particle [81, 102, 108].
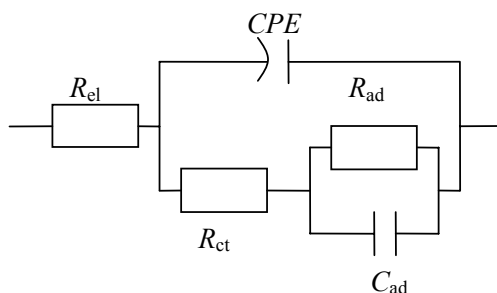


Results of the non-linear regression analysis of the Nyquist; Bode; $\log Z'$, $\log f$- and $\log|Z''|$, $\log f$-plots (solid lines in Figs 10–12) for solutions with $c_{K_3[Fe(CN)_6]} < 1\cdot10^{-4}$ M show that these plots can be simulated by this equivalent circuit very well because there is a very good accordance of experimental and fitted results. The $\chi^2$ function for the circuit has comparatively low values ($\chi^2 < 8\cdot10^{-4}$) and the relative errors of individual parameters obtained are lower than those obtained using other EC discussed in paper [108]. The parameters obtained are given in Figs. 13–15.

According to the fitting results the fractional exponent $\alpha$ has values from 0.92 to 0.95 depending slightly on $E$ and $c_{K_3[Fe(CN)_6]}$ in a good agreement with $\alpha$ values obtained from the slope of $\log|Z''|$, $\log f$-plots. The $Q$ values (Fig. 13a) obtained for solutions with different additions of $[Fe(CN)_6]^{3-}$ have reasonable values. At $E > -1.6$ V, the values of $Q$ for the $[Fe(CN)_6]^{3-}$ containing solutions are systematically lower than those for the pure base electrolyte, which points to the surface blocking effect of the Cd(0001) electrode surface in the solutions with addition of the $[Fe(CN)_6]^{3-}$ anions [102, 108]. $Q$ starts to increase in the region of $E_{min}$ if $c_{K_3[Fe(CN)_6]} > 2\cdot10^{-4}$ M, thus if the diffuseness of the edl decreases and the weak specific adsorption of the electrolyte starts. In the case of more concentrated solutions $Q$ is minimal at $E_{min} = -1.00$ V, which is in a good agreement with experimental series capacitance data at fixed ac frequency presented in Fig. 5.
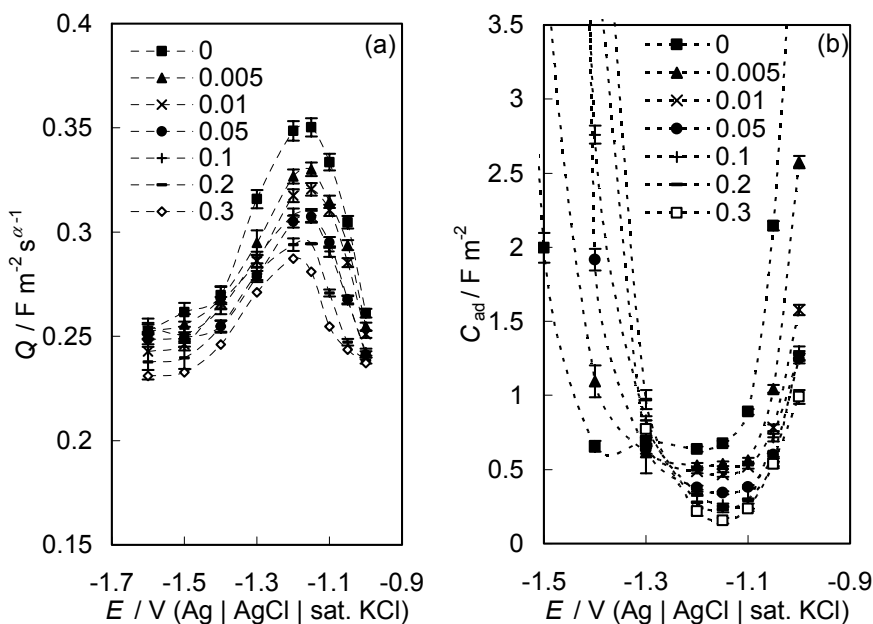
**Figure 13.** Dependences of CPE constant $Q$ (a) and adsorption capacitance (b) on the electrode potential for the EP Cd(0001) plane in 0.002 M KF solution with different additions of $K_3[Fe(CN)_6]$ (mM, noted in figure).

Adsorption capacitance (Fig. 13b) has somewhat higher values than $Q$ at potentials $E < -1.3$ V, thus, the weak non-blocking adsorption of the cations or cationic complexes is possible [102, 108]. In the region of potentials from -1.3 to -1.0 V, $C_{ad}$ decreases with $c_{K_3[Fe(CN)_6]}$, which indicates the weak blocking adsorption of the $[Fe(CN)_6]^{3-}$ ions or $K_{ml}[Fe(CN)_6]^{ml-3}$ ion-pairs [89, 90], caused by the squeezing out effect of big anions from the bulk solution by the $F^-$ anions. In the case of higher concentrations of $[Fe(CN)_6]^{3-}$ and at $E > -1.3$ V, the surface blocking is very probable as the very low values of $C_{ad}$ have been obtained compared with the adsorption capacitance obtained at -1.5 V to -1.3 V [102, 108]. The decrease of adsorption capacitance at slightly negatively charged surface has been established for other anions ($I^-$, $Br^-$) adsorbing at the Cd(0001) plane from solutions with $I =$ const [93]. However, at $E > -1.1$ V the noticeable increase of the $C_{ad}$ can be seen, which is connected to the occurring of the Faradaic oxidation reaction of surface or formation covalent bond between adsorbed $[Fe(CN)_6]^{3-}$ and Cd(0001) surface with a noticeable capacitive component. In the more concentrated KF solutions, $C_{ad}$ has maximum within the potential region from -1.5 to -1.3 V (not shown in Fig. 13b) [94, 102, 108].
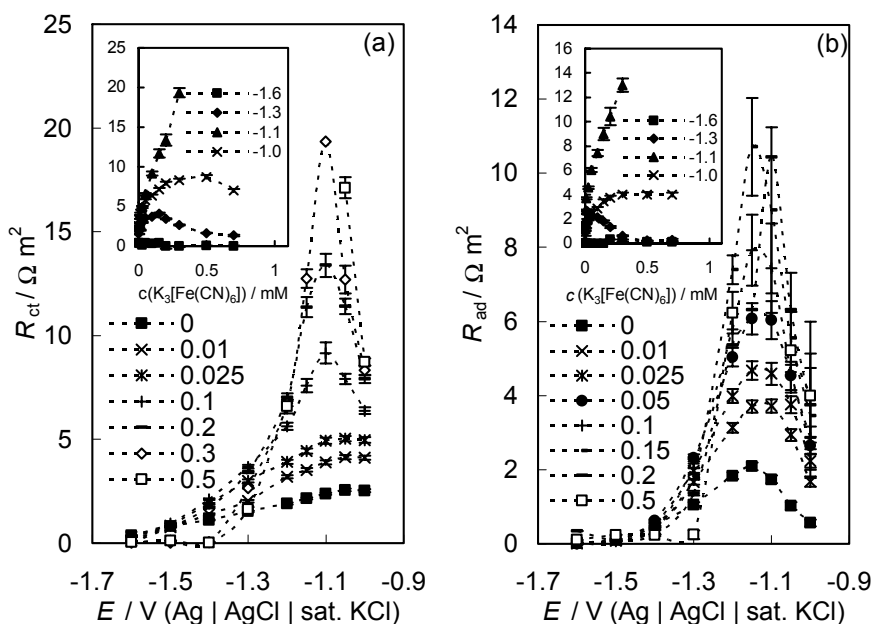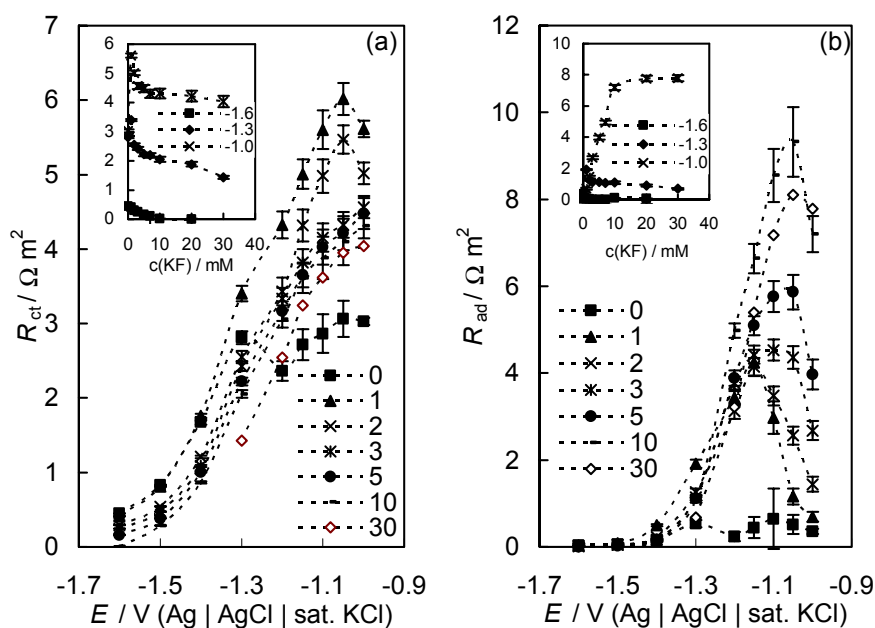
**Figure 14.** Dependences of charge transfer resistance (a) and adsorption resistance (b) on the electrode potential for the EP Cd(0001) plane in 0.002 M KF solution with different additions of $K_3[Fe(CN)_6]$ (mM, noted in figure). Insets: Dependences of $R_{ct}$ (a) and $R_{ad}$ (b) on the concentration of the surface-active anion at different $E$ (V, noted in figure).

The charge transfer and adsorption resistances depend noticeably on $c_{K_3[Fe(CN)_6]}$ and $c_{base.el}$ as well as on the electrode potential applied (Figs. 14 and 15). In the case of fixed solution composition, the charge transfer and adsorption resistances increase nearly exponentially with decreasing the negative potential in the region of potentials from $-1.6$ to $-1.1$ V. The maximum in the $R_{ct}$, $E$- and $R_{ad}$, $E$-dependences appears at $-1.15$ V, where the maximal increase in the electrostatic work term takes place [28, 36, 49, 88–90, 94, 95, 99, 102, 108]. In the region of peaks in the $R_{ct}$, $E$-curves the data for more concentrated $[Fe(CN)_6]^{3-}$ solutions can not be fitted because the $R_{ct}$ value approaches to infinity in the relatively dilute $[Fe(CN)_6]^{3-}$ solutions already. At $E < -1.2$ V the charge transfer resistance decreases as $c_{K_3[Fe(CN)_6]} > 1 \cdot 10^{-4}$ M

rises, thus in the analogous way as the current density for standing electrode [94]. Thus, at these conditions the new reaction pathways (in addition to the traditional Frumkin long-range charge transfer mechanism direct charge transfer through the adsorption state) are simultaneously possible [102, 108]. At $E = -1.0$ V the charge transfer and adsorption resistances tend to the constant value at higher reactant concentrations. Thus, the surface is probably partly blocked

by the specifically adsorbed $[Fe(CN)_6]^{3-}$ or reaction intermediates at $E > -1.1$ V. In the region of very pronounced increase of the electrostatic work term at $-1.1 < E < -0.95$ V (where $|d\psi_1/dE|$ is maximal) [28, 36, 49, 88–90, 94, 95, 99, 102, 108] the noticeable increase of the adsorption resistance has been observed, rising with the reactant concentration (Fig. 14b). Thus, the adsorption resistance has maximum values just before the region of the so-called current pits in the $j, E$-curves, which have been observed using the rotating disc electrode method [94]. At $E < -1.5$ V the value of $R_{ad}$ lower than 0.1 $\Omega$ m$^2$ has been established, which corresponds to the very quick adsorption of the K$^+$ ions as well as K$_{ml}$[Fe(CN)$_6$]$^{ml-3}$ ion pairs at the Cd(0001) electrode and the following electroreduction process at the Cd(0001) surface.



**Figure 15.** Dependences of charge transfer resistance (a) and adsorption resistances (b) on the electrode potential for the EP Cd(0001) plane in $1 \times 10^{-4}$ M K$_3$[Fe(CN)$_6$] solutions with different additions of KF (mM, noted in figure). Insets: Dependences of $R_{ct}$ (a) and $R_{ad}$ (b) on the concentration of the surface-active anion at different $E$ (V, noted in figure).

At constant $c_{K_3[Fe(CN)_6]}$ the charge transfer resistance is inversely proportional to $c_{base.el}$ (inset in Fig. 15a) and nearly exponentially decreases with increasing the negative electrode potential (Fig. 15a). Thus, $R_{ct}$ depends on thickness of the diffuse layer, i.e. on the $\psi_1$ potential at the Cd(0001) electrode surface and on the concentration of cations, $c_{K^+}$. The adsorption resistance $R_{ad}$ (inset in Fig. 15b) decreases with the rise of c$_{base.el}$ in the region of potentials from $-1.6$ to

−1.15 V and approaches to the nearly constant value at higher $c_{base.el}$ ($> 1 \cdot 10^{-2}$ M) [102, 108]. At $E = -1.1$ V, $R_{ad}$ increases with the rise of $c_{base.el}$, indicating to the blocking adsorption of $[Fe(CN)_6]^{3-}$ or $K_{ml}[Fe(CN)_6]^{ml-3}$ ion pairs at the Cd(0001) electrode at small negative surface charge densities ($|q| \leq 0.2$ C m$^{-2}$).

The values of the adsorption capacitance and resistance give only indirect information about the mechanism of the reaction and therefore the parameters $A$, $B$ and $C$ have been calculated using Eqs. 4.4.18–20, respectively [96, 102, 108]. As $c_{K_3[Fe(CN)_6]}$ increases the parameter $A$ increases at $E < -1.5$ V, i.e. the surface coverage $\theta$ increases as $-\alpha_1 \overrightarrow{k_1} - (1-\alpha_2)\overleftarrow{k_{-2}} + (1-\alpha_1)\overleftarrow{k_{-1}} + \alpha_2 \overrightarrow{k_2} > 0$. At $E > -1.2$ V the parameter $A$ increases until it becomes constant at $c_{K_3[Fe(CN)_6]} > 3 \cdot 10^{-4}$ M, thus probably corresponding to the condition where the surface coverage $\theta \rightarrow$ const. At intermediate $K_3[Fe(CN)_6]$ concentrations and electrode potentials from $-1.4$ to $-1.3$ V the parameter $A$ goes through the minimum [102, 108]. The addition of KF into the $1 \cdot 10^{-4}$ M $[Fe(CN)_6]^{3-}$ solution causes the increase in $A$ (if the value of $\theta$ rises) with the decrease of the thickness of the diffuse layer and the surface activity of $[Fe(CN)_6]^{3-}$ increases in a good agreement with the data for other anions adsorption at Bi(hkl) and Cd(0001) [91–93, 96, 97]. Thus, at these conditions the Frumkin correction depends on the edl thickness (i.e. Debye screening length) and Gibbs adsorption value of the $[Fe(CN)_6]^{3-}$ anions or $K_{ml}[Fe(CN)_6]^{ml-3}$ ion pairs at the Cd(0001) surface. The parameter $|B|$ in Eq. 4.4.19 changes in the analogous manner as parameter $A$. If $c_{KF} < 3 \cdot 10^{-2}$ M and $c_{K_3[Fe(CN)_6]} < 3 \cdot 10^{-4}$ M at $-1.4 < E < -1.0$ V then the parameter $C$ in Eq. 4.4.20 could be considered to be independent of $c_{KF}$ and $c_{K_3[Fe(CN)_6]}$, indicating the constancy of $(\overrightarrow{k_1} + \overleftarrow{k_{-1}} + \overrightarrow{k_2} + \overleftarrow{k_{-2}})/\Gamma_{max}$ at Cd(0001)| $K_3[Fe(CN)_6]$ + KF aqueous. The same conclusion has been made by Damaskin et al [21] for the Hg|$[Fe(CN)_6]^{3-}$ interface too.

The results obtained indicate that the adsorption of $[Fe(CN)_6]^{3-}$ or reaction intermediates of electroreduction process, $K_{ml}[Fe(CN)_6]^{ml-3}$, and base electrolyte ions is possible. The strong inhibition of the very slow Faradaic process occurring in the pure base electrolyte solution with the addition of $K_3[Fe(CN)_6]$ into the solution demonstrates that the Faradaic processes are strongly influenced by the adsorption processes and therefore mainly the same surface sites (active centres) are used for the occurring of various adsorption and simultaneous charge transfer reactions (hydrogen evolution, electroreduction of $[Fe(CN)_6]^{3-}$, electroreduction of $K^+$-$[Fe(CN)_6]^{3-}$ complex, electroreduction of $K^+$, $H_2O$ decomposition (only if $E < -1.6$ V)). Taking into account that there is only one low frequency semi-circle in $Z''$, $Z'$-plot (as well as one maximum at $|Z|$, log$f$- and $|\phi|$, log$f$-plots), therefore these parallel processes have very similar time constants and have to be viewed as conjugated

processes, not very well separated ones. Analysis of ac impedance spectroscopy data gives only the complex charge transfer parameters for the total cathodic complex electroreduction reaction (interrelated with each other). Therefore the in situ FTIR, second harmonic generation and in situ Raman spectroscopy data are inevitable for the more detailed analysis of simultaneous reactions in progress in our laboratory.

# 7. CONCLUSIONS

Electrochemical reduction of the hexacyanoferrate(III) anions on the electro-chemically polished Cd(0001) plane has been studied by the linear sweep, rotating disc electrode voltammetry, constant ionic strength and impedance spectroscopy methods.

The rate of electroreduction of the $[Fe(CN)_6]^{3-}$ anion depends on the potential of the Cd(0001) electrode, as well as on concentrations of the base electrolyte and $K_3[Fe(CN)_6]$. According to the rotating disc electrode voltammetry the electroreduction of the $[Fe(CN)_6]^{3-}$ anion in the region of zero charge potential is limited mainly by the rate of diffusion of the $[Fe(CN)_6]^{3-}$ anions to the Cd(0001) surface. Diffusion coefficient values ($7 \cdot 10^{-6}$ cm$^2$s$^{-1}$ for $1 \cdot 10^{-2}$ M KF) obtained from the linear Levich plots were in a reasonable agreement with the literature data [24]. The inhibition of the $[Fe(CN)_6]^{3-}$ anion electroreduction takes place in the region of small negative surface charge densities, this is explained by the $\psi_1$ potential effect as well as by the adsorption of reactant and reaction intermediates at Cd(0001) surface. At more negative surface charge densities the acceleration of $[Fe(CN)_6]^{3-}$ anion electroreduction is explained by diminishing of the $\psi_1$ potential effect since at negative potentials far from the zero charge potential the value of $d\psi_1/dE$ is approximately constant; and also by weak specific adsorption of the $K^+$ cations on the electrochemically polished Cd(0001) surface at $q \leq -14$ μC cm$^{-2}$. The cationic catalysis can take place at $E < -1.5$ V.

The apparent rate constant values $k_{het}$ were calculated using the kinetic current densities $j_k$ obtained from the linear Koutecký–Levich plots. The corrected Tafel plots for the electroreduction of the $[Fe(CN)_6]^{3-}$ on the Cd(0001) electrode, using the classical diffuse layer potential values obtained according to the Gouy–Chapman theory, were calculated. At higher cathodic polarization ($E$ - $\psi_0 \leq$ -1.2 V) the corrected Tafel plots for the electrochemically polished Cd(0001) electrodes are linear with the slope corresponding to the apparent transfer coefficient $\alpha_{app} \approx 0.35$. At smaller negative surface charge densities the corrected Tafel plots are non-linear and there is noticeable decrease of corrected current density values with the rise of $c_{KF}$. The values of $\alpha_{app}$ obtained for $[Fe(CN)_6]^{3-}$ electroreduction are noticeably higher than $\alpha_{app}$ calculated for Cd(0001) | $Na_2S_2O_8$ + NaF interface where nearly activationless charge transfer takes place [99].

It was found that near the zero charge potential the $[Fe(CN)_6]^{4-}$ and $[Fe(CN)_6]^{3-}$ anions adsorb specifically. The adsorption activity of polyvalent anions increases from $[Fe(CN)_6]^{4-}$ to $[Fe(CN)_6]^{3-}$ as the negative charge number of the anion and the solvation energy decrease. The inner layer structure depends on the anion adsorbed at the Cd(0001) surface as well as on the surface

charge density applied. The Gibbs adsorption energy for $[Fe(CN)_6]^{3-}$ anions is comparable with $Br^-$ anions at the Cd(0001) plane [93].

It can be concluded from the analysis of the experimental impedance data, that the rate determining steps at potentials −1.4 to −1.2 V, where the current pits have been observed in the current density versus electrode potential plots for the rotating Cd(0001) electrode, are slow adsorption of reactant anions and/or co-adsorption processes of the cations and ion-pairs (reaction intermediate) and the following electroreduction process in parallel to the "true" long-range Frumkin charge transfer process. In the case of more concentrated electrolyte solutions at potentials more negative than −1.4 V mixed kinetics (slow charge transfer and adsorption steps) was observed. The dependence of the fitted parameters on concentrations of the hexacyanoferrate(III) anions and base electrolyte indicates clearly that the mixed kinetic process of the $[Fe(CN)_6]^{3-}$ electroreduction at the electrochemically polished Cd(0001) electrode occures. The weak specific adsorption of the $[Fe(CN)_6]^{3-}$ anions or $K^+$-$[Fe(CN)_6]^{3-}$ ion pairs is in a agreement with the diffuse layer minimum potential and adsorption capacitance dependence on the reactant concentration.

The shape of the complex plane, phase angle, total impedance, and imaginary and real parts of the impedance demonstrate that the electroreduction of $[Fe(CN)_6]^{3-}$ or ionic complex is not limited by the classical semi infinite diffusion step at the standing electrode. The rate of electroreduction reaction increases with the increase of the base electrolyte concentration, i.e. with decreasing the electrostatic work and $\psi_1$-potential influence that is in a good agreement with the classical Frumkin conception. The charge transfer resistance decreases nearly exponentially with the rise of the negative electrode potential that is in a agreement with the slow charge transfer theory. However the increase of base electrolyte concentration shifts the process from the mixed kinetic (mainly adsorption limited) towards purely adsorption limitation (toward the totally blocked electrode).

# 8. REFERENCES

[1]     W.R. Fawcett, in J. Lipkowski, P.N. Ross (Eds.), Electrocatalysis, Wiley, New York, 1998 (Chapter 8).

[2]     W.R. Fawcett, M. Hromadova, G.A. Tsirlina, R.R. Nazmutdinov, J. Electroanal. Chem. 498 (2001) 93.

[3]     M.J. Weaver, F.C. Anson, J. Am. Chem. Soc. 97 (1975) 4403.

[4]     A. Hamelin, M.J. Weaver, J. Electroanal. Chem. 209 (1986) 109.

[5]     A. Hamelin, M.J. Weaver, J. Electroanal. Chem. 223 (1987) 171.

[6]     G.J. Brug, M. Sluyters-Rehbach, J.H. Sluyters, A. Hamelin, J. Electroanal. Chem. 181 (1984) 245.

[7]     J. Peres, E.R. Gonzalez, H.M. Villullas, J. Phys. Chem. B 102 (1998) 10931.

[8]     Z. Samec, A.M. Bittner, K. Doblhofer, J. Electroanal. Chem. 432 (1997) 205.

[9]     W. Fawcett, M. Fedurco, Z. Ková čova, J. Electrochem. Soc. 141 (1994) L30.

[10]    M. Hromadová, W.R. Fawcett, J. Phys. Chem. A 104 (2000) 4356.

[11]    G.A. Tsirlina, N.V. Titov, R.R. Nazmutdinov, O.A. Petrii, Elektrokhimiya 37 (2001) 21.

[12]    F. Kitamura, N. Nanbu, T. Ohsaka, K. Tokuda, J. Electroanal. Chem. 456 (1998) 113.

[13]    L.M. Peter, W. Dürr, P. Bindra, H. Gerischer, J. Electroanal. Chem. 71 (1976) 31.

[14]    S.A. Campbell, L.M. Peter, J. Electroanal. Chem. 364 (1994) 257.

[15]    P. Kulesza, T. Jędral, Z. Galus, J. Electroanal. Chem. 109 (1980) 141.

[16]    A. Więckowski, M. Szklarczyk, J. Electroanal. Chem. 142 (1982) 157.

[17]    J. Kawiak, T. Jędral, Z. Galus, J. Electroanal. Chem. 145 (1983) 163.

[18]    J. Kawiak, P.J. Kulesza, J.E.C. Z. Galus, J. Electroanal. Chem. 226 (1987) 305.

[19]    C. Beriet, J.E.C. D. Pletcher, J. Electroanal. Chem. 361 (1993) 93.

[20]    C. Lee, F.C. Anson, J. Electroanal. Chem. 323 (1992) 381.

[21]    B.B. Damaskin, J.V. Stenina, O.A. Baturina, L.N. Sviridova, Elektrokhimiya 34 (1998) 1083.

[22]    D.E. Khoshtariya, T.D. Dolidze, D. Krulic, N. Fatouros, P. Devilliers, J. Phys. Chem. B 102 (1998) 7800.

[23]    V. Mareček, Z. Samec, J. Weber, J. Electroanal. Chem. 94 (1978) 169.

[24]    O.A. Petrii, N.V. Nikolaeva–Fedorovich, Zhurn. Fis. Khim. 35 (1961) 1999.

[25]    A.N. Frumkin, G.M. Florianovich, Dokl. Akad. Nauk USSR 80 (1951) 907.

[26]    A.N. Frumkin, O.A. Petrii, N.V. Nikolaeva–Fedorovich, Dokl. Akad. Nauk. USSR 128 (1959) 1006.

[27]    A.N. Frumkin, in P. Delahay (Ed.), Adv. Electrochem., Vol. 1, Intersci. Publ., NY, 1961, p. 65.

[28]    A.N. Frumkin, Z. Elektrochem 59 (1955) 807.

[29]    A.N. Frumkin, Z. Phys. Chem. 164 (1933) 121.

[30]    B.B. Damaskin, O.A. Petrii, Vvedenie v elektrokhimicheskuyu kinetiku, Moscow, 1975.

[31]    B.B. Damaskin, Praktikum po elektrokhimii, Vysshaya shkola, Moscow, 1991.

[32]    N.V. Fedorovich, Reports in Science and Technology, Vol. 14, Viniti, Moscow, 1979, p. 5 (in Russian).

[33] E. Gileadi, Electrode Kinetics for Chemist, Chemical Engineers and Material Scientists, VCH Publishers, Inc, New York, Weinheim, Cambridge, 1993.

[34] B.B. Damaskin, N.V. Fedorovich, Zh. Fiz. Khim. 36 (1962) 1483.

[35] K. Asada, P. Delahay, A. Sundaram, J. Am. Chem. Soc. 83 (1961) 3396.

[36] E. Lust, R. Truu, K. Lust, J. Russ. Electrochem. 36 (2000) 1195.

[37] R. Jäger, E. Härk, P. Möller, J. Nerut, K. Lust, E. Lust, J. Electroanal. Chem. 566 (2004) 217.

[38] W. Nernst, Z. Phys. Chem. 47 (1904) 52.

[39] V.G. Levich, Fiziko-khimicheskaya gidrodinamika, Fizmatgiz, Moscow, 1959.

[40] Y.V. Pleskov, V.Y. Filonovskiy, Vrashchayushchiisya diskovyi elektrod, Nauka, Moscow, 1972.

[41] R. Parsons, Surf. Sci. 2 (1964) 418.

[42] A.N. Frumkin, N.V. Nikolaeva-Fedorovich, N.P. Berezina, H.E. Keis, J. Electroanal. Chem. 58 (1975) 189.

[43] S. Trasatti, in H. Gerisher, C.W. Tobias (Eds.), Adv. in Electrochem. and Electrochem. Eng., Vol. 19, Wiley, NY, 1977, p. 297.

[44] R.R. Nazmutdinov, G.A. Tsirlina, Y.I. Kharkats, O.A. Petrii, M. Probst, J. Phys. Chem. B 102 (1998) 677.

[45] G.A. Tsirlina, Y.I. Kharkats, R.R. Nazmutdinov, O.A. Petrii, Russ. J. Electrochem. 35 (1999) 23.

[46] G.A. Tsirlina, O.A. Petrii, Y.I. Kharkats, A.M. Kuznetsov, Russ. J. Electrochem. 35 (1999) 1210.

[47] R.R. Nazmutdinov, I.V. Pobelov, G.A. Tsirlina, O.A. Petrii, J. Electroanal. Chem. 491 (2000) 126.

[48] I.V. Pobelov, G.A. Tsirlina, M.I. Borzenko, O.A. Petrii, Russ. J. Electrochem. 37 (2001) 270.

[49] T. Thomberg, E. Lust, J. Electroanal. Chem. 485 (2000) 89.

[50] Z. Samec, J. Electroanal. Chem. 146 (1995) 3349.

[51] H.D. Hurwitz, J. Electroanal. Chem. 10 (1965) 35.

[52] E. Dutkiewicz, R. Parsons, J. Electroanal. Chem. 11 (1966) 100.

[53] R. Parsons, in J.O.M. Bockris, B.E. Conway, E. Yeager (Eds.), Comprehensive Treatise of Electrochemistry, Vol. 1, Plenum Press, New York, CR. 1, p. 1.

[54] M.D. Levi, A.V. Shlepakov, B.B. Damaskin, I.A. Bagotskaya, J. Electroanal. Chem. 138 (1982) 1.

[55] U.V. Palm, B.B. Damaskin, Itogi nauki i tekhniki. Elektrokhimiya 12 (1979) 99.

[56] D.C. Grahame, R. Parsons, J. Am. Chem. Soc. 83 (1961) 1291.

[57] J.M. Parry, R. Parsons, Trans Faraday Soc. 59 (1963) 24 1.

[58] Y.A. Alekseev, Y.A. Popov, Y.M. Kolotyrkin, J. Electroanal. Chem. 62 (1975) 135.

[59] B. Damaskin, S. Karpov, S. Dyatkina, U. Palm, M. Salve, J. Electroanal. Chem. 189 (1985) 183.

[60] B. Damaskin, I. Pankratova, U. Palm, K. Anni, M. Väätnõu, M. Salve, J. Electroanal. Chem. 234 (1987) 31.

[61] B. Damaskin, U. Palm, M. Salve, J. Electroanal. Chem. 218 (1987) 65.

[62] M.A. Vorotyntsev, J. Res. Inst. Catalysis, Hokkaido Univ. 30 (1982) 167.

[63] M.A. Vorotyntsev, K. Golub, Elektrokhimiya 29 (1984) 256.

[64] A.V. Scheglov, M.A. Vorotyntsev, B.B. Damaskin, R.V. Ivanova, Elektrokhimiya 21 (1985) 1262.

[65] M.A. Vorotyntsev, Itogi nauki i tekhniki. Elektrokhimiya 26 (1988) 3.

[66] C.V. D'Alkaine, E. Conzalez, R. Parsons, J. Electroanal. Chem. 32 (1971) 57.

[67] B. Damaskin, U. Palm, E. Petyarv, M. Salve, J. Electroanal. Chem. 11 (1966) 100.

[68] B. Damaskin, U. Palm, M. Salve, J. Electroanal. Chem. 209 (1986) 233.

[69] B. Damaskin, U. Palm, Väärtnõu, J. Electroanal. Chem. 70 (1976) 103.

[70] D.C. Grahame, J. Am. Chem. Soc. 80 (1958) 4201.

[71] R. Parsons, Trans. Faraday Soc. 51 (1955) 1518.

[72] G. Valette, A. Hamelin, R. Parsons, Z. Phys. Chem. Neue Folge 113 (1978) 71.

[73] Z. Chi, J. Lipkowski, J. Electroanal. Chem. 403 (1996) 225.

[74] Z. Chi, J. Lipkowski, S. Mirwald, B. Pettinger, J. Chem. Soc. Faraday Trans. 92 (1996) 3737.

[75] K. Bange, B. Straehler, J.K. Sass, R. Parsons, J. Electroanal.Chem. 229 (1987) 87.

[76] M. Sluyters-Rehbach, in A. Bard (Ed.), Electroanalytical Chemistry, Vol. 4, Marcel Dekker, New York, 1970, p. 1.

[77] R.D. Armstrong, M. Henderson, J. Electroanal. Chem. 39 (1972) 81.

[78] M. Sluyters-Rehbach, J.H. Sluyters, in E. Yeager, J.O.M. Bockris, B.E. Conway, S. Sarangapani (Eds.), Comprehensive Treatise of Electrochem, Vol. 9, Plenum Press, New York, 1984, p. 177.

[79] I.D. Raistrick, J.R. MacDonald, D.R. Franceschetti, in J.R. MacDonald (Ed.), Impedance Spectroscopy, Wiley, New York, 1987.

[80] M. Sluyters-Rehbach, Pure Appl. Chem. 66 (1994) 1831.

[81] A. Lasia, in B.E. Conway, J.O.M. Bockris, R.E. White (Eds.), Modern Aspects of Electrochemistry, Vol. 32, Kluwer Academic/Plenum Publishers, New York, 1999, p. 143.

[82] J. Barber, S. Morin, B.E. Conway, J. Electroanal. Chem. 446 (1998) 125.

[83] C. Deslouis, I. Epelboin, M. Keddam, J.C. Lestrade, J. Electroanal. Chem. 28 (1970) 57.

[84] J.S. Chen, J.-P. Diard, R. Durand, C. Montella, J. Electroanal. Chem. 406 (1996) 1.

[85] L. Bai, D.A. Harrington, B.E. Conway, Electrochim. Acta 32 (1987) 1713.

[86] B. Breyer, H.H. Bauer, in P.J. Elving, I.M. Kolthoff (Eds.), Alternating Current Polarography and Tensammetry, Chemical Analysis Series, Vol. 13, Wiley-Interscience, New York, 1963.

[87] O.A. Petrii, A.N. Frumkin, Dokl. Akad. Nauk SSSR 146 (1962) 1121.

[88] A.N. Frumkin, O.A. Petrii, Dokl. Akad. Nauk SSSR 147 (1962) 418.

[89] A.N. Frumkin, Elektrodnye Protsessy (The Electrode Processes), Nauka, Moscow, 1987.

[90] T. Thomberg, J. Nerut, E. Lust, J. Electroanal. Chem. 586 (2006) 237.

[91] E. Lust, A. Jänes, K. Lust, M. Väärtnõu, Electrochim. Acta 42 (1997) 771.

[92] K. Lust, M. Väärtnõu, E. Lust, Electrochim. Acta 45 (2000) 353.

[93] R.R. Nazmutdinov, T.T. Zinkicheva, M. Probst, K. Lust, E. Lust, Surf. Sci. 577 (2005) 112.

[94] J. Nerut, P. Möller, E. Lust, Electrochim. Acta 49 (2004) 1597.

[95]   T. Thomberg, J. Nerut, E. Lust, Electrochim. Acta 49 (2004) 1271.
[96]   E. Lust, K. Lust, A. Jänes, J. Electroanal. Chem. 413 (1996) 111.
[97]   E. Lust, in A.J. Bard, M. Stratman (Eds.), Encyclopedia of Electrochemistry, Wiley, New York, 2002, p. 188.
[98]   R. Gonzalez, F. Sanz, Electroanalysis 9 (1997) 169
[99]   T. Thomberg, J. Nerut, R. Jäger, P. Möller, K. Lust, E. Lust, J. Electroanal. Chem. 582 (2005) 130.
[100]  T. Wandlowski, J.X. Wang, B.M. Ocko, J. Electroanal. Chem. 500 (2001) 418.
[101]  B.B. Damaskin, N.S. Polyanovskaya, Elektrokhimiya 21 (1985) 45.
[102]  E. Lust, J. Nerut, E. Härk, R. Jäger, K. Lust, K. Tähnas, ECS Trans. 1 (17) (2006) 9.
[103]  J. Nerut, K. Lust, E. Lust, J. Electroanal. Chem. D-06–00250R2 (2007) in review.
[104]  J.W. Schultze, K.J. Vetter, J. Electroanal. Chem. 44 (1973) 63.
[105]  P.K. Sukla, M.E. Orazem, G. Nelissen, Electrochim. Acta 51 (2006) 1514.
[106]  M.E. Orazem, M. Durbha, C. Deslouis, H. Takenouti, B. Tribollet, Electrochim. Acta 44 (1999) 4403.
[107]  K. Lust, M. Väärtnõu, E. Lust, J. Electroanal. Chem. 532 (2002) 303.
[108]  J. Nerut, K. Lust, E. Lust, J. Electrochem. Soc. (2007) Submitted.
[109]  S.B. Emery, J.L. Hubbley, D. Roy, Electrochim. Acta 50 (2005) 5659.
[110]  M.E. Orazem, N. Pebere, B. Tribollet, J. Electrochem. Soc. 153 (2006) B129.
[111]  P. Zoltowski, J. Electroanal. Chem. 443 (1998) 149.
[112]  Z. Kerner, T. Pajkossy, J. Electroanal. Chem. 448 (1998) 139.
[113]  B. Barsoukov, J.R. Macdonald, Impedance spectroscopy, Wiley, Hoboken, New Jersey, 2005.
[114]  D. Johnson, ZView for Windows (Version 2.3) fitting program  Scribner Inc.
[115]  C.M. Pharr, P.R. Griffiths, Anal. Chem. 69 (1997) 4665.
[116]  C.M. Pharr, P.R. Griffiths, Anal. Chem. 69 (1997) 4673.

15

# 9. SUMMARY IN ESTONIAN

## Heksatsüanoferraat(III) aniooni redutseerimine kaadmium (0001) monokristalli tahul

Heksatsüanoferraat(III) anioonide redutseerimise uurimiseks elektrokeemiliselt poleeritud Cd(0001) elektroodil kasutati tsüklilist voltamperomeetriat kombineerituna pöörleva ketaselektroodi metoodikaga ning konstantse ioonse jõu ja impedantsspektroskoopia meetodeid.

$[Fe(CN)_6]^{3-}$ anioonide redutseerumine sõltub Cd(0001) elektroodi potentsiaalist ning foonelektrolüüdi ja $K_3[Fe(CN)_6]$ kontsentratsioonidest. Pöörleva ketaselektroodi andmete järgi on elektroodi null-laengupotentsiaali alas $[Fe(CN)_6]^{3-}$ aniooni redutseerumise kiirus limiteeritud peamiselt $[Fe(CN)_6]^{3-}$ anioonide difusiooniga Cd(0001) pinnale. Fikseeritud potentsiaalidel konstrueeritud Levich'i sõltuvustest leitud difusioonikoefitsientide väärtused ($7 \cdot 10^{-6}$ cm$^2$s$^{-1}$ $1 \cdot 10^{-2}$ M KF vesilahuses) on heas kooskõlas kirjanduses toodutega [24]. Väikestel negatiivsetel pinnalaengutel $[Fe(CN)_6]^{3-}$ aniooni redutseerumise kiirus pidurdub, mille põhjuseks on $\psi_1$-potentsiaali järsk muutus, kuid ka $[Fe(CN)_6]^{3-}$ anioonide ja vaheproduktide adsorptsioon Cd(0001) pinnal. $[Fe(CN)_6]^{3-}$ aniooni redutseerumise kiirenemine kõrgematel negatiivsetel pinnalaengutel on seletatav nii $\psi_1$-potentsiaali osatähtsuse vähenemisega (sest kui $E \ll E_{q=0}$, siis $d\psi_1/dE \approx const$), kui ka K$^+$ ioonide nõrga spetsiifilise adsorptsiooniga elektrokeemiliselt poleeritud Cd(0001) monokristalli tahul, kui $q \leq -14$ µC cm$^{-2}$. Katoodsetel potentsiaalidel $E < -1.5$ V võib toimuda katioonne katalüüs.

Heterogeense reaktsiooni kiiruskonstandi $k_{het}$ väärtused arvutati Koutecký–Levich'i meetodil leitud kineetilistest voolutihedustest. Konstrueeriti parandatud Tafeli sõltuvused $[Fe(CN)_6]^{3-}$ redutseerumisprotsessile elektrokeemiliselt poleeritud Cd(0001) elektroodil, kasutades klassikalisi difuusse kihi potentsiaali väärtusi, mis arvutati lähtudes Gouy-Chapmani teooriast. Kõrgematel katoodsetel potentsiaalidel ($E - \psi_0 \leq -1.2$ V) saavutati parandatud Tafeli sõltuvuste kokkulangevus Cd(0001) elektroodil. Parandatud Tafeli sirge tõusule vastav ülekandekoefitsient oli $\alpha_{app} \approx 0.35$. Väikestel negatiivsetel pinnalaengutel osutusid parandatud Tafeli sõltuvused mittelineaarseteks ning foonelektrolüüdi kontsentratsiooni kasvades parandatud voolutihedused langesid märgatavalt. $[Fe(CN)_6]^{3-}$ redutseerumise $\alpha_{app}$ väärtused olid oluliselt suuremad kui Cd(0001) | Na$_2$S$_2$O$_8$ + NaF piirpinna jaoks leitud $\alpha_{app}$, kus toimub ligilähedaselt aktivatsiooni energiata laenguülekanne [99].

Null-laengupotentsiaali lähedases alas adsorbeeruvad $[Fe(CN)_6]^{3-}$ ja $[Fe(CN)_6]^{4-}$ spetsiifiliselt. Polüvalentsete anioonide adsorptsiooniline aktiivsus kasvab üleminekul $[Fe(CN)_6]^{4-}$ anioonilt $[Fe(CN)_6]^{3-}$ anioonile, ehk kui negatiivne laenguarv ja solvatatsioonienergia vähenevad. Sisekihi ehitus sõltub Cd(0001) pinnale adsorbeerunud anioonidest ja elektroodi laengutihedusest.

Cd(0001) elektroodil on $[Fe(CN)_6]^{3-}$ ja $Br^-$ Gibbsi adsorptsioonienergiad võrreldavad [93].

Pöörleva ketaselektroodiga mõõdetud tsükliliste voltamperogrammide miinimumi alas (potentsiaalide vahemikus $-1.2$ V kuni $-1.4$ V), mõõdetud impedantsi spektritest järeldub, et limiteerivateks protsessideks võib olla reageerivate anioonide adsorptsioon, katioonide kaasadsorptsioon ja/või ioonpaaride (vaheühendite) adsorptsioon koos järgneva elektrokeemilise redutseerumisega paralleelselt nn. tõelise kaugdistantse laenguülekandega. Modelleerimistulemustest leitud parameetrite sõltuvus heksatsüanoferraat(III) anioonide ja foonelektrolüüdi kontsentratsioonist näitab, et $[Fe(CN)_6]^{3-}$ anioonide redutseerumine elektrokeemiliselt poleeritud Cd(0001) elektroodil on segakineetiline protsess. $[Fe(CN)_6]^{3-}$ anioonide või $K^+\text{-}[Fe(CN)_6]^{3-}$ ioonide nõrk spetsiifiline adsorptsioon on kooskõlas difuusse kihi miinimumpotentsiaali nihke ja mahtuvuse muutusega reageerivate osakeste kontsentratsiooni kasvades.

Kompleksimpedantsi, faasinurga, summaarse impedantsi, ning impedantsi imaginaar- ja reaalosa sõltuvused näitavad, et $[Fe(CN)_6]^{3-}$ anioonide või ioonse kompleksi redutseerumine pole seisval elektroodil limiteeritud klassikalise Ficki difusiooniga. Reaktsiooni kiirus kasvab foonelektrolüüdi kontsentratsiooni kasvades, st. elektrostaatilise töö ja $\psi_1$-potentsiaali osakaal väheneb, mis on kooskõlas Frumkini kontseptsiooniga. Laenguülekande takistus väheneb ligilähedaselt eksponentsiaalselt negatiivse potentsiaali kasvades. Foonelektrolüüdi kontsentratsiooni kasvuga nihkub segakineetiline protsess puhtalt adsorptsioon limiteeritud protsessi suunas, st. täielikult blokeeritud elektroodi suunas.

# 10. ACKNOWLEDGEMENTS

# 11. PUBLICATIONS

# Electroreduction of hexacyanoferrate(III) anions on electrochemically polished Cd(0 0 0 1) plane

J. Nerut, P. Möller, E. Lust[*],[1]

*Institute of Physical Chemistry, University of Tartu, 2 Jakobi Street, Tartu 51014, Estonia*

## Abstract

Electroreduction of hexacyanoferrate(III) anion on an electrochemically polished Cd(0 0 0 1) plane in aqueous KF solutions with different additions of $K_3[Fe(CN)_6]$ was studied by rotating disc voltammetry. The rate of electroreduction of $[Fe(CN)_6]^{3-}$ depends on the electrode potential and base electrolyte concentration. The kinetic current densities obtained have been used for the determination of the rate constant values for the heterogeneous electroreduction reaction of the $[Fe(CN)_6]^{3-}$ anion on the Cd(0 0 0 1) plane. The diffuse layer potential values $\psi_d$ calculated according to the Gouy–Chapman–Grahame (GCG) model have been used for the construction of the corrected Tafel plots, which were linear in the limited region of negative potentials $(-1.35\,\text{V} \leq (E - \psi_d) \leq -1.15\,\text{V}$ versus $Hg|Hg_2Cl_2|4\,\text{M KCl})$ giving the apparent transfer coefficient value $\alpha_{app} \approx 0.35$ for $1 \times 10^{-3}$ M KF solution.
© 2003 Elsevier Ltd. All rights reserved.

*Keywords:* Hexacyanoferrate(III); Complex anion; Electroreduction; Cd(0 0 0 1); Heterogeneous rate constant

## 1. Introduction

The electroreduction kinetics of the hexacyanoferrate(III) anion has been an object of many studies [1–18]. These studies have included an investigation of the effect of the chemical nature of the electrode metal for a wide variety of polycrystalline electrodes [1–3,5–33]. However, it should be noted that there is only very few data discussed about the influence of the crystallographic structure of the electrode surface on the reduction kinetics of the $[Fe(CN)_6]^{3-}/[Fe(CN)_6]^{4-}$ redox couple [4].

According to the Frumkin slow discharge theory [27–33], the rate-determining step can be characterized by an apparent rate constant of the heterogeneous reaction:

$$k_{het} = k_{cor} \exp\left(\frac{-z_i F\psi_1}{RT}\right)$$
$$= k_0 \exp\left(\frac{-z_i F\psi_1}{RT}\right) \exp\left[\frac{-\alpha F(E - \psi_1)}{RT}\right] \quad (1)$$

where $k_{cor}$ is the rate constant corrected for the diffuse layer effect (so-called Frumkin correction ($\psi_1$ effect); $z_i$

the point charge at the site $i$; $F$ the Faraday constant; $\psi_1$ the potential experienced by the point charge in the double layer at the reaction site; $\alpha$ the transfer coefficient; and $k_0$ the potential-independent rate constant. As shown in [1–8,13,34–38], this picture is oversimplified even for the Hg electrode.

Systematic analysis of the experimental data shows that for the so called simple redox reactions $(Co(NH_3)_6^{3+}$ and other Co(III) and Cr(III) complexes [1–3,19–26], where the redox transfer occurs by an outer-sphere mechanism) the kinetic parameters depend noticeably on the chemical nature of the electrode metal and on the crystallographic structure of the electrode surface [1,24,26].

The kinetic data for electroreduction of $S_2O_8^{2-}$ on the Au, Bi and Cd single crystal plane electrodes demonstrate the noticeable dependence of $k_{het}$ and the apparent transfer coefficient, $\alpha_{app}$, values on the chemical nature and crystallographic structure of the electrode surface studied [39–41].

Based on *ac* impedance spectroscopy it was found that the apparent rate constant values $k_{het}$ for the redox couple $[Fe(CN)_6]^{3-}/[Fe(CN)_6]^{4-}$ largely depend on the surface structure of the Pt electrode and $k_{het}$ increases along the series: $(1\,1\,0) < (1\,0\,0) < (1\,1\,1)$, i.e. with increase of the reticular density of plane [4]. The in situ IR spectroscopy data indicate the presence of adsorbates ascribable to the cyanide

group on every Pt($h\,k\,l$) surface and the spectral features on
the Pt(1 1 1) surface were found to be different from Pt(1 1 0)
and Pt(1 0 0) planes [4]. Strong adsorption of reactants and
intermediates on the Pt electrode surface is also recognized
in other works [4–8] which has been explained simultane-
ously with the surface blocking effect. It has been pointed
out that the "true" rate constant of this couple should be
obtained in the very dilute solutions of the $[Fe(CN)_6]^{3-}$ or
$[Fe(CN)_6]^{4-}$ ions, when the surface coverage of the adsor-
bates is low [6,9–11].

The main aim of this work was to study the charge-transfer
mechanism and the electroreduction kinetics of the
$[Fe(CN)_6]^{3-}$ anion on the electrochemically polished (EP)
Cd(0 0 0 1) electrode.

## 2. Experimental

Electrolyte solutions were prepared from KF and
$K_3[Fe(CN)_6]$, triply recrystalized from Milli-Q+ water,
which was used for the preparation of solutions. Air was re-
moved from the solution by bubbling argon (Ar: 99.993%)
through or over prior to or during measurements, respec-
tively [39–42].

Electrochemically polished (EP) Cd(0 0 0 1) single-crystal
plane electrodes were prepared according to the method
described in [39,42]. After the electrochemical polish-
ing the EP Cd(0 0 0 1) plane was rinsed carefully with
Milli-Q+ water and submerged into a solution at $E =
-1.2$ V versus $Hg|Hg_2Cl_2|4$ M KCl in water. In this paper,
all potentials are referenced against the $Hg|Hg_2Cl_2|4$ M KCl
reference electrode. Electrochemical measurements were
performed at $T = 298$ K in a three-compartment glass cell
with a separated platinum counter electrode and a reference
electrode. PINE rotating disc electrode system with a com-
puter controlled potentiostat was used for the stationary and
rotating disc voltammetry measurements.

For the accurate determination of precision of the exper-
imental data, a statistical treatment of results was carried
out [39,40]. A total number of the independent experiments
$n \geq 6$, and at least two different electrodes with the same
crystallographic orientation were used [39,40,42]. The rel-
ative error in current density at constant potential did not
exceed 5–10%.

## 3. Results and discussion

### 3.1. Cyclic and rotating disc electrode voltammetry data
for electroreduction of hexacyanoferrate(III) anion

The voltammograms of the hexacyanoferrate(III) anion
reduction on the EP Cd(0 0 0 1) electrode in the KF solu-
tions (from $1 \times 10^{-3}$ to $1 \times 10^{-1}$ M) are displayed in Figs. 1
and 2 (the current densities $j$ in Fig. 1 are not corrected and
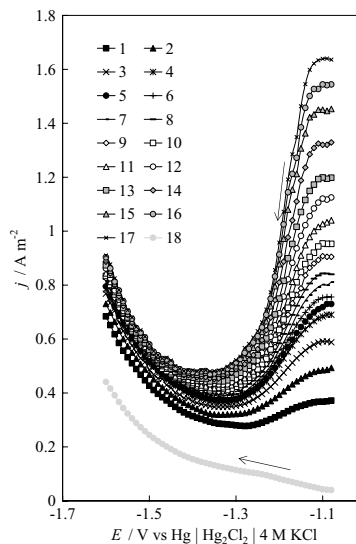in Fig. 2 the $j$ values are corrected for the current density in



Fig. 1. Rotating disc voltammetry ($j$, $E$) curves (scan rate $v = 10$ mV s$^{-1}$,
not corrected for the base electrolyte current density) for electropolished
Cd(0 0 0 1) electrode in $1 \times 10^{-4}$ M $K_3[Fe(CN)_6] + 1 \times 10^{-3}$ M KF solution
at rotation velocities $\upsilon$ (rev min$^{-1}$): 1, 500; 2, 1000; 3, 1500; 4, 2000;
5, 2200; 6, 2430; 7, 2690; 8, 3000; 9, 3370; 10, 3810; 11, 4340; 12,
4990; 13, 5800; 14, 6830; 15, 8150; 16, 9000; and 17, 9900. 18, ($j$,
$E$) curve ($v = 10$ mV s$^{-1}$) for electropolished Cd(0 0 0 1) electrode at
$\upsilon = 0$ rev min$^{-1}$ in $1 \times 10^{-3}$ M KF solution. (Here and further arrows
represent the direction of the potential scan).

the base electrolyte solution). It should be noted that in Fig. 1
the dependence of the current density for the base elec-
trolyte solution on the electrode potential is given for com-
parison (Curve 18). According to these data, the noticeable
increase of current density for the base electrolyte solution
takes place only at $E < -1.4$ V. It is probably caused by the
cathodic hydrogen evolution reaction, because the current
density is practically independent of the rotation velocity
of the EP Cd(0 0 0 1) electrode. For that reason, the current
densities for the base electrolyte solution were subtracted
from the data for systems with addition of $[Fe(CN)_6]^{3-}$ in
the base electrolyte to study the electroreduction kinetics of
the $[Fe(CN)_6]^{3-}$ anion on Cd(0 0 0 1) plane (Figs. 2 and 3).
According to the data in Figs. 1 and 2, the rate of electrore-
duction of $[Fe(CN)_6]^{3-}$ to $[Fe(CN)_6]^{4-}$ depends noticeably
on the electrode potential, as well as on the base electrolyte
and $[Fe(CN)_6]^{3-}$ concentrations. Unlike Pt electrodes [4],
no hysteresis of current density between the negative and
positive scans of potential in the region of mixed kinetics
was observed if concentration was $5 \times 10^{-5} \leq c_{K_3[Fe(CN)_6]} \leq
7 \times 10^{-4}$ M. In the region of potentials $-1.1 \leq E \leq -1.0$ V,
the very clear current plateaus were found. The limiting

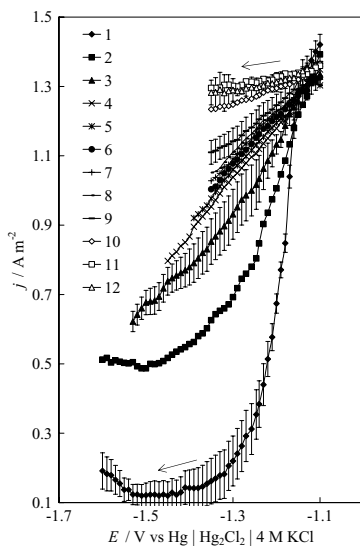Fig. 2. (*j*, *E*) curves ($v = 10\,\text{mV}\,\text{s}^{-1}$, corrected for the base electrolyte current density) for electropolished Cd(0 0 0 1) electrode at $v = 9000\,\text{rev}\,\text{min}^{-1}$ in $1 \times 10^{-4}$ M $K_3[Fe(CN)_6]$ solution with different additions of base electrolyte (KF, M): 1, 0.001; 2, 0.002; 3, 0.003; 4, 0.004; 5, 0.005; 6, 0.006; 7, 0.008; 8, 0.01; 9, 0.015; 10, 0.02; 11, 0.05; and 12, 0.1.

current density $j_d$ at constant potential measured at the rotating EP Cd(0 0 0 1) disc electrode was found to fit very well to the Levich ($j$, $\omega^{1/2}$) plot ($0.997 \le r^2 \le 0.999$):

$$j_d = 0.620 n_i F v^{-1/6} D^{2/3} \omega^{1/2} c_i \tag{2}$$

where $n_i$ is the number of electrons consumed in the reduction of an ion $i$; $c_i$ the bulk concentration of the discharging ion; $v$ the kinematic viscosity; and $D$ the diffusion coefficient. Taking $n_i = 1$ and $v = 0.01\,\text{cm}^2\,\text{s}^{-1}$ [1–3], the values of the diffusion coefficient for the $[Fe(CN)_6]^{3-}$ anion have been calculated ($D = 7 \times 10^{-6}\,\text{cm}^2\,\text{s}^{-1}$ for a $1 \times 10^{-2}$ M KF solution), which are in a good agreement with the literature data [4,16,43]. Thus, in this region of potentials, the electroreduction of the $[Fe(CN)_6]^{3-}$ anion on the EP Cd(0 0 0 1) plane is mainly limited by the rate of diffusion of the $[Fe(CN)_6]^{3-}$ anions to the electrode surface.

According to the data in Figs. 1 and 2, with increasingly negative potential ($\sigma \le -2.0\,\mu\text{C}\,\text{cm}^{-2}$; $E < -1.1$ V), the inhibition of $[Fe(CN)_6]^{3-}$ electroreduction begins, caused by the increase of the negative value of the $\psi_1$ potential, and a minimum of current density at $-1.4 \le E \le -1.3$ V appears in the dilute KF solutions. At constant concentration of $c_{K_3[Fe(CN)_6]}$ $E_{min}$ slightly depends on concentration of base electrolyte.

According to the data in Fig. 3a, the current density (corrected for the base electrolyte current density) at fixed constant potential systematically increases with the rise of reactant concentration in the solution. The results of the systematic kinetic analysis show that the current values are stable and very well reproducible if the electrode potential has been cycled in the region $-1.6 \le E \le -1.0$ V. The attempts to study the $[Fe(CN)_6]^{3-}$ electroreduction process on the Cd(0 0 0 1) plane at more positive potentials than $E \ge -0.95$ V cause a very quick decrease of the current density values in all the region of potential studied which indicates the surface "blocking effect" similarly to the Pt electrodes [4,7–9]. The surface "blocking effect" might be caused by irreversible adsorption of the $[Fe(CN)_6]^{3-}$ or $[Fe(CN)_6]^{4-}$ anions on the electrode surface. But the situation might be more complex and the oxidation of the cadmium electrode to cadmium hexacyanoferrate could take place at $E > -0.95$ V. This oxidation current can partly counter-balance the electroreduction current of $[Fe(CN)_6]^{3-}$ and, as a result, the decrease of the resulting current might be observed. In addition, cadmium ferrocyanide which can be formed on the electrode presumably inhibits the process studied. Differently from Pt electrodes [4,7–9] there is no hysteresis in the current density versus potential curves as well as no dependence of $j$ on time (i.e. on the cycle number) if $E \le -1.0$ V. The data in Fig. 3b show that there is a really linear dependence of the limiting diffusion current density $j_d$ (corrected for the base electrolyte current density) on $c_{K_3[Fe(CN)_6]}$ if $c_{K_3[Fe(CN)_6]} < 8 \times 10^{-4}$ M. At higher $c_{K_3[Fe(CN)_6]}$ the surface blocking, i.e. the irreversible adsorption of solution components or intermediates is possible. Therefore, in the experiments where the influence of the base electrolyte concentration on the reaction rate was investigated the concentration of $K_3[Fe(CN)_6]$ was $1 \times 10^{-4}$ M and the potential interval was limited to $-1.6 \le E \le -1.1$ V. Choosing these experimental conditions ensures that the reduction is not influenced by the formation and adsorption of the cadmium hexacyanoferrate because there is no deviation of the limiting diffusion current density from linearity in Levich plot (Fig. 3b) and accordingly cadmium hexacyanoferrate has not been formed on the electrode surface. Otherwise, there has to be noticeable decrease of the limiting diffusion current density.

At more negative surface charge densities ($\sigma \le -10\,\mu\text{C}\,\text{cm}^{-2}$) in the dilute KF solutions acceleration of the $[Fe(CN)_6]^{3-}$ anion electroreduction in the region of potentials where the value of $d\psi_1/dE$ is approximately constant has been observed. Acceleration of the reaction is mainly caused by the increase of negative electrode potential, i.e. by the dependence of activation energy $E_a$ on $E - E_0 = \eta$, where $E_0$ is the equilibrium potential of the redox system and $\eta$ is so-called overpotential. According to the Frumkin slow discharge theory [27–29,44,45] $E_a$ can be expressed as:

$$E_a = -F(\alpha - z_R)\psi_1 - \alpha F\eta \tag{3a}$$

where $\alpha$ is the true transfer coefficient and $z_R$ the reactant charge number. On the other hand, the increase of $j_k$ at $E$
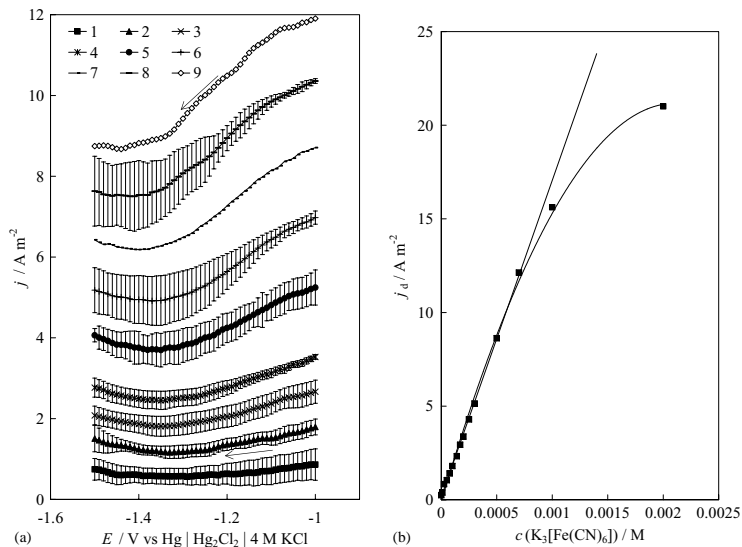
Fig. 3. (a) $(j, E)$ curves ($v = 10\,\mathrm{mV\,s^{-1}}$, corrected for the base electrolyte current density) for electropolished Cd(0 0 0 1) electrode at $\upsilon = 9000\,\mathrm{rev\,min^{-1}}$ in 0.01 M KF solution with different additions of $K_3[Fe(CN)_6]$ (M): 1, $5 \times 10^{-5}$; 2, $1 \times 10^{-4}$; 3, $1.5 \times 10^{-4}$; 4, $2 \times 10^{-4}$; 5, $3 \times 10^{-4}$; 6, $4 \times 10^{-4}$; 7, $5 \times 10^{-4}$; 9, $8 \times 10^{-4}$; and 9, $7 \times 10^{-4}$. (b) Dependences of the limiting diffusion current density (corrected for the base electrolyte current density) on $K_3[Fe(CN)_6]$ concentration for electropolished Cd(0 0 0 1) electrode in 0.01 M KF at $v = 9000\,\mathrm{rev\,min^{-1}}$.

$< -1.4\,\mathrm{V}$ (for dilute KF solutions) can be explained by the beginning of the weak specific adsorption of the base electrolyte cations at the negatively charged Cd(0 0 0 1) electrode surface ($\sigma \leq -13\,\mu\mathrm{C\,cm^{-2}}$) and thus by the charge transfer through the adsorbed ion-pair [16,18,27–29,44,45]. This result is in a good agreement with the impedance data (Figs. 4 and 5) as in this region of potential ($E \leq -1.4\,\mathrm{V}$) a strong rise in the differential capacitance $C$ values with $c_{KF}$ is observed. It should be noted that the capacitance values for the 0.1 M KF solution are somewhat higher than for the 0.1 M NaF solution ($\Delta C \sim 1.0\,\mu\mathrm{F\,cm^{-2}}$), demonstrating that weak adsorption of the $K^+$ ions is possible on the Cd(0 0 0 1) plane at $\sigma \leq -14\,\mu\mathrm{C\,cm^{-2}}$ [42]. In this region of potentials ($E \leq -1.4\,\mathrm{V}$), the current density for $[Fe(CN)_6]^{3-}$ reduction on the Cd(0 0 0 1) plane increases noticeably with increasing the base electrolyte concentration (Fig. 1). The dependences of surface charge density $\sigma$ on $c_{KF}$ at various fixed potentials (Fig. 5) are in good agreement with this conclusion as at $E = -1.6\,\mathrm{V}$ the difference between $\sigma$ values $\Delta\sigma \geq 1.5\,\mu\mathrm{C\,cm^{-2}}$ for $1 \times 10^{-3}$ and $1 \times 10^{-1}\,\mathrm{M}$ KF solutions has been established.

### 3.2. Kinetic analysis

The apparent rate constant for the heterogeneous electroreduction reaction of the $[Fe(CN)_6]^{3-}$ anions, $k_{het}$, was defined by Eq. (4):

$$j_k = n_i F k_{het} c_i \tag{4}$$

where $j_k$ is the kinetic current density. The values of kinetic current density at constant potential were obtained from the linear Koutecký–Levich plots ($0.997 \leq r^2 \leq 0.999$) according to Eq. (5):[2]

$$\frac{1}{j} = \frac{1}{j_k} + \frac{1}{j_d} \tag{5}$$

The logarithmic dependences of the apparent rate constant (calculated from the current densities, which were corrected for the base electrolyte effects), on the electrode potential at the different base electrolyte concentrations are presented in Fig. 6. At constant potential, $\log k_{het}$ increases with $c_{KF}$ in the solution, but at constant concentration of KF it is practically independent of $c_{K_3[Fe(CN)_6]}$, if $c_{K_3[Fe(CN)_6]} \leq 8 \times 10^{-4}\,\mathrm{M}$.

Analysis of the experimental data shows that there is a good linear dependence of $\ln j_k$ values on $\ln c_{KF}$ ($0.995 \leq r^2 \leq 0.999$), if $c_{KF} \leq 0.01\,\mathrm{M}$ and $\sigma \leq -5\,\mu\mathrm{C\,cm^{-2}}$. Using these data the charge number of the reacting particle $z_i$ was

---

[2] In the literature, this equation is named Koutecký–Levich equation. However, it should be noted that this method was derived for the first time by Frumkin and Aikazian [46] and used by Frumkin and Tedoradze [47] for the interpretation of experimental results.

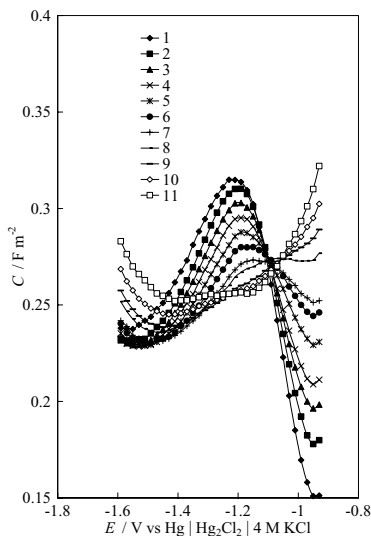Fig. 4. Differential capacitance vs. electrode potential curves (at ac frequency $f = 5$ Hz) for electropolished Cd(0 0 0 1) electrode in KF solution with concentrations (M): 1, 0.001; 2, 0.002; 3, 0.003; 4, 0.004; 5, 0.005; 6, 0.007; 7, 0.01; 8, 0.02; 9, 0.03; 10, 0.05; and 11, 0.1.
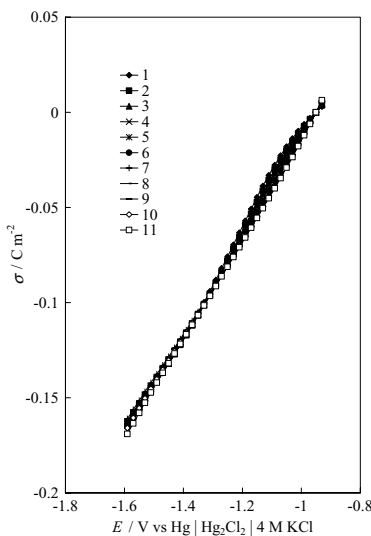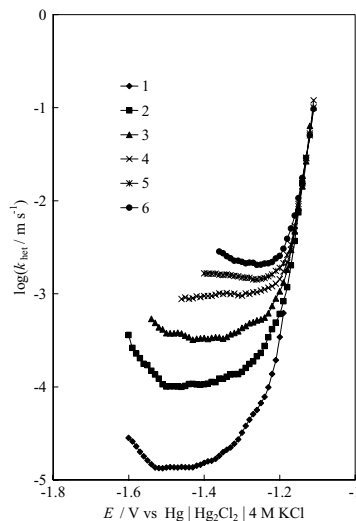


Fig. 6. The $\log k_{het}$, $E$ curves for electropolished Cd(0 0 0 1) electrode in $1 \times 10^{-4}$ M $K_3[Fe(CN)_6]$ with different additions of base electrolyte (KF, M): 1, 0.001; 2, 0.002; 3, 0.003; 4, 0.004; 5, 0.005; and 6, 0.006.

obtained according to the Frumkin–Petrii method (described in more detail in [45]) according to Eq. (6):

$$\left( \frac{\partial \ln j_k}{\partial \ln c_{KF}} \right)_{E-(RT/z_2 F) \ln c_{KF}, c_i} = -\frac{z_i}{z_2}, \tag{6}$$

where $z_2$ is the charge number of the base electrolyte cations (i.e. $z_2 = +1$); and $c_i$ is the bulk concentration of the reacting particles. According to the data in Fig. 7 the values of $z_i$ obtained depend on the electrode charge density and absolute value of $z_i$ increases with $\sigma$ if $\sigma \leq -5\,\mu C\,cm^{-2}$. The comparatively low values of $|z_i|$ at $\sigma \geq -5\,\mu C\,cm^{-2}$ indicate that there are noticeable deviations from the classical Frumkin model and the condition $\Gamma_{A^-} \ll \Gamma_{C^+}$ at $\sigma \geq -5\,\mu C\,cm^{-2}$ is not satisfied for the Cd(0 0 0 1)|[Fe(CN)$_6$]$^{3-}$+KF+H$_2$O interface ($\Gamma_{A^-}$ and $\Gamma_{C^-}$ are the Gibbs adsorption of the anions and cations, respectively). For more conclusive remarks the future more detailed experimental impedance studies in various base electrolyte solutions are planned. The value of $z_i \approx -3$ obtained at the very negative values of the surface charge densities indicates that the ion-pairing effect is probably unimportant in determination of the reacting particle charge for the Cd(0 0 0 1)|K$_3$[Fe(CN)$_6$] + KF + H$_2$O interface.

### 3.3. Corrected Tafel plots

The corrected Tafel plots (cTp) [48] for the [Fe(CN)$_6$]$^{3-}$ anion electroreduction on the EP Cd(0 0 0 1) have been calculated according to $j_k$ values, using the $\psi_d$ values calculated from the impedance data for the pure base electrolyte



Fig. 5. Surface charge density vs. electrode potential curves for electropolished Cd(0 0 0 1) electrode in KF solution with concentrations (M): 1, 0.001; 2, 0.002; 3, 0.003; 4, 0.004; 5, 0.005; 6, 0.007; 7, 0.01; 8, 0.02; 9, 0.03; 10, 0.05; and 11, 0.1.
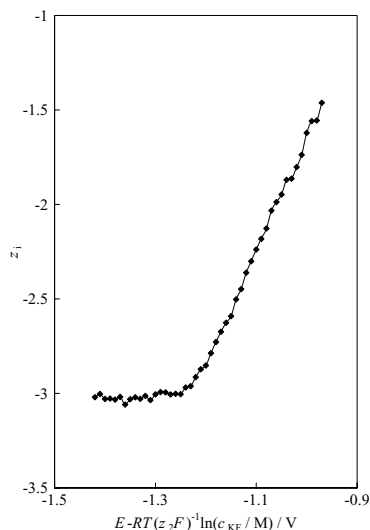
Fig. 7. Charge of the reacting particle $z_i$ at various surface charge densities for electropolished Cd(0001) electrode in $1 \times 10^{-4}$ M $K_3[Fe(CN)_6]$.



Fig. 8. Corrected Tafel plots for EP Cd(0001)|$1 \times 10^{-4}$ M $K_3[Fe(CN)_6] + x$ M KF system (1–6) and for Hg|$3.3 \times 10^{-4}$ M $K_3[Fe(CN)_6] + x$ M KCl interface (1′–4′) (data taken from [3,16,18]) at fixed KF concentration $x$ (M): 1, 0.001; 2, 0.002; 3, 0.003; 4, 0.004; 5, 0.005; and 6, 0.006 and at fixed KCl concentration $x$ (M): 1′, 0; 2′, 0.0005; 3′, 0.001; and 4′, 0.0015.

solutions (Figs. 4 and 5) [17,18,44]. Thus, to a first approximation, the value of the $\psi_d$ potential has been taken equal to the value of the $\psi_1$ potential, i.e. to the mean potential of the plane at which the centres of the charges of the reacting particles in the transition state of the reaction are located. As can be seen in Fig. 8 (Curves 1–6) the cTps for the EP Cd(0001) interface in the less concentrated base electrolyte solution with addition of $[Fe(CN)_6]^{3-}$ are linear at $(E - \psi_d) \leq -1.1$ V, if we assume that $z_i = -3$. The apparent transfer coefficient $\alpha_{app} \approx 0.35$ for the most diluted KF solution can be obtained. For more concentrated base electrolyte solution these plots are nonlinear at $(E - \psi_d) > -1.15$ V, which is probably caused by the dependence of the adsorption energies of the reactant and product on the electrode potential. The attempts to use various new approximations, discussed in works [1–3,34–38,49], did not give better fit of the experimental data in the region of $(E - \psi_d) > -1.15$ V and, therefore, the more correct adsorption data of the $K^+$ ions as well as $[Fe(CN)_6]^{3-}$ and $[Fe(CN)_6]^{4-}$ ions on the EP Cd(0001) plane are needed. Thus, the verification of the applicability of the Tafel equation for the electroreduction of the $[Fe(CN)_6]^{3-}$ anions under conditions of the weakly adsorbed base electrolyte anions for EP Cd(0001) requires future experimental studies in the various base electrolyte solutions with anions of a different nature ($F^-$, $BF_4^-$, $Cl^-$, $SO_4^{2-}$, i.e. anions with the different values of Gibbs adsorption energy) [50,51].

It should be noted that Damaskin et al. [13] developed a new model and method for the double-layer correction,
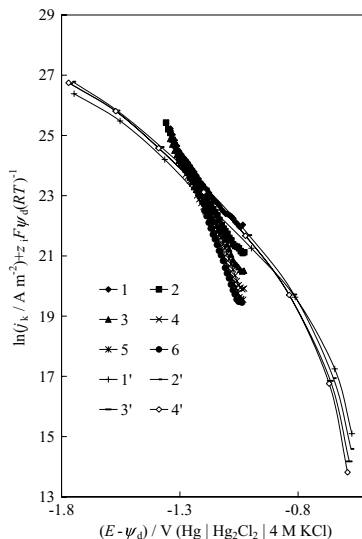
taking into account the new diffuse layer theory developed by Gonzalez and Sanz [52]. Our calculations show that for the KF + $K_3[Fe(CN)_6]$ system these corrections under discussion are comparatively small and in the region of $(E - \psi_d) > -1.15$ V the non-linear shape of the corrected Tafel plots practically does not change. It should be noted that the further theoretical studies based on the new diffuse layer models (Monte Carlo method as well as mean generalized spherical approximation [53–55]) are in progress now.

Comparison of the results for EP Cd(0001)|$1 \times 10^{-4}$ M $K_3[Fe(CN)_6] + x$ M KF interface with the data for Hg|$3.3 \times 10^{-4}$ M $K_3[Fe(CN)_6] + x$ M KCl ($5 \times 10^{-4}$ M $\leq x \leq 1.5 \times 10^{-3}$ M) interface [3,16,18] (Fig. 8, Curves 1′–4′) shows a good agreement of the cTps at the moderate negative electrode potentials in the dilute base electrolyte solutions. However, exact comparison of our results with the data obtained in works [3,16,18] is impossible because the different base electrolyte with the different solution concentrations have been used.

## 4. Conclusions

Electrochemical reduction of the hexacyanoferrate(III) anions on the electrochemically polished Cd(0001) plane

has been studied by the linear sweep and rotating disc electrode voltammetry methods. The rate of electroreduction of the $[Fe(CN)_6]^{3-}$ anion depends on the polarization of the EP Cd(0001) electrode, as well as on the base electrolyte concentration. In the region of zero charge potential the electroreduction of the $[Fe(CN)_6]^{3-}$ anion is mainly limited by the rate of diffusion of the $[Fe(CN)_6]^{3-}$ anions to the EP Cd(0001) surface. Diffusion coefficient values ($7 \times 10^{-6}\,cm^2\,s^{-1}$ for $1 \times 10^{-2}$ M KF) obtained from the linear Levich plots, constructed in the region of zero charge potential, were in a reasonable agreement with the literature data [16,43]. In the region of small negative surface charge densities the inhibition of the $[Fe(CN)_6]^{3-}$ anion electroreduction takes place, which has been explained by the diffuse layer effect. At more negative surface charge densities, the acceleration of $[Fe(CN)_6]^{3-}$ anion electroreduction in the dilute base electrolyte solution has been explained by diminishing the diffuse layer potential effect as at potentials far negative from the zero charge potential the diffuse layer potential very weakly depends on potential, as well as by weak specific adsorption of the $K^+$ cations on the electrochemically polished Cd(0001) surface at $\sigma \leq -14\,\mu C\,cm^{-2}$.

The apparent rate constant values $k_{het}$ have been calculated using the kinetic current densities $j_k$ obtained from the linear Koutecký–Levich plots. At potentials far negative from the zero charge potential the $k_{het}$ values increase strongly with the base electrolyte concentration. At constant electrode potential $k_{het}$ is practically independent of reactant concentration, if $c_{K_3[Fe(CN)_6]} \leq 7 \times 10^{-4}$ M.

The corrected Tafel plots for the electroreduction of the $[Fe(CN)_6]^{3-}$ anion on the EP Cd(0001) electrode have been calculated, using the classical diffuse layer potential values obtained according to the Gouy–Chapman theory. In the limited region of cathodic polarizations ($-1.35\,V \leq (E - \psi_d) \leq -1.15$ V versus $Hg|Hg_2Cl_2|4$ M KCl in water) the corrected Tafel plots for the EP Cd(0001) electrodes are linear with the slope corresponding to the apparent transfer coefficient $\alpha_{app} \approx 0.35$ for most diluted KF solution. At smaller negative surface charge densities the cTps are nonlinear. Comparison of our data with the data for $Hg|3.3 \times 10^{-4}$ M $K_3[Fe(CN)_6] + x$ M KCl ($5 \times 10^{-4} = x = 1.5 \times 10^{-3}$ M) interface [3,16,18] shows a good agreement of the cTps at moderate negative electrode potentials in the dilute base electrolyte solutions.

## Acknowledgements

## References

[1] W.R. Fawcett, in: J. Lipkowski, P.N. Ross (Eds.), Electrocatalysis, Wiley, New York, 1998, p. 323.

[2] W.R. Fawcett, M. Hromadova, G.A. Tsirlina, R.R. Nazmutdinov, J. Electroanal. Chem. 498 (2001) 93.

[3] G.A. Tsirlina, N.V. Titova, R.R. Nazmutdinov, O.A. Petrii, Elektrokhimiya 37 (2001) 21.

[4] F. Kitamura, N. Nanbu, T. Ohsaka, K. Tokuda, J. Electroanal. Chem. 456 (1998) 113.

[5] L.M. Peter, W. Dürr, P. Bindra, H. Gerischer, J. Electroanal. Chem. 71 (1976) 31.

[6] S.A. Campbell, L.M. Peter, J. Electroanal. Chem. 364 (1994) 257.

[7] P. Kulesza, T. Jêdral, Z. Galus, J. Electroanal. Chem. 109 (1980) 141.

[8] A. Wiêckowski, M. Szklarczyk, J. Electroanal. Chem. 142 (1982) 157.

[9] J. Kawiak, T. Jêdral, Z. Galus, J. Electroanal. Chem. 145 (1983) 163.

[10] J. Kawiak, P.J. Kulesza, Z. Galus, J. Electroanal. Chem. 226 (1987) 305.

[11] C. Beriet, D. Pletcher, J. Electroanal. Chem. 361 (1993) 93.

[12] C. Lee, F.C. Anson, J. Electroanal. Chem. 323 (1992) 381.

[13] B.B. Damaskin, J.V. Stenina, O.A. Baturina, L.N. Sviridova, Elektrokhimiya 34 (1998) 1083.

[14] D.E. Khoshtariya, T.D. Dolidze, D. Krulic, N. Fatouros, P. Devilliers, J. Phys. Chem. B 102 (1998) 7800.

[15] V. Mareèek, Z. Samec, J. Weber, J. Electroanal. Chem. 94 (1978) 169.

[16] O.A. Petrii, N.V. Nikolaeva-Fedorovich, Zhurn. Fis. Khim. 35 (1961) 1999.

[17] A.N. Frumkin, G.M. Florianovich, Dokl. Akad. Nauk. USSR 80 (1951) 907.

[18] A.N. Frumkin, O.A. Petrii, N.V. Nikolaeva-Fedorovich, Dokl. Akad. Nauk. USSR 128 (1959) 1006.

[19] M.J. Weaver, F.C. Anson, J. Am. Chem. Soc. 97 (1975) 4403.

[20] A. Hamelin, M.J. Weaver, J. Electroanal. Chem. 209 (1986) 109.

[21] A. Hamelin, M.J. Weaver, J. Electroanal. Chem. 223 (1987) 171.

[22] G.J. Brug, M. Sluyters-Rehbach, J.H. Sluyters, A. Hamelin, J. Electroanal. Chem. 181 (1984) 245.

[23] J. Peres, E.R. Gonzalez, H.M. Villullas, J. Phys. Chem. B 102 (1998) 10931.

[24] Z. Samec, A.M. Bittner, K. Doblhofer, J. Electroanal. Chem. 432 (1997) 205.

[25] W. Fawcett, M. Fedurco, Z. Kováèova, J. Electrochem. Soc. 141 (1994) L30.

[26] M. Hromadová, W.R. Fawcett, J. Phys. Chem. A 104 (2000) 4356.

[27] A.N. Frumkin, Z. Phys. Chem. 164 (1953) 121.

[28] A.N. Frumkin, Z. Elektrochem. 59 (1955) 807.

[29] A.N. Frumkin, in: P. Delahay (Ed.), Advance Electrochemistry, vol. 1, Interscience, New York, 1961, p. 65.

[30] R. Parsons, Surf. Sci. 2 (1964) 418.

[31] A.N. Frumkin, N.V. Nikolaeva-Fedorovich, N.P. Berezina, H.E. Keis, J. Electroanal. Chem. 58 (1975) 189.

[32] S. Trasatti, in: H. Gerischer, C.W. Tobias (Eds.), Advances in Electrochemistry and Electrochemical Engineering, vol. 19, Wiley, New York, 1977, p. 297.

[33] N.V. Fedorovich, Reports in Science and Technology, vol. 14, Viniti, Moscow, 1979, p. 5 (in Russian).

[34] R.R. Nazmutdinov, G.A. Tsirlina, Y.I. Kharkats, O.A. Petrii, M. Probst, J. Phys. Chem. B 102 (1998) 677.

[35] G.A. Tsirlina, Y.I. Kharkats, R.R. Nazmutdinov, O.A. Petrii, Russ. J. Electrochem. 35 (1999) 23.

[36] G.A. Tsirlina, O.A. Petrii, Y.I. Kharkats, A.M. Kuznetsov, Russ. J. Electrochem. 35 (1999) 1210.

[37] R.R. Nazmutdinov, I.V. Pobelov, G.A. Tsirlina, O.A. Petrii, J. Electroanal. Chem. 491 (2000) 126.

[38] I.V. Pobelov, G.A. Tsirlina, M.I. Borzenko, O.A. Petrii, Russ. J. Electrochem. 37 (2001) 270.

[39] T. Thomberg, E. Lust, J. Electroanal. Chem. 485 (2000) 89.

[40] E. Lust, R. Truu, K. Lust, Russ. Elektrokhim. 36 (2000) 1349.

[41] Z. Samec, J. Electroanal. Chem. 146 (1995) 3349.

*J. Nerut et al. / Electrochimica Acta 49 (2004) 1597–1604*

[42] E. Lust, A. Jänes, K. Lust, M. Väärtnõu, Electrochim. Acta 42 (1997) 771.

[43] I.-F. Hu, D.H. Karweik, T. Kuwana, J. Electroanal. Chem. 189 (1985) 59.

[44] A.N. Frumkin, Z. Phys. Chem. A 164 (1933) 121.

[45] O.A. Petrii, A.N. Frumkin, Dokl. Akad. Nauk. USSR 147 (1962) 418.

[46] A.N. Frumkin, E.A. Aikazian, Dokl. Akad. Nauk. USSR 100 (1955) 333.

[47] A.N. Frumkin, E. Tedoradze, Z. Elektrochem. 62 (1958) 252.

[48] K. Asada, P. Delahay, A.K. Sundram, J. Am. Chem. Soc. 83 (1961) 3396.

[49] G.A. Tsirlina, O.A. Petrii, R.R. Nazmutdinov, D.V. Gluhov, Elektrokhimiya 38 (2002) 154.

[50] K. Lust, M. Väärtnõu, E. Lust, Electrochim. Acta 45 (2000) 3543.

[51] K. Lust, M. Väärtnõu, E. Lust, J. Electroanal. Chem. 532 (2002) 303.

[52] R. Gonzalez, F. Sanz, Electroanalysis 9 (1997) 169.

[53] D. Boda, K.Y. Khan, D. Henderson, J. Chem. Phys. 110 (1999) 5346.

[54] W.R. Fawcett, J. Electroanal. Chem 500 (2001) 264.

[55] W.R. Fawcett, D.J. Henderson, J. Phys. Chem. 104 (2000) 6837.

**II**

# The kinetics of electroreduction of peroxodisulfate anion on electrochemically polished Cd(0 0 0 1) plane

T. Thomberg, J. Nerut, K. Lust, E. Lust*

*Institute of Physical Chemistry, University of Tartu, 2 Jakobi Street, 51014 Tartu, Estonia*

## Abstract

The electroreduction of the peroxodisulfate anion on the electrochemically polished (EP) Cd(0 0 0 1) plane has been studied by cyclic voltammetry and rotating disc electrode methods. The rate constant of the heterogeneous electroreduction reaction of the $S_2O_8^{2-}$ anion on the EP Cd(0 0 0 1) plane dependent on electrode polarisation and base electrolyte concentration has been established. The values of apparent transfer coefficient $\alpha_{app}$ corrected for the double layer effect, noticeably lower than 0.5 for the EP Cd(0 0 0 1) plane, only very weakly depend on the electrode potential but noticeably on the electrolyte concentration, decreasing with the base electrolyte concentration. The very low values of the apparent charge transfer coefficient show that the activationless charge transfer mechanism is probably valid for EP Cd(0 0 0 1) | NaF + Na$_2$S$_2$O$_8$ aqueous solution interface in a good agreement with the theoretical models for the high hydrogen overvoltage metals based on the diabatic charge transfer mechanism from the metal to an ion.
© 2003 Elsevier Ltd. All rights reserved.

*Keywords:* Electroreduction; Peroxodisulfate; Cadmium single crystal; Heterogeneous rate constant; Formal charge transfer coefficient

## 1. Introduction

Electroreduction of the peroxodisulfate anion has been suggested as a probe reaction for studying the influence of the electrical double layer (edl) structure on the charge transfer mechanism from a metal to an anion [1–23]. Experimental data for Hg [1–4,13–17] and various polycrystalline sp-metals like Bi, Sb, Pb, Sn, Cd and Ag [5,7–9], as well as for single-crystal Ag(1 1 1) and Ag(1 0 0) planes [10–12] in the limited concentration region of the base electrolyte solution have implied that the reduction rate of the overall two-electron peroxodisulfate anion is controlled by a single one electron rate-determining step. This rate-determining step can be characterised by an apparent heterogeneous rate constant $k_{het}$ [3–7]

$$k_{het} = k_{cor} \exp\left(\frac{-z_i F \psi_1}{RT}\right)$$
$$= k_0 \exp\left(\frac{-z_i F \psi_1}{RT}\right) \exp\left[\frac{-\alpha F(E - \psi_1)}{RT}\right] \quad (1)$$

---

* Corresponding author. Tel.: +372-7-375-165; fax: +372-7-375-160.
*E-mail address:* enn@chem.ut.ee (E. Lust).

where $k_{cor}$ is the rate constant corrected for the double layer effect (so-called Frumkin correction ($\psi_1$ effect)); $\psi_1$ the electrical potential at the optimum point, where the charge transfer from metal to ion takes place; $z_i$ the charge number of a reactant ion, $\alpha$ the transfer coefficient; and $k_0$ is the potential-independent rate constant. It should be noted that in the case of $S_2O_8^{2-}$ the electroreduction is irreversible due to breaking of the O–O bond [4–8]. As shown and discussed in Refs. [22–36] and noted by Samec and coworkers [18–21], the classical conception is oversimplified even for the Hg electrode. It should be noted, that the very low values of the apparent transfer coefficient $\alpha_{app}$ ($\alpha_{app} = 0.22$ if $z_i = -2$) have been reported [1–5,30–35] and, according to Gierst [13], $\alpha_{app}$ depends on the electrode potential ($\alpha_{app} \approx 0$ at $E \leq E_{\sigma=0}$, if $z_i = -2$; and $\alpha_{app} \approx 0.2$ or 0.4 at $E \ll E_{\sigma=0}$, if $z_i = -1$). Thus, as it was pointed out in Ref. [13], there is a noticeable change in a mechanism from an activationless discharge of the divalent anion to a normal discharge of the univalent ion-pair [31,32]. Results of quantum chemical calculations [27,28] show that the electroreduction of the $S_2O_8^{2-}$ anion belongs to the group of the reactions with a very complicated mechanism and the transfer of the first electron to the $S_2O_8^{2-}$ anion takes place according to Eq. (2)

[25–28]

$$S_2O_8{}^{2-} + e^- \rightarrow SO_4{}^{2-} + SO_4{}^{-\bullet} \qquad (2)$$

It was found that the transfer of the first electron is probably the rate determining step and the standard potential for the redox couple $E^0_{S_2O_8{}^{2-}/SO_4{}^{2-};SO_4{}^{-\bullet}} = 1.45$ V versus SHE [25–28]. According to the experimental results, there is no specific adsorption of the $S_2O_8{}^{2-}$ anions on the Hg electrode and the reaction centre lies in the diffuse layer [1–9,17,27,28]. The very low values of $\alpha_{app}$ for the Hg electrode have been explained theoretically by Petrii and coworkers [27,28] by the diabatic and activationless charge transfer mechanism [31,32].

It should be noted that Damaskin et al. [30] have discussed the possibility to use the new diffuse layer theory, developed by Gonzalez and Sanz [36] where the activity of the $S_2O_8{}^{2-}$ anions at the outer Helmholtz plane has been used as the concentration variable to construct the so-called corrected Tafel plots (cTp) [37]. It was found that for $Hg \mid K_2S_2O_8 + K_2SO_4$ system the new model gives reasonable results (with $\alpha_{app} = 0.11$), but for $Hg \mid K_2S_2O_8 + KF$ system the influence of the activity of the anions and corresponding corrections are very small [30].

According to the new so-called microscopic double layer $\psi_i$ potential correction model [27–29,38–42], the interaction of reactants with the electrical double layer field can be modelled on the basis of the so called "microscopic $\psi_i$" approach, taking into account the effective charges of the atoms forming the complex ions.

Another more usual representation is based on the location of the effective point charge at a certain distance $x_i$ with subsequent calculation of the effective value $z_{eff}$ [3,4,37]. In the papers published by Petrii, Frumkin et al. [3–7,43,44], there has been developed a formal conception taking into account that the $\psi_1$ potential is different from the Gouy–Chapman diffuse layer potential $\psi_d$ for aqueous NaF base electrolyte solution and the effective double layer potential at the reaction site, $\psi_x(x_i)$, has been calculated as [29,37,46–50]

$$\psi_x(x_i) = \frac{4RT}{F}\text{arctanh}\left\{\tanh\left(\frac{F\psi_d}{4RT}\right)\exp(-\kappa x)\right\} \qquad (3)$$

where $\psi_d$ is the classical Gouy–Chapman diffuse layer potential for the base electrolyte, and $\kappa$ is the Gouy screening length (i.e. the inverse Debye length) for the electrolyte solution with concentration $c$ and $\kappa$ is expressed as

$$\kappa = \left(\sqrt{\frac{\varepsilon_0 \varepsilon RT}{2cF^2}}\right)^{-1} \qquad (4)$$

In Eq. (3), the variable $x = x_i - x_d$ is a distance of the reaction site from the outer Helmholtz plane with distance $x_d$ from the electrode surface [29]. It was approximated that the potential drops linearly from the value of $\phi^m$ at the interface to the value $\psi_d$ at the outer Helmholtz plane and $\psi_x(x_i) = \phi^m - (\phi^m - \psi_d)(x_i/x_d)$ [29] if the reaction site lies in the inner layer region.

For electroreduction of the $S_2O_8{}^{2-}$ anion on Hg it was found that the linear corrected Tafel plots can be established if the reaction site is assumed to lie in the inner layer, i.e. at the distance somewhat smaller than the parameter of the effective ellipsoid formed by the $S_2O_8{}^{2-}$ anion (0.32 and 0.68 nm, respectively) [4,27–29,51]. However, for electroreduction of $[Fe(CN)_6]^{3-}$ ions on Hg very large values of the distance from the outer Helmholtz plane, $x$, have been established (i.e. $x \geq 1.0$ nm) [5,7,43,44] and according to these data this distance is more than two times larger than the effective diameter of the $[Fe(CN)_6]^{3-}$ ion (equal to 0.41 nm) [41]. Thus, the double layer correction for electroreduction of the complex anions at the so-called Hg-like metals is an open question.

Electrochemical reduction of peroxodisulfate anion on Au electrodes has been suggested to proceed via two parallel pathways [18–21]. Samec and Doblhofer [18–20] have demonstrated that the first pathway gives rise in a current at positively charged polycrystalline Au, Au(1 1 1) and Au(0 1 1) electrodes and involves a stronger interaction of the discharging $S_2O_8{}^{2-}$ anion with the electrode surface resulting in an electrocatalysis of this process. At more negative potentials, the direct electroreduction of the $S_2O_8{}^{2-}$ anions (i.e. the Frumkin mechanism) has been observed for the Au electrodes. A dynamic model of a $S_2O_8{}^{2-}$ electrochemical oscillator was put forward, which refers to conclusions derived from studies of peroxodisulfate reduction on Hg [18–21].

The first experimental studies at electrochemically polished (EP) Cd(0 0 0 1) plane electrode [34] demonstrated a noticeable concentration dependence of the corrected Tafel plots indicating the deviation of Cd(0 0 0 1) $\mid S_2O_8^{2-}$ + NaF system from the classical Frumkin slow discharge theory [3–9].

The main aim of this work was to test the applicability limits of the various new theoretical and empirical approximations and to characterise the charge transfer mechanism and kinetics of electroreduction of the $S_2O_8{}^{2-}$ anion at the Cd(0 0 0 1) plane in a wide region of the base electrolyte concentrations and electrode polarisations.

## 2. Experimental

Base electrolyte solutions were prepared from the triply recrystallised from the Milli-Q+ water NaF and $Na_2S_2O_8$ salts. The Milli-Q+ water was used for preparation of the solutions studied. Air was removed from the solutions by bubbling argon (Ar, 99.998%) through or over solution prior to or during measurements, respectively.

Electrochemically polished Cd(0 0 0 1) single crystal plane electrode used was prepared according to the methods described in Refs. [34,46–49]. After the electrochemical polishing the Cd(0 0 0 1) electrode was rinsed carefully with Milli-Q+ water and submerged into the solution at $E = -1.2$ V versus calomel electrode in 4 M KCl (4M

CE). Electrochemical measurements were performed at $T = 298$ K in a three-compartment glass cell with a separated platinum counter electrode, as well as by a separated (by Luggin capillary) reference electrode (calomel electrode in 4 M KCl).

Conventional electrochemical equipment (Pine Company) was used for the stationary and rotating disc voltammetry (rotation velocity $\nu = 0$–9990 rev min$^{-1}$). Dependence of differential capacitance $C$ on the electrode potential $E$ was measured using Autolab PGSTAT with FRA2 system [52]. The differential capacitance was evaluated for the equivalent circuit consisting of a resistor and a capacitor in series and measured at ac frequencies $f$ from 0.1 to 1000 Hz. The equilibrium capacitance values $C(f = 0)$ obtained by the linear extrapolation (in the region $0.5 \leq f \leq 500$ Hz) have been used for calculating the charge density versus electrode potential dependences. The diffuse layer potential has been calculated using the Gouy–Chapman–Grahame model [53,54].

For the accurate determination of precision of the experimental data, a statistical treatment of the results was carried out. A total number of independent experiments $n \geq 8$, and at least two different electrodes with the same crystallographic orientation were used [34,46–49]. The relative error in current density at $E = $ const. did not exceed 4–9%.

## 3. Results and discussion

### 3.1. Cyclic and rotating disc electrode voltammetry of peroxodisulfate anion

The experimental voltammograms of the peroxodisulfate anion reduction at the EP Cd(0 0 0 1) electrode in NaF+Na$_2$S$_2$O$_8$ aqueous solutions are displaced in Figs. 1(a) and 2 (corrected for the current densities for the base electrolyte solution). According to the experimental results, the current densities in the base electrolyte solution (Fig. 1b) are noticeably smaller than for the system with addition of S$_2$O$_8$$^{2-}$ anion (Fig. 1c) and only at very negative potentials ($E < -1.4$ V versus 4 M CE) there is a noticeable increase of cathodic current (Fig. 1b) practically independent of the rotation velocity of the disk electrode. Thus, the main kinetically limited process is probably hydrogen evolution at $E < -1.4$ V as the current density at fixed potential only slightly increases with the base electrolyte concentration indicating the weak specific adsorption of cations at EP Cd(0 0 0 1) plane. For that reason, all the kinetic data for less concentrated base electrolyte solutions $c_{NaF} \leq 3 \times 10^{-2}$ M were calculated from the experimental $j, E$ curves within the range $-1.6 \leq E \leq -1.2$ V (4 M CE), taking into account the current densities in the base electrolyte solution, i.e. the current densities for the pure NaF solution (Fig. 1b) were subtracted from the $j, E$ curves for the Na$_2$S$_2$O$_8$ + NaF solution (Fig. 1c). According to the data in Figs. 1(a) and 2, the rate of electroreduction of S$_2$O$_8$$^{2-}$ to SO$_4$$^{2-}$ depends


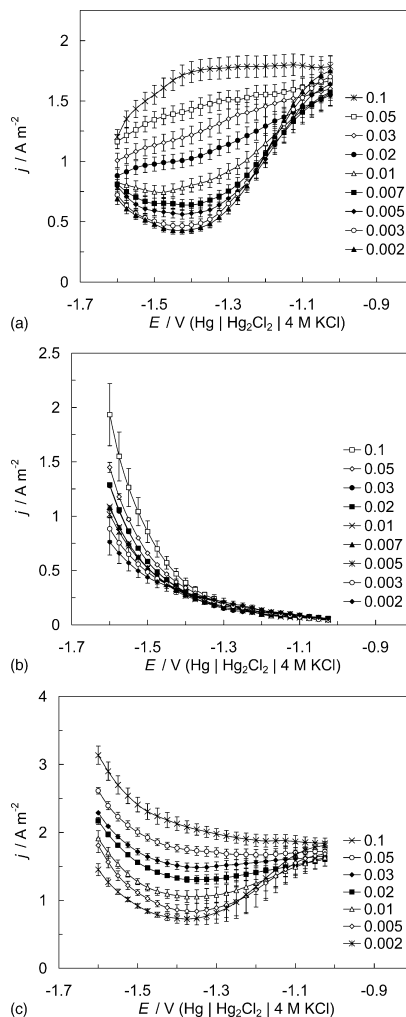
Fig. 1. Rotating disc voltammetry curves (scan rate 10 mV s$^{-1}$; rotation velocity $\nu = 9000$ rev min$^{-1}$) for the electrochemically polished Cd(0 0 0 1) plane in $4 \times 10^{-5}$ M Na$_2$S$_2$O$_8$ + $x$ M NaF solution (noted in figure) corrected for the base electrolyte current densities in the different base electrolyte solutions (b); and curves for $4 \times 10^{-5}$ M Na$_2$S$_2$O$_8$ in the base electrolyte solution with different concentrations (noted in figure) (c).

noticeably on the electrode potential, as well as on the base electrolyte concentration. Differently from Au electrodes [18–21] no hysteresis of current density between the negative and positive scans of potential was observed in the region
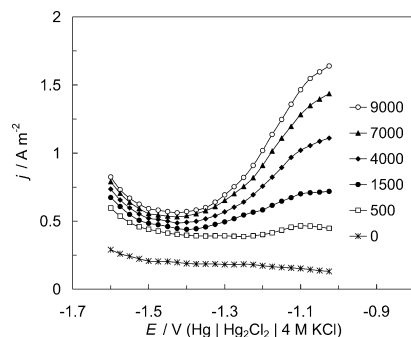
Fig. 2. Rotating disc voltammetry curves (corrected for the base electrolyte current densities; scan rate $10\,\mathrm{mV\,s^{-1}}$) for the electrochemically polished Cd(0 0 0 1) plane in $4 \times 10^{-5}$ M $Na_2S_2O_8 + 0.01$ M NaF solution at various rotation velocities $\nu$ (rev min$^{-1}$), noted in figure.

of mixed kinetics if $c_{Na_2S_2O_8} \leq 4 \times 10^{-5}$ M. In the region of zero charge potential ($-1.1 \leq E \leq -0.9$ V (4 M CE)), the very well exposed current plateaus were found. The current density values ($j$) at $E = $ const. measured at the rotating EP Cd(0 0 0 1) disc electrode (corrected for the current densities for the base electrolyte solution) were found to fit very well to the Levich ($j$, $\omega^{1/2}$) plot [31,32] ($0.997 \leq R^2 \leq 0.999$)

$$j_d = 0.620 n_i F \upsilon^{-1/6} D^{2/3} \omega^{1/2} c_i \quad (5)$$

where $j_d$ is the limiting current density, $n_i$ the number of electrons consumed in the reaction of the ion $i$; $c_i$ the bulk concentration of the discharging ion; $\upsilon$ the kinematic viscosity; $\omega$ the angular frequency and $D$ is the diffusion coefficient. Taking $n_i = 2$ and $\nu = 0.01$ cm$^2$ s$^{-1}$ [1–9], the diffusion coefficient values of the peroxodisulfate anion have been calculated ($D = 1.1 \times 10^{-5}$ cm$^2$ s$^{-1}$ for a $1 \times 10^{-2}$ M NaF solution) in a good agreement with literature data [1–9]. Thus, in this region of potentials, the electroreduction of the $S_2O_8^{2-}$ anion on the EP Cd(0 0 0 1) plane is mainly limited by the diffusion step of the $S_2O_8^{2-}$ anions to the electrode surface.

According to Figs. 1(a) and 2, with increasingly negative polarisation ($E < -1.2$ V versus 4 M CE), the inhibition of $S_2O_8^{2-}$ electroreduction begins, caused by the rise of the negative value of the $\psi_1$ potential. In the dilute NaF solutions a minimum of current density at $-1.5 \leq E_{min} \leq -1.3$ V (4 M CE) was found. At more negative surface charge densities ($E \leq -1.4$ V (4 M CE)), acceleration of $S_2O_8^{2-}$ anion electroreduction occurs as $d\psi_1/dE \approx$ const. in this potential region. Acceleration of reaction is mainly caused by the increase of the negative electrode potential, as well as, probably, by the beginning of the weak specific adsorption of the base electrolyte cations at the negatively charged EP Cd(0 0 0 1) electrode surface ($E \leq -1.4$ V versus 4 M CE). This result is in a good agreement with the impedance data as in this region of potentials ($E < -1.4$ V (4 M CE)) the weak rise of the differential capacitance values with $c_{NaF}$

was observed [45,46]. It should to be noted that the values of differential capacitance in the 0.1 M NaF solution are higher than those in 0.1 M LiClO$_4$ solution ($\Delta C \sim 1.0\,\mu\mathrm{F\,cm^{-2}}$), demonstrating that weak specific adsorption of the Na$^+$ ions is possible on the EP Cd(0 0 0 1) plane at $E \leq -1.4$ V (versus 4 M CE). In this region of potentials, the current density mainly linearly increases with increase of the base electrolyte concentration (Figs. 1(a) and 2). Thus, at the very negatively charged Cd(0 0 0 1) surface the exchange of the electroreduction mechanism of $S_2O_8^{2-}$ anions is possible, i.e. additionally to the usual charge transfer process the simultaneous charge transfer through the adsorbed ion-pairs is probable. It should be noted that for more concentrated base electrolyte solutions ($c_{NaF} \geq 3 \times 10^{-2}$ M), the corrected current densities are lower than the limiting diffusion currents at $E > -1.2$ V (versus 4 M CE). This effect can be explained by adsorption of the Na$^+$ ions and co-adsorption of the $S_2O_8^{2-}$ ions [34,35] and by formation of the Na$^+S_2O_8^{2-}$ ion pairs in the inner layer region of the electrical double layer (i.e. by the so-called "surface blocking effect", caused by adsorption of the reactants). This effect seems to be important only for the more concentrated base electrolyte systems because the adsorption of Na$^+$ cations is weak. However, it should be noted that for more detailed analysis the systematic impedance data are inevitable in addition to cyclic voltammetry and rotating disc electrode data and these measurements are in progress now.

### 3.2. Kinetic analysis

The apparent rate constant of the heterogeneous reaction of the electroreduction of $S_2O_8^{2-}$ anions, $k_{het}$, was defined by Eq. (6)

$$j_k = n_i F k_{het} c_i \quad (6)$$

where $j_k$ is the kinetic current density. The kinetic current density values at $E = $ const. were obtained from the linear Koutecky–Levich plots ($0.994 \leq R^2 \leq 0.999$) [5–9].

Fig. 3 demonstrates the statistically treated log $k_{het}$, $E$ dependences for EP Cd(0 0 0 1) plane (obtained from the current densities corrected for the base electrolyte current densities). As it can be seen, log $k_{het}$ decreases with dilution of the base electrolyte but the decrease of $k_{het}$ is somewhat smaller than that predicted according to the Frumkin slow charge transfer theory [4–7]. Statistical analysis of the log $k_{het}$, $E$ plots shows that the values of log $k_{het}$ do not depend on the reactant concentration if $c_{S_2O_8^{2-}} \leq 5 \times 10^{-5}$ M. At higher $c_{S_2O_8^{2-}}$ the small decrease of log $k_{het}$ begins at fixed $E$ more pronounced at less negatively charged EP Cd(0 0 0 1), indicating the possible weak adsorption of the reactant on the EP Cd(0 0 0 1) plane (i.e. the so-called surface blocking effect [18–20] has been established caused by the adsorption of the $S_2O_8^{2-}$ anions or reaction intermediates at Cd(0 0 0 1)). For that reason only the data for $c_{S_2O_8^{2-}} \leq 5 \times 10^{-5}$ M have been used for the quantitative analysis. The heterogeneous rate
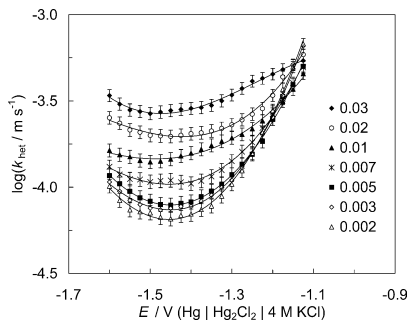
Fig. 3. Heterogeneous rate constant vs. electrode potential dependences (obtained from the $j$, $E$ curves corrected for the base electrolyte current densities) for electrochemically polished (EP) Cd(0 0 0 1) electrode in $4 \times 10^{-5}$ M $Na_2S_2O_8$ solution with different additions of the base electrolyte NaF (M), noted in figure.

constant values for Au($h\,k\,l$) [19,20] are somewhat higher than that for the EP Cd(0 0 0 1) plane. The heterogeneous rate constant values for Bi($h\,k\,l$) are on the same order as for EP Cd(0 0 0 1) electrode but for Bi(1 1 1) the dependence of $k_{het}$ on $c_{NaF}$ is comparatively weak [35].

### 3.3. Corrected Tafel plots

The corrected Tafel plots have been calculated using various empirical approximations for the $\psi_1$ potential value [1–9,37–42]. At first the classical Frumkin approximation was used (i.e. it was assumed that $\psi_1 = \psi_d$ and $z_i = -2$ for the $S_2O_8{}^{2-}$ anion). As it can be seen from Fig. 4, there is a noticeable dependence of the corrected kinetic current density values on the base electrolyte concentration, and the cTp values at fixed $(E - \psi_d)$ decrease with increasing $c_{NaF}$. The slope of the cTp, giving the value of the apparent transfer coefficient $\alpha_{app}$, decreases with increasing $c_{NaF}$ ($\alpha_{app} = 0.14$ for 0.002 M NaF and $\alpha_{app} = 0.1$ for 0.03 M NaF) (Fig. 4(b)). It should be noted that the charge transfer mechanism through the adsorbed ion-pairs has been discussed by Frumkin and coworkers [2–9]. The data in Fig. 5 shows that noticeably less pronounced dependence of the corrected kinetic current values on $c_{NaF}$ has been established if the ion-pair formation at the outer Helmholtz plane (i.e. in the reaction zone) has been taken into account [7–9]. Thus, if we assume that $z_i = -1$ and $\psi_1 = \psi_d$ then there is a very good concordance of the cTps in the region 0.005 M $\leq c_{NaF} < 0.03$ M and in the region of moderate surface charge densities $\sigma \approx -7.0$ to $-2.0\,\mu C\,cm^{-2}$ ($-1.0 < E - 1.25$ V versus 4 M CE). However, the cTps are nonlinear near the zero charge potential. At $E \ll E_{\sigma=0}$, the noticeable dependence of cTps on $c_{NaF}$ has been established, indicating the dependence of $\alpha_{app}$ on $c_{NaF}$ (Fig. 4(b)). Thus, according to the data in Figs. 4(b) and 5, the higher $\alpha_{app}$ values correspond to the less concentrated base electrolyte solutions.
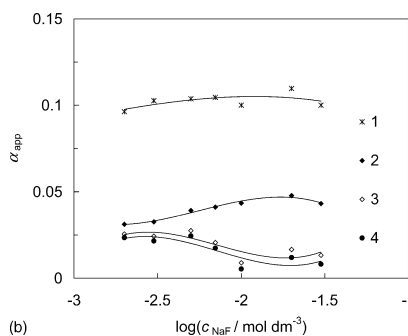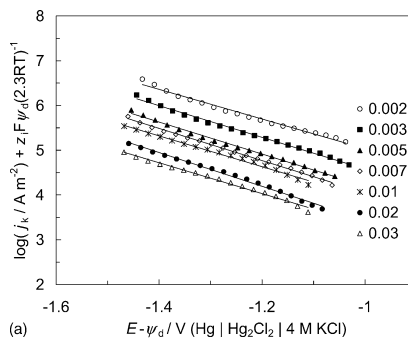


(a)

(b)

Fig. 4. (a) Corrected Tafel plots (cTp) ($z_i = -2$ and $\psi_1 = \psi_d$, i.e. classical Frumkin correction) for the EP Cd(0 0 0 1) plane in $4 \times 10^{-5}$ M $Na_2S_2O_8$ solutions with different additions of NaF (M), noted in figure. (b) Apparent transfer coefficient vs. log $c_{NaF}$ dependences calculated at various approximations of the $\psi_1$ potential: $z_i = -2$, $\psi_1 = \psi_d$ (1); $z_i = -1$, $\psi_1 = \psi_d$ (2); $z_i = -2$ and $\psi_x$ calculated according to Eq. (3) at the fixed distances of reaction site from the outer Helmholtz plane, $x$ (nm): (3) 0.20 and (4) 0.43.
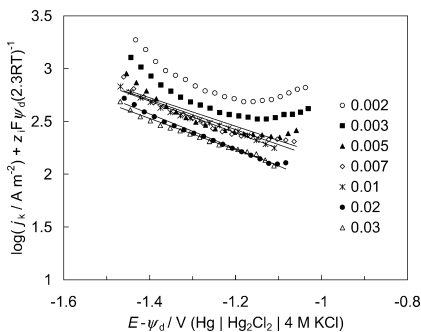


Fig. 5. Corrected Tafel plots for the EP Cd(0 0 0 1) plane in $4 \times 10^{-5}$ M $Na_2S_2O_8$ solutions with different additions of NaF (M, noted in figure) at $z_i = -1$ and $\psi_1 = \psi_d$.

As mentioned in Ref. [41] the ionic association process of the polycharged complex anions (including $S_2O_8^{2-}$ anions) with the base electrolyte cations is possible in the solution phase. The ionic association process in the solution phase has been simulated according to the Fuoss equation [56]

$$K_A = \frac{4\pi N_A a^3 e_0^b}{3000} \tag{7}$$

where $b = e_0^2/a\varepsilon kT$, $e_0$ the elementary charge, $\varepsilon$ the dielectric constant of the solvent and $N_A$ is the Avogadro number. The values of the association constant $K_A$, calculated according to Eq. (7) assuming that the distance of the closest approach of various ions $a = 0.36$, 0.6 and 0.8 nm, are comparatively low ($K_A = 0.118$ for 0.36 nm). As shown in Ref. [41], the association of the ions can be a reason for the possible simultaneous electroreduction of the variously charged species. In these conditions, the kinetic current density is expressed as [41]

$$j_k = kc_1 \exp\left[\frac{-\alpha(E - \psi_d)F}{RT}\right] \exp\left[\frac{-z_i F \psi_d}{RT}\right]$$
$$+ k_A c_2 \exp\left[\frac{(-z_i + 1)(F\psi_d)}{RT}\right] \tag{8}$$

where $z_i = -2$ (charge of the $S_2O_8^{2-}$ anion) and $(z_i + 1)$ is the charge of associated $S_2O_8^{2-}$ anion with $Na^+$ (base electrolyte cation); $k_A$ the relative rate constant for the reduction reaction of the reactant(s) with $(z_i + 1) = -1$ ($NaS_2O_8^-$); $c_1$ and $c_2$ are the effective volume concentrations of the $S_2O_8^{2-}$ anion and $NaS_2O_8^-$ ion complex, respectively; and $k$ is the rate constant [41]. The results calculated by Eq. (8) demonstrate a very large difference between the cTps for 0.002 and 0.03 M NaF solutions, and therefore, the ionic association in the solution phase has not a remarkable influence on the shape and coincidence of cTps for the $Cd(0001) \mid Na_2S_2O_8 + NaF$ system.

According to the results of classical works [4,5,7,43,44], the linear corrected Tafel plots for $Hg \mid S_2O_8^{2-}$ system were obtained if it was assumed that the reaction site lies in the inner layer (i.e. $x_i - x_d < 0$) but for $Hg \mid [Fe(CN)_6]^{3-}$ system the reaction site has to lie in the diffuse layer ($x = x_i - x_d > 0$). The results of simulation of the data for the EP $Cd(0001) \mid NaF + Na_2S_2O_8$ system shows that in spite of the selected fixed values of $x = x_i - x_d > 0$ (0, 0.23, 0.43, 0.68 nm) in Eq. (3) the cTps obtained for EP $Cd(0001)$ are nonlinear and there is no concordance for cTps measured in a wide concentration region (Fig. 6). The values of the apparent transfer coefficient are comparatively low and depend on concentration of the base electrolyte in the solution (Fig. 4(b)).

Analysis of the experimental Tafel plots shows that the coincidence and linearity of the cTps can be obtained if we assume that the distance of the closest approach of the reacting anions to the EP $Cd(0001)$ plane surface, $x = x_i - x_d$, depends on the base electrolyte concentration (i.e. $x = f(c_{NaF})$). Analysis of the Tafel plots shows
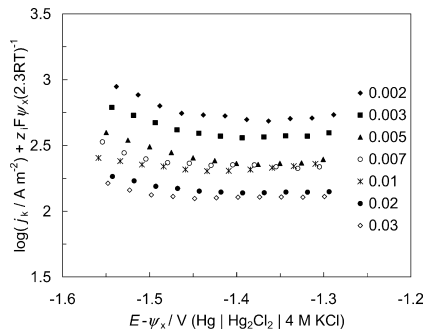


Fig. 6. Corrected Tafel plots calculated according to Eq. (3) ($z_i = -2$ and $\psi_1 = \psi_x$) for the EP $Cd(0001)$ plane in $4 \times 10^{-5}$ M $Na_2S_2O_8$ solutions with different additions of NaF (M, noted in figure) at the fixed distance $x = 0.2$ nm of the reaction site from the outer Helmholtz plane.

that the concordance of cTps can be reached if the term in the last brackets of Eq. (3) $[-\kappa(x_i - x_d)] \approx$ const. at $E = $ const. Thus, if we assume that the diffuse layer theory is correct [47–50] (and the Gouy length $\kappa$ can be calculated using this theory) and the value of the $\psi_x$ potential at the reaction site can be calculated using Eq. (3) then it is possible to calculate the effective distance values of the reaction site from the outer Helmholtz plane $x = f(c_{NaF})$, assuming that the cTps have to be linear and coincide for different $c_{NaF}$. The results in Fig. 7(a) show that this is valid if we assume that $x$ is an exponential function of the base electrolyte concentration (Fig. 7(b)). Thus, if this effect has a real physical background then we can conclude that the effective distance of the reaction site from the EP $Cd(0001)$ surface (as well as from the outer Helmholtz plane) increases exponentially with diluting the electrolyte solution, i.e. with increasing the effective ion atmosphere according to the Debye–Hückel theory. However, the better fit of the experimental data has been established in the case of comparatively small $x$ values (Fig. 7(b)) and thus, the reaction site lies not far from the outer Helmholtz plane for the EP $Cd(0001)$ plane. The weak dependence of the effective distance of the reaction site on the base electrolyte concentration can be explained by the so-called "squeezing out" effect [5,47,48], i.e. by the dependence of the distance of the closest approach [47,57,58] of the reacting ions to the electrode on the base electrolyte concentration, but for more detailed analysis the experimental data in other base electrolyte solutions are needful. It should be noted that there are deviations from the classical Gouy–Chapman–Grahame model for $Bi(hkl)$ and $Cd(hkl)$ electrodes in NaF solutions with different concentration [45–49], i.e. the inner layer capacitance depends on the electrolyte concentration. The electrical double layer (i.e. $\psi_d$-potential) correction for the systems with the weak specific adsorption of anions is a very complicated problem even for systems with
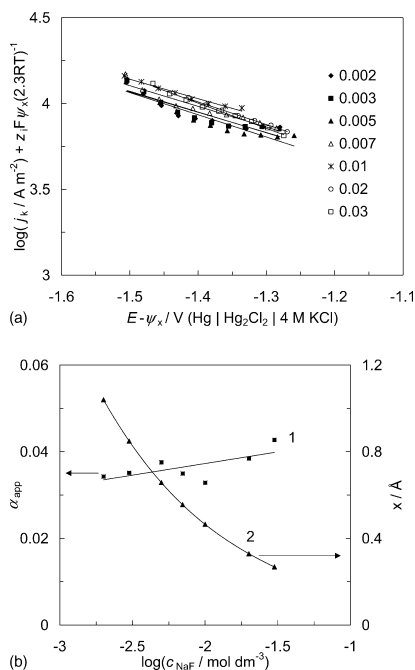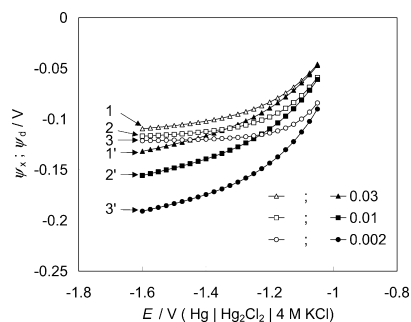
(a)



Fig. 8. Dependences of the classical Gouy–Chapman $\psi_d$ potential ($1'$–$3'$) on $E$ and of the effective $\psi_x$ potential (1–3) on $E$ (used for the calculation of cTps in Fig. 7(a)) at the conditions $x = f(c_{NaF})$ and the term $[-\kappa x] = $ const. in Eq. (3).



(b)

Fig. 7. (a) Corrected Tafel plots calculated according to Eq. (3) ($z_i = -2$ and $\psi_1 = \psi_x$) for the EP Cd($0\,0\,0\,1$) plane in $4 \times 10^{-5}$ M Na$_2$S$_2$O$_8$ solutions with different additions of NaF (M, noted in figure), assuming that $x = f(c_{NaF})$ and the term $[-\kappa x] = $ const. in Eq. (5). (b) The corresponding dependences of the apparent transfer coefficient $\alpha_{app}$ (1) and effective distance of the reaction site from the outer Helmholtz plane (2) on the base electrolyte concentration.

the constant ionic strength where is no electrochemical reaction [59–62]. The systematic analysis of experimental data for Bi($h\,k\,l$) [59–62] as well as Cd($0\,0\,0\,1$) electrodes [63] shows that the $\psi_d$-potential values calculated using classical Gouy–Chapman–Grahame model [53–55] are overestimated (i.e. negative values of $\psi_d$ are too large to give the linear corrected virial isotherms). The situation is more complicated for the systems with the smaller ionic strength. Thus, it can be concluded that the classical $\psi_d$ potential corrections are too high to give the concordance for the cTps at $\sigma \ll 0$ within the wide base electrolyte concentration region. This conclusion is in a good agreement with the results for [Co(NH$_3$)$_6$]$^{3+}$ and [Fe(CN)$_6$]$^{3-}$ electroreduction on Bi($h\,k\,l$) and Cd($0\,0\,0\,1$) electrodes [64,65] as well as for S$_2$O$_8^{2-}$ electroreduction on Bi($1\,1\,1$) plane [35].

Comparison of the $\psi_d$ values with the $\psi_x$ potential values, calculated according to Eq. (3) assuming that $x = f(c_{NaF})$, shows (Fig. 8) that the values of $|\psi_x|$ are somewhat lower than $|\psi_d|$ and at very high negative surface charge den-

sity values ($E < -1.4$ V versus 4 M CE) there is only a weak dependence of $\psi_x$ on $c_{NaF}$ if $c_{NaF} \geq 5 \times 10^{-3}$ M. Thus, at comparatively negative surface charge densities the influence of diffuse layer on the charge transfer kinetics is very small caused probably by the charge transfer through the adsorbed ion-pairs [5,7,30–32]. For a more detailed analysis the impedance data as well as the theoretical quantum-chemical calculations are inevitable.

The data in Fig. 7(b) show that the values of transfer coefficient $\alpha_{app}$, obtained from Fig. 7(a), are practically independent of the base electrolyte concentration. The very low values of $\alpha_{app}$ for the EP Cd($0\,0\,0\,1$) | NaF + Na$_2$S$_2$O$_8$ system indicates that the activationless electroreduction process is probably possible at high negative surface charge densities (i.e. at $E \ll E_{\sigma=0}$), which is in a good agreement with the Levich model [31,32] and Petrii and coworkers analysis data for the Hg electrode [27,51].

## 4. Conclusions

The influence of the base electrolyte concentration and electrode polarisation on the electroreduction of the peroxodisulfate anion at the electrochemically polished Cd($0\,0\,0\,1$) plane has been studied by cyclic voltammetry and rotating disc electrode methods. The rate constant of the heterogeneous electroreduction reaction of the S$_2$O$_8^{2-}$ anion on the EP Cd($0\,0\,0\,1$) plane dependent on the base electrolyte concentration and electrode polarisation has been established. It was found that there is a dependence of the kinetic parameters on the chemical nature of the metal studied. The values of apparent transfer coefficient $\alpha_{app}$ corrected for the double layer effect, noticeably lower than 0.5 for the EP Cd($0\,0\,0\,1$) plane, only very weakly depend on the electrode potential but noticeably on the electrolyte concentration, decreasing with the base electrolyte concentration. The different models for the calculation of the

21

diffuse layer potential correction of the kinetic current density have been used to construct the so called corrected Tafel plots. The coincidence of the corrected Tafel plots for the solutions with different base electrolyte concentrations has been established if the effective distance of the reaction site from the outer Helmholtz plane is assumed to be inversely proportional to the base electrolyte concentration in the solution. The very low values of the apparent charge transfer coefficient show that the activationless charge transfer mechanism is probably valid for EP Cd(0 0 0 1) | NaF + Na$_2$S$_2$O$_8$ aqueous solution interface in a good agreement with the theoretical models for the high hydrogen overvoltage metals (mainly the Hg electrode) based on the diabatic charge transfer mechanism from the metal to an ion.

## References

[1] A.N. Frumkin, G.M. Florianovich, Dokl. Akad. Nauk SSSR 80 (1951) 907.

[2] G.M. Florianovich, A.N. Frumkin, Zh. Fiz. Khim. 29 (1955) 1827.

[3] O.A. Petrii, A.N. Frumkin, Dokl. Akad. Nauk SSSR 146 (1962) 1121.

[4] A.N. Frumkin, O.A. Petrii, Dokl. Akad. Nauk SSSR 147 (1962) 418.

[5] A.N. Frumkin, Potentsialy nulevogo zaryada (The Potentials of Zero Charge), Nauka, Moscow, 1979.

[6] A.N. Frumkin, Z. Elektrochem. 59 (1955) 807.

[7] A.N. Frumkin, Elektrodnye protsessy (The Electrode Processes), Nauka, Moscow, 1987.

[8] N.V. Fedorovich, A.N. Frumkin, Kh.E. Keis, Collect. Czech. Chem. Commun. 36 (1971) 722.

[9] A.N. Frumkin, N.V. Nikolaeva-Fedorovich, N.P. Berezina, Kh.E. Keis, J. Electroanal. Chem. 58 (1975) 189.

[10] N.V. Nikolaeva-Fedorovich, M.D. Levi, S.I. Kulakovskaya, Elektrokhimiya 13 (1977) 904.

[11] N.V. Fedorovich, F.S. Sarbash, Dokl. Akad. Nauk SSSR 255 (1980) 923.

[12] M.D. Levi, N.V. Fedorovich, B.B. Damaskin, Can. J. Chem. 59 (1981) 2019.

[13] L. Gierst, in: E. Yeager (Ed.), in: Transactions of the Symposium on Electrode Processes, Wiley, New York, 1961, 109 pp.

[14] W. Fawcett, S. Levie, J. Electroanal. Chem. 43 (1973) 301.

[15] W. Fawcett, D. Bieman, M. Mackey, Collect. Czech. Chem. Commun. 36 (1971) 503.

[16] W. Fawcett, J. Electroanal. Chem. 22 (1969) 19.

[17] P. Delahay, A. Aramata, J. Phys. Chem. 66 (1962) 1194.

[18] Z. Samec, K. Doblhofer, J. Electroanal. Chem. 367 (1994) 141.

[19] Z. Samec, K. Doblhofer, J. Electroanal. Chem. 409 (1996) 165.

[20] Z. Samec, K. Doblhofer, J. Electroanal. Chem. 432 (1997) 205.

[21] Z. Samec, K. Kirscher, K. Doblhofer, J. Electroanal. Chem. 499 (2001) 129.

[22] R.R. Nazmutdinov, G.A. Tsirlina, Yu.I. Kharkats, O.A. Petrii, M. Probst, J. Phys. Chem. 52 (1998) 677.

[23] W.R. Fawcett, in: J. Lipkowski, P.N. Ross (Eds.), Electrcatalysis, Wiley, New York, 1998 (Chapter 8).

[24] J.-M. Saveant, J. Am. Chem. Soc. 114 (1992) 10595.

[25] D.M. Stanbury, Adv. Inorg. Chem. 33 (1989) 69.

[26] J. Song, H. Fu, W. Guo, J. Electroanal. Chem. 511 (2001) 31.

[27] R.R. Nazmutdinov, D.V. Gluhov, G.A. Tsirlina, O.A. Petrii, Elektrokhimiya 38 (2002) 812.

[28] R.R. Nazmutdinov, G.A. Tsirlina, Y.I. Kharkats, O.A. Petrii, M. Probst, J. Phys. Chem. B 102 (1998) 627.

[29] W.R. Fawcett, M. Hromadova, G.A. Tsirlina, R.R. Nazmutdinov, J. Electroanal. Chem. 498 (2001) 93.

[30] B.B. Damaskin, E.V. Stenina, O.A. Baturina, L.N. Sviridova, Elektrokhimiya 34 (1998) 1083.

[31] V.G. Levich, Fiziko-khimicheskaya gidrodinamika (Physicochemical Hydrodynamics), Fizmatgiz, Moscow, 1959, 161 pp.

[32] V.G. Levich, Dokl. Akad. Nauk SSSR 124 (1959) 869.

[33] W.R. Fawcett, in: J. Lipkowski, P.N. Ross (Eds.), Electrocatalysis, Wiley-VCH, New York, 1998, pp. 323–371.

[34] T. Thomberg, E. Lust, J. Electroanal. Chem. 485 (2000) 89.

[35] E. Lust, R. Truu, K. Lust, Russ. Electrochem. 36 (2000) 1195.

[36] R. Gonzalez, F. Sanz, Electroanalysis 9 (1997) 169.

[37] P. Delahay, Double Layer and Electrochemical Kinetics, Interscience, New York, 1965.

[38] G.A. Tsirlina, Y.I. Kharkats, R.R. Nazmutdinov, O.A. Petrii, Russ. J. Electrochem. 35 (1999) 23.

[39] G.A. Tsirlina, O.A. Petrii, Y.I. Kharkats, A.M. Kuznetsov, Russ. J. Electrochem. 35 (1999) 1372.

[40] R.R. Nazmutdinov, I.V. Pobelov, G.A. Tsirlina, O.A. Petrii, J. Electroanal. Chem. 491 (2000) 126.

[41] G.A. Tsirlina, N.V. Titova, R.R. Nazmutdinov, O.A. Petrii, Russ. J. Electrochem. 37 (2001) 21.

[42] R.R. Nazmutdinov, G.A. Tsirlina, Y.I. Kharkats, O.A. Petrii, A.M. Kuznetsov, Electrochim. Acta 45 (2000) 3521.

[43] A.N. Frumkin, O.A. Petrii, N.V. Nikolayeva-Fedorovich, Dokl. Akad. Nauk SSSR 128 (1959) 1006.

[44] O.A. Petrii, N.V. Nikolayeva-Fedorovich, J. Fhiz. Khim. 35 (1961) 1999.

[45] E. Lust, K. Lust, A. Jänes, J. Electroanal. Chem. 413 (1996) 111.

[46] E. Lust, A. Jänes, K. Lust, M. Väärtnõu, Electrochim. Acta 42 (1997) 771.

[47] S. Trasatti, E. Lust, in: R.E. White, B.E. Conway, J.O'M. Bockris (Eds.), Modern Aspects of Electrochemistry, vol. 33, Kluwer Academic/Plenum Publishers, New York, London, 1999, 1 pp.

[48] E.J. Lust, A.A.-J. Jänes, K.K. Lust, J.J. Ehrlich, Russ. J. Electrochem. 32 (1996) 597.

[49] E.J. Lust, K.K. Lust, A.A.-J. Jänes, Russ. J. Electrochem. 31 (1995) 807.

[50] W. Schmickler, Interfacial Electrochemistry, Oxford University Press, New York, Oxford, 1996, pp. 215–274.

[51] G.A. Tsirlina, O.A. Petrii, R.R. Nazmutdinov, D.V. Gluhov, Russ. J. Electrochem. 38 (2002) 154.

[52] G. Nurk, A. Jänes, K. Lust, E. Lust, J. Electroanal. Chem. 515 (2001) 17.

[53] G. Gouy, J. Phys. Radium 9 (1910) 457.

[54] D. Chapman, Phil. Magn. 25 (1913) 475.

[55] D.C. Grahame, Chem. Rev. 41 (1947) 441.

[56] R.M. Fuoss, J. Am. Chem. 80 (1958) 5059.

[57] S. Amokrane, J.P. Badiali, J. Electroanal. Chem. 266 (1989) 21.

[58] S. Amokrane, J.P. Badiali, in: R.E. White, J.O'M. Bockris, B.E. Conway (Eds.), Modern Aspects of Electrochemistry, vol. 22, Plenum Press, New York, 1991, 1 pp.

[59] B. Damaskin, U. Palm, M. Väärtnõu, J. Electroanal. Chem. 70 (1976) 103.

[60] U.V. Palm, B.B. Damaskin, Itogi nauki i tekhniki, vol. 12, VINITI, Moscow, 1977, 99 pp.

[61] K. Lust, M. Väärtnõu, E. Lust, Electrochim. Acta 45 (2000) 3543.

[62] K. Lust, E. Lust, E. Lust, Influence of geometrical structure of the anions on the adsorption parameters at the Bi(0 0 1) electrode, J. Electroanal. Chem. 552 (2003) 129.

[63] K. Lust, E. Lust, Adsorption of halide ions on electrohemically polished Cd(0 0 0 1) plane (in preparation).

[64] R. Jäger, E. Härk, P. Möller, J. Nerut, K. Lust, E. Lust, The kinetics of eletroreduction of hexaamminecobalt(III) cation on Bi planes in aqueous HClO$_4$ solutions, J. Electroanal. Chem., in press.

[65] J. Nerut, P. Möller, E. Lust, Electroreduction of hexacyanoferrat(III) anions on electrochemically polished Cd(0 0 0 1) plane, Electrochim. Acta, in press DOI:10.1016/j.electacta.2003.11.021

**III**

ELSEVIER

# Impedance spectroscopy data for $S_2O_8^{2-}$ anions electroreduction kinetics at Cd(0001) plane electrode

Thomas Thomberg, Jaak Nerut, Enn Lust *

*Institute of Physical Chemistry, University of Tartu, 2 Jakobi Street, 51013 Tartu, Estonia*

## Abstract

Kinetics of electroreduction of peroxodisulfate anions on electrochemically polished single crystal Cd(0001) electrode has been studied using impedance spectroscopy. The influence of the electrode potential, the electrolyte as well as reactant concentrations on the kinetic parameters has been established. The fitting analysis of results demonstrates the influence of adsorption of the base electrolyte as well as reactant components (Na$^+$ or ion complex at more negative electrode potentials and $S_2O_8^{2-}$ or reaction intermediates at less negative surface charge densities) on the electroreduction rate of the $S_2O_8^{2-}$ anions.
© 2005 Elsevier B.V. All rights reserved.

## 1. Introduction

Electroreduction kinetics of the $S_2O_8^{2-}$ and $[Fe(CN)_6]^{3-}$ anions at Bi($hkl$) and Cd(0001) planes from various base electrolyte solutions has been studied [1–4] and it was found that there are some deviations from the simplified version of Frumkin slow discharge theory [5–9] where the specific adsorption of reacting particles has not been taken into account. For the more detailed analysis of $S_2O_8^{2-}$ electroreduction mechanism, the impedance spectroscopy method [10–17] has been used in this work for studying the complicated electroreduction reaction mechanism of $S_2O_8^{2-}$ anions to the $SO_4^{2-}$ anions at the Cd(0001) electrode with the high hydrogen evolution overpotential, i.e., at the so-called Hg-like (Bi, Sb, Sn, Pb, Cd and Zn) electrode [1–9].

Rate of the heterogeneous charge transfer reaction

$$Ox + ze^- \underset{k_b}{\overset{k_f}{\longleftrightarrow}} Red \qquad (1)$$

is given by the expression

---

* Corresponding author. Tel.: +372 7375 165; fax: +382 7375 160.
  *E-mail address:* enn.lust@ut.ee (E. Lust).

$$-j_F = zF[k_f c_{Ox} - k_b c_{Red}], \qquad (2)$$

where $j_F$ is the Faradaic current density, $k_f$ and $k_b$ are the forward and reverse rate constants, $z$ is the charge number of the electrons transferred in reaction, $c_{Ox}$ and $c_{Red}$ are the concentrations of reactant (oxidiser) and product (reductant), respectively [9–24]. Using impedance spectroscopy method, the current is composed of a steady-state (or direct) part (determined by the mean dc potential $E$ and the mean dc concentrations at the interface, $c_{Ox}$ and $c_{Red}$) and an ac part $\Delta j_F$ (determined by the ac perturbing signal $\Delta E$ and concentration fluctuations, $\Delta c_{Ox}$ and $\Delta c_{Red}$). The Faradaic impedance is given by the ratio of the Laplace transform of the ac parts of the voltage and current density [10–24]

$$Z_F = \{\Delta E\}/\{\Delta j_F\}. \qquad (3)$$

The presence of an electric field at the interface affects differently the energies of the variously charged species as they approach the interfacial region [5–12]. Therefore, the activation energy barriers for the reaction depends on the potential difference across the interface. It is convenient to express the potential dependence of the rate constants in the following manner [6–13,23]:

$$k_f = k_0 \exp\left[-\alpha(E - E^0)\frac{nF}{RT}\right], \tag{4}$$

$$k_b = k_0 \exp\left[(1-\alpha)(E - E^0)\frac{nF}{RT}\right], \tag{5}$$

where $k_0$ is the rate constant at the formal electrode potential $E^0$, $\alpha$ is the apparent cathodic transfer coefficient and $n$ is a number of electrons transferred in the limiting step.

Generally $\Delta j_F$ is expressed as an expansion of the ac parts of the concentrations and electrode potential [10–23]

$$\Delta j_F = \sum\left(\frac{\partial j_F}{\partial c_i}\right)\Delta c_i + \left(\frac{\partial j_F}{\partial E}\right)\Delta E$$
$$+ \text{higher-order terms.} \tag{6}$$

Neglecting all but the first-order terms (linearisation) and solving for $\Delta E$

$$-\Delta E = \frac{1}{(\partial j_F/\partial E)}\left[\sum\left(\frac{\partial j_F}{\partial c_i}\right)\Delta c_i - \Delta j_F\right] \tag{7}$$

the Faradaic impedance has a form

$$Z_F = \frac{1}{(\partial j_F/\partial E)}\left[1 - \sum\left(\frac{\partial j_F}{\partial c_i}\right)\frac{\{\Delta c_i\}}{\{\Delta j_F\}}\right]. \tag{8}$$

The first term is the so-called charge transfer resistance $((\partial j_F/\partial E)^{-1} = R_{ct})$, the second term contains the influence of the ac part of the mass transfer step on the impedance. The value $\{\Delta c_i\}/\{\Delta j_F\}$ can be expressed as a solution of the diffusion equation and under condition of semi-infinite diffusion to a planar electrode [10–17,23]

$$\frac{\{\Delta c_i\}}{\{\Delta j_F\}} = \frac{1}{nF\sqrt{(pD_i)}}, \tag{9}$$

where $p$ is the complex frequency variable ($p = \sigma + j\omega$, where $\sigma$ is conductivity, j is imaginary unit, and $\omega = 2\pi f$, where $f$ is ac frequency) and $D_i$ is the diffusion coefficient of the particle $i$. Under equilibrium conditions the charge transfer resistance

$$R_{ct} = \frac{RT}{nFj_0}, \tag{10}$$

where the exchange current density is expressed as

$$j_0 = nFk_0c_{Ox} * \exp\left[-\alpha(E_r - E^0)\frac{nF}{RT}\right]$$
$$= nFk_0(c_{Ox}^*)^{1-\alpha}(c_{Red}^*)^\alpha. \tag{11}$$

For heterogeneous charge transfer (Faradaic) reaction involving one adsorbed particle [24] the following stages can be separated [23]:

$$A_{sol} + e^- \underset{k_{-1}}{\overset{k_1}{\rightleftarrows}} B_{ads}, \tag{12a}$$

$$B_{ads} + e^- \underset{k_{-2}}{\overset{k_2}{\rightleftarrows}} C_{sol}, \tag{12b}$$

where the indexes sol and ads denote the particles in solution and adsorbed state, respectively. The rates of these reactions may be written, assuming a Langmuir adsorption isotherm for B [23,24], as

$$v_1 = k_1^0\Gamma_s a_A \exp\left[-\alpha_1\frac{F}{RT}(E - E_1^0)\right]$$
$$- k_1^0\Gamma_B \exp\left[(1-\alpha_1)\frac{F}{RT}(E - E_1^0)\right], \tag{13a}$$

$$v_2 = k_2^0\Gamma_B \exp\left[-\alpha_2\frac{F}{RT}(E - E_2^0)\right]$$
$$- k_2^0\Gamma_s a_C \exp\left[(1-\alpha_2)\frac{F}{RT}(E - E_2^0)\right], \tag{13b}$$

where $k_1^0$ and $k_2^0$ are the standard rate constants of these reactions; $\alpha_1$ and $\alpha_2$ are the symmetry coefficients (transfer coefficients); $\Gamma_B$ and $\Gamma_s$ are the surface concentrations of the species B and of free adsorption sites $S$, respectively; $a_A$ and $a_C$ are the surface concentrations of A and C (assumed as equal to the bulk concentrations); and $E_1^0$ and $E_2^0$ are the standard redox potentials of the reactions 1 and 2, respectively. At equilibrium potential, $E_r$, the net rates of both reactions are zero and the following relations are obtained:

$$\exp\left[\frac{F}{RT}(E_r - E_1^0)\right] = \Gamma_s^0 a_A/\Gamma_B^0 = (1-\theta_0)a_A/\theta_0, \tag{14a}$$

$$\exp\left[\frac{F}{RT}(E_r - E_2^0)\right] = \Gamma_B^0/\Gamma_s^0 a_C = \theta_0/(1-\theta_0)a_A, \tag{14b}$$

where the index 0 indicates equilibrium conditions, and a following relation is introduced: $\Gamma_i = \theta_i\Gamma_{max}$ (where $\Gamma_{max}$ is the maximal surface concentration [24]).

The total current density observed is given as

$$j = F(v_1 + v_2) \tag{15}$$

and the Faradaic admittance is given by

$$\widehat{Y}_t = A + \frac{B}{j\omega + G}, \tag{16}$$

where the inverse charge transfer resistance $A = R_{ct}^{-1}$ is obtained as [23]

$$A = \frac{1}{RT}\left[\alpha_1\overrightarrow{k}_1(1-\theta) + (1-\alpha_1)\overleftarrow{k}_{-1}\theta + \alpha_2\overrightarrow{k}_2\theta\right.$$
$$\left. + (1-\alpha_2)\overleftarrow{k}_{-2}(1-\theta)\right] \tag{17a}$$

and

$$B = \frac{1}{RT\Gamma_{max}}\left(-\overrightarrow{k}_1 - \overleftarrow{k}_{-1} + \overrightarrow{k}_2 + \overleftarrow{k}_{-2}\right)\left[\alpha_1\overrightarrow{k}_1(1-\theta)\right.$$
$$\left. + (1-\alpha_1)\overleftarrow{k}_{-1}\theta - \alpha_2\overrightarrow{k}_2\theta - (1-\alpha_2)\overleftarrow{k}_{-2}(1-\theta)\right] \tag{17b}$$

and

$$G = \frac{1}{\Gamma_{max}}\left(\overrightarrow{k}_1 + \overleftarrow{k}_{-1} + \overrightarrow{k}_2 + \overleftarrow{k}_{-2}\right)$$
$$= \frac{F}{\sigma_1}\left(\overrightarrow{k}_1 + \overleftarrow{k}_{-1} + \overrightarrow{k}_2 + \overleftarrow{k}_{-2}\right). \tag{17c}$$

It should be noted that the quantity $F\Gamma_{max} = \sigma_1$ is the charge necessary for the total surface coverage by $B$. The more complicated cases, taking into account the slow diffusion step to the fractal and disc electrodes, have been discussed by Laisa et al. [23].

## 2. Experimental details

The Cd(0001) single crystal electrodes, electrochemically polished in 1:1 $H_3PO_4 + H_2O$ solution, have been studied in the region of electrode potential from $-1.0$ to $-1.6$ V vs. Ag|AgCl (all potentials have been measured vs. Ag|AgCl| aqueous saturated KCl solution reference electrode, noted as Ag|AgCl for simplicity), using electrochemical impedance and cyclic voltammetry [1–4,25–28]. The impedance spectra were measured at ac frequency from $1 \times 10^{-2}$ to $1 \times 10^{4}$ Hz and at ac voltage amplitude 5 mV, using the Autolab PGSTAT 20 FRA2 system [27]. Base electrolyte solutions were prepared from the triply recrystallised from the Milli-Q+ water $Na_2SO_4$ and $Na_2S_2O_8$ salts. The Milli-Q+ water was used for preparation of the solutions studied. Air was removed from the solutions by bubbling argon (Ar, 99.998%) through or over solution prior to or during measurements, respectively.

Electrochemically polished Cd(0001) single crystal plane electrode used was prepared according to the methods described in [2–4,25,28]. After the electrochemical polishing the Cd(0001) electrode was rinsed carefully with Milli-Q+ water and submerged into the solution at $E = -1.2$ V (vs. Ag|AgCl electrode in sat. KCl). Electrochemical measurements were performed at $T = 298$ K in a three-compartment glass cell with a separated platinum counter electrode, as well as by a separated (by Luggin capillary) reference electrode (Ag|AgCl electrode in sat. KCl).

## 3. Experimental results

### 3.1. Impedance data (Nyquist and Bode plots)

The impedance spectra were measured at ac frequency, $f$, from $1 \times 10^{-2}$ to $1 \times 10^{4}$ Hz within the region of the electrode potential $-1.6 < E < -1.0$ V. The complex plane impedance $Z''$, $Z'$ (i.e., Nyquist) plots are given in Figs. 1–5. The data in Figs. 1–3 show that the shape of the Nyquist plots depends on the electrode potential, as well as on the base electrolyte and reactant concentrations in the solution (Figs. 4 and 5). The similar behaviour of $Hg|S_2O_8^{2-}$ + base electrolyte system has been observed by Peter et al. [17,18]. At given base electrolyte ($Na_2SO_4$) concentrations, $c_{base.el.}$, the active ($Z'$) and imaginary ($Z''$) parts of impedance depend noticeably on concentration of the $S_2O_8^{2-}$ ions and on the electrode potential (Figs. 1–3). The so-called total polarisation resistance $R_p$, obtained from the difference between the high-frequency resistance $R_{ex}$ and low-frequency resistance $R_{lf}$, and $|Z''|$ increase with decreasing the negative potential. At fixed potential and base electrolyte concentration ($E = -1.6$ V, $c_{base.el.} = 10$ mM), $Z''$ and $R_p$ increase with decreasing $c_{S_2O_8^{2-}}$.

Differently from the data at $E > -1.5$ V (Figs. 2 and 3(a)) there is an additional semicircle in the Nyquist plots at $E$ $-1.6$ V (Fig. 1(a)) in the very high frequency region. Thus, at very negative potentials ($E \leqslant -1.6$ V) there is probably another very quick Faradaic reaction (probably hydrogen evolution or electroreduction of cation adsorbed
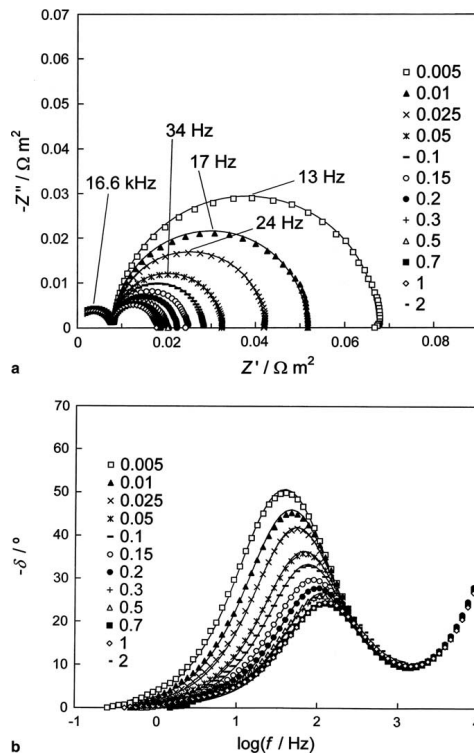


Fig. 1. Complex plane (a) and phase angle ($\delta$) vs. ac frequency plots (b) for the electrochemically polished (EP) Cd(0001) plane in aqueous 0.01 M $Na_2SO_4$ solution with different additions of $Na_2S_2O_8$ (mM), noted in figure, at the electrode potential $E = -1.6$ V vs. Ag|AgCl| sat. KCl (marks – experimental, solid lines – data calculated according to the circuit 'c' in Fig. 8).

or electroreduction of very small amounts of residual oxygen) at the Cd(0001) electrode. However, these very high frequency semicircles can be caused or influenced by the experimental artefacts connected with the uncompensated impedance of the reference electrode [23]. In any case, the shape of these very high frequency semicircles is very well reproducible, depends on the base electrolyte concentration (Fig. 4(a)) (i.e., on the total high frequency series resistance) as well as on the electrode potential (i.e., on the current density) and these semicircles are unimportant and undetectable at $E > -1.4$ V (Fig. 3(a)). It should be noted that the additional experimental studies by other experimental techniques (SNIFTIR, etc.) are inevitable for the more detailed analysis of the reaction mechanism at more negative potentials than $-1.6$ V.

The complex plane plots show complicated behaviour at low frequencies, deviation to lower (Figs. 1(a)) or higher
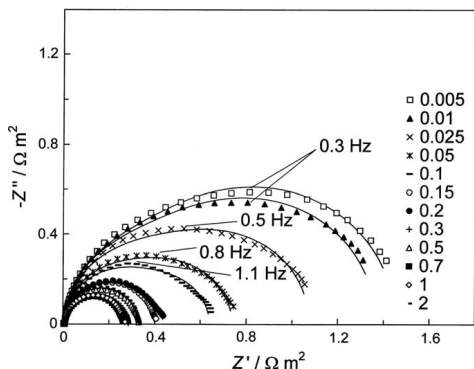
Fig. 2. Complex plane plots for the EP Cd(0 0 0 1) plane in aqueous 0.01 M $Na_2SO_4$ solution with different additions of $Na_2S_2O_8$ (mM), noted in figure, at $E = -1.3$ V vs. Ag|AgCl| sat. KCl (marks – experimental, solid lines – data calculated according to the circuit 'c' in Fig. 8).

(4(a)) $Z'$ values. This effect might be related to the changes of the impedance with time. However, the time stability of the system has been tested many times and in the region of potentials $E \geqslant -1.5$ V the time stability of system is good. The shape of the low-frequency part of $Z''$, $Z'$-plots depends on potential as well as on the reactant concentration and the decrease of $Z'$ with the decrease of frequency can be explained by the weak induction effect, possible to simulate with the equivalent circuit (d) in Fig. 8, i.e., with adsorption effect of the intermediate species at the electrode [23]. The adsorption of the intermediate species depends strongly on $E$ as well as concentration of $S_2O_8^{2-}$ ions in solution. According to the results obtained the migration effects are unimportant at $c_{\text{base electrolyte}} \geqslant 5 \times 10^{-3}$ M $Na_2SO_4$.

According to the data in Figs. 1(a), 2(a) and 3(a), the frequency of the main maximum in the $Z''$, $Z'$ plots ($f_{\max}$, given in figures) shifts toward lower values and the values of $|Z''|$ decrease with increasing $c_{S_2O_8^{2-}}$ in the solutions with given base electrolyte concentration. Thus, the characteristic time constant $\tau_{\max}$ obtained from experimental data ($\tau_{\max} = (2\pi f_{\max})^{-1}$), decreases with increasing $c_{S_2O_8^{2-}}$ (Figs. 6 and 7). The noticeable dependence of $\tau_{\max}$ on $c_{S_2O_8^{2-}}$ and the depressed shape of the low frequency region of the $Z''$, $Z'$-semicircles indicate the complicated mixed kinetic behaviour of $S_2O_8^{2-}$ electroreduction at the Cd(0 0 0 1) electrode. Thus, the characteristic relaxation time, $\tau_{\max}$, obtained is not the simple valued quantity, but is distributed continuously or discretely around a mean $\tau_{\max}$ value and shows that the balance of the various rate-determining processes changes with $c_{S_2O_8^{2-}}$ and electrode potential as well (Figs. 1(a), 2(a) and 3(a)).

The total experimental series differential capacitance ($C_s$), obtained from the $Z''$, $Z'$ plots (using the relation $Z'' = (j\omega C_s)^{-1}$), only very weakly decreases with $c_{S_2O_8^{2-}}$ and has the values between 15 and 20 μF cm$^{-2}$ for solu-
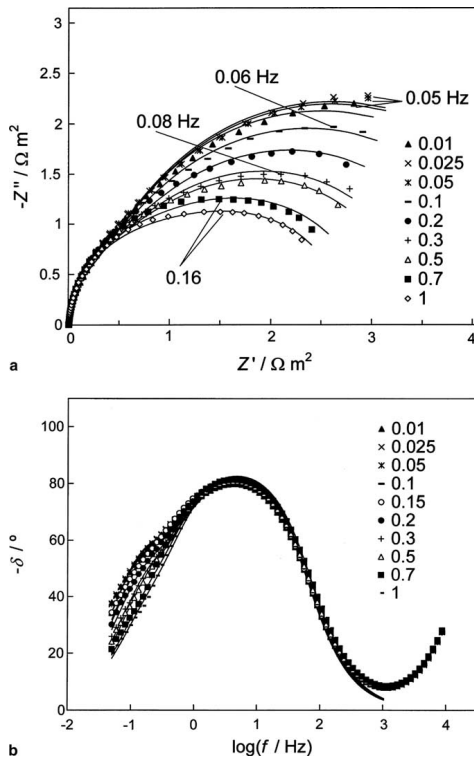




Fig. 3. Complex plane (a) and phase angle ($\delta$) vs. ac frequency plots (b) for the EP Cd(0 0 0 1) plane in aqueous 0.01 M $Na_2SO_4$ solution with different additions of $Na_2S_2O_8$ (mM), noted in figure, at $E = -1.1$ V vs. Ag|AgCl| sat. KCl (marks – experimental, solid lines – data calculated according to the circuit 'c' in Fig. 8).

tions with additions from $1 \times 10^{-2}$ to 1 mM $S_2O_8^{2-}$ at $f \geqslant 100$ Hz and at $E > -1.6$ V (Ag|AgCl). The dependences of $C_s$ on $f^{-1/2}$ show that, at $f < 100$ Hz, there is a noticeable increase in the Faradaic pseudocapacitance $C_s$ with increasing $c_{S_2O_8^{2-}}$ in the solution at $E = -1.60$ V, caused by electroreduction of $S_2O_8^{2-}$ ions as well as by the hydrogen evolution reaction at the potentials more negative than the zero charge potential.

Some phase angle $\delta$ vs. $\log f$ dependences are given in Figs. 1(b) and 3(b), because the Nyquist plots do not show all details [11–23]. On the other hand, the complex impedance $|Z|$ and $\delta$, $\log f$ plots (so-called Bode plots) contain all the necessary information. That is why, in parallel with Nyquist plots, the Bode plots are used in the circuit analysis. The shapes of the Nyquist and Bode plots (Figs. 1(a), 3(b), 4(b) and 5(b)) show that a very complicated reaction mechanism is characteristic of the electroreduction reaction of the $S_2O_8^{2-}$ anions at the Cd(0 0 0 1) plane.
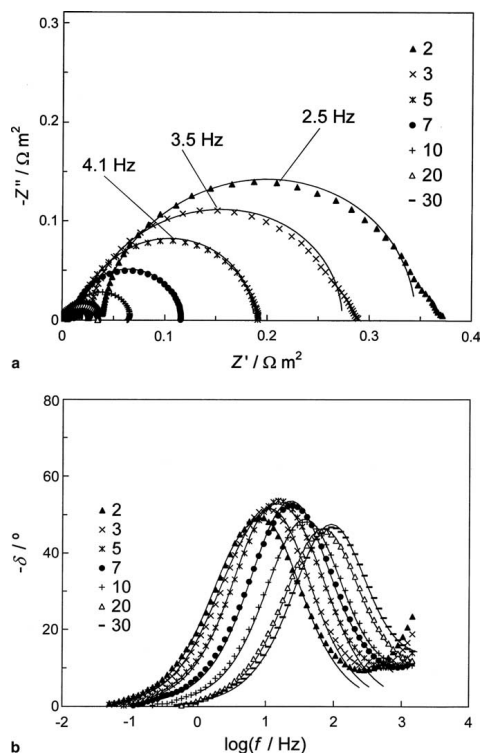
Fig. 4. Complex plane (a) and phase angle ($\delta$) vs. ac frequency plots (b) for the EP Cd(0001) plane in $4 \times 10^{-5}$ M $Na_2S_2O_8$ solutions with different additions of $Na_2SO_4$ (mM), noted in figure, at $E = -1.6$ V vs. Ag|AgCl| sat. KCl.
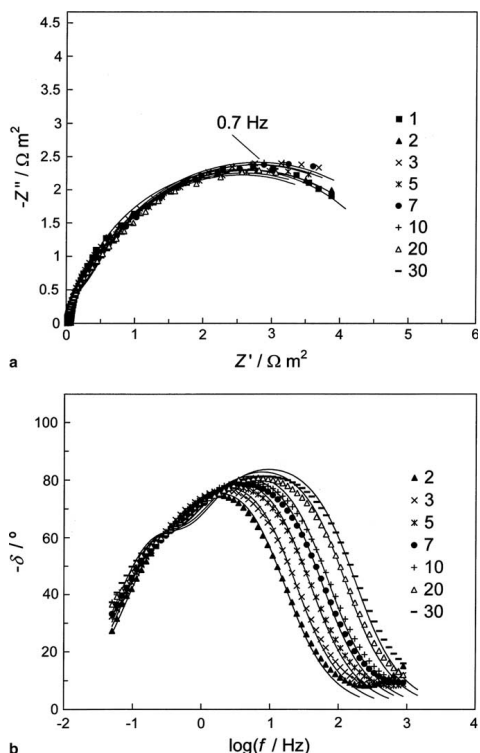


Fig. 5. Complex plane (a) and phase angle ($\delta$) vs. ac frequency plots (b) for the EP Cd(0001) plane in $4 \times 10^{-5}$ M $Na_2S_2O_8$ solutions with different additions of $Na_2SO_4$ (mM), noted in figure, at $E = -1.1$ V vs. Ag|AgCl| sat. KCl.

At given potential $E = -1.6$ V, the shape of the phase angle ($\delta$) vs. $\log f$ plots depends noticeably on $c_{S_2O_8^{2-}}$ and there is a maximum in the $\delta$, $\log f$ plots with $|\delta| \geqslant 50°$ at ac frequency from 10 to 300 Hz. The absolute values of $\delta$ decrease with increasing $c_{S_2O_8^{2-}}$, indicating the deviation of mixed kinetic process toward the charge transfer limited process at higher $c_{S_2O_8^{2-}}$. The phase angle values near zero at low ac frequency ($f < 1$ Hz) indicate that the heterogeneous charge transfer is a rate-limiting step at $E \leqslant -1.5$ V.

The noticeably higher total polarisation resistance values have been established in the potential region from $-1.2$ to $-1.4$ V (Fig. 2(a)), where the inhibition of the electroreduction of $S_2O_8^{2-}$ (i.e., the decrease in cathodic current density) takes place [1–4]. The noticeably higher $|Z''|$ values have been obtained in comparison with those at $E = -1.6$ V, corresponding to somewhat higher capacitance values ($27 < C_s < 32$ μF m$^{-2}$) and weakly decreasing with increasing $c_{S_2O_8^{2-}}$. At these potentials, the noticeably higher absolute values of the phase angle have been

established at lower $f_{max}$, compared with potentials more negative than $-1.5$ V. Thus, with decreasing the negative potential of the Cd(0001) electrode, the characteristic relaxation time increases (Figs. 6 and 7). At $\log f \leqslant -1$, the noticeably higher $|\delta|$ values ($|\delta| > 70°$) point to the kinetically mixed reaction mechanism for $S_2O_8^{2-}$ electroreduction reaction at potentials from $-1.4$ to $-1.2$ V. $f_{max}$ somewhat increases (i.e., $\tau_{max}$ decreases) with $c_{S_2O_8^{2-}}$ and this effect is less pronounced than at $E < -1.5$ V.

The data in Fig. 3(a) show that at $E \geqslant -1.1$ V, the shape of the Nyquist plots is different from that demonstrated at $E = -1.6$ V or at $E = -1.3$ V, and the very high values of total polarisation resistance have been obtained. The values of characteristic time constant calculated are independent of $c_{S_2O_8^{2-}}$ (except solutions with very high $c_{S_2O_8^{2-}}$, where the values of $\tau_{max}$ are smaller and weak specific adsorption of anions at Cd(0001) is possible [29]) and are somewhat higher than those at $E = -1.6$ V. Hence, the values of $C_s$ obtained from the values of $|Z''|$ at $\tau_{max}$ are
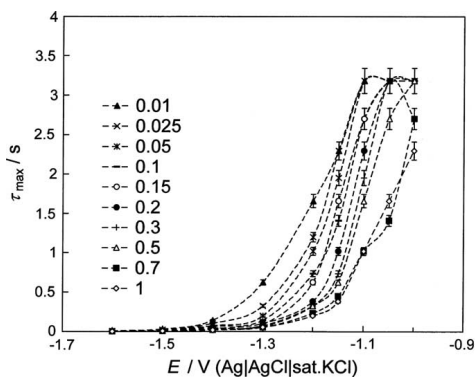
Fig. 6. Characteristic relaxation time $\tau_{max}$, $E$ – dependences for the EP Cd(0001) plane in aqueous 0.01 M $Na_2SO_4$ solution with different addition of $Na_2S_2O_8$ (mM), noted in figure.



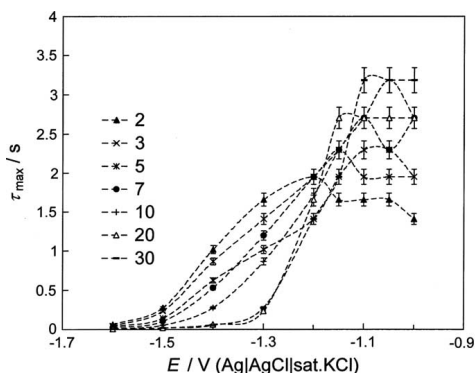Fig. 7. $\tau_{max}$, $E$ – dependences for the EP Cd(0001) plane in $4 \times 10^{-5}$ M $Na_2S_2O_8$ solutions with different additions of $Na_2SO_4$ (mM), noted in figure.

noticeably higher than those obtained at $E = -1.6$ V and at $E = -1.3$ V. In the region of moderate frequency, $C_s$ decreases with $c_{S_2O_8^{2-}}$. At very low ac frequency, the values of $C_s$ are very high and independent of $c_{S_2O_8^{2-}}$. The shape of $\delta$, $\log f$ plots is practically independent of $c_{S_2O_8^{2-}}$ (Fig. 3(b)) if $f > 1$ Hz, and only at very low ac frequency the small decrease of $|\delta|$ takes place with increasing $c_{S_2O_8^{2-}}$. In most dilute $S_2O_8^{2-}$ solutions, where adsorption effects can be neglected, the phase angle has a value near $-45°$, indicating the mainly diffusion limited reaction mechanism at $E = -1.1$ V, where the limiting diffusion current plateaus in the cyclic voltammograms for the rotating Cd(0001) electrode have been established [2–4]. However, in a good agreement with the data for the rotating disc electrode, the deviation from the purely diffusion limited reaction

mechanism toward the adsorption limited mechanism has been established with rising $c_{S_2O_8^{2-}}$ higher than $1 \times 10^{-3}$ M in the solution.

The shape of the Nyquist plots (Figs. 4(a) and 5(a)) (i.e., the polarisation resistance) and the Bode phase angle plots (Figs. 4(b) and 5(b)) depends noticeably on the base electrolyte concentration. At $E = -1.6$ V and at fixed $c_{S_2O_8^{2-}}$, the low frequency polarisation resistance $R_p$ decreases with increasing the base electrolyte concentration (Fig. 4(a)). The values of $|Z''|$ decrease with rising the base electrolyte concentration and, thus, the differential capacitance increases weakly with $c_{base.el.}$ because $f_{max}$ increases noticeably with $c_{base.el.}$. Thus, like for the higher reactant concentration, the higher base electrolyte concentration (smaller diffuse layer thickness) causes the decrease in the characteristic relaxation time (Fig. 7) for the $S_2O_8^{2-}$ electroreduction process. The phase angle has comparatively low values (Fig. 4(b)) and is practically independent of $c_{base.el.}$. The dependence of $\tau_{max}$ on the reactant as well as base electrolyte concentration points to the mixed kinetics behaviour in the case of $S_2O_8^{2-}$ electroreduction (comparable speeds of the diffusion, adsorption and charge transfer steps). The same tendency is valid at $E = -1.3$ V, but the values of $R_p$ and $|Z''|$ are noticeably higher than at more negative potentials. At $E = -1.1$ V (Fig. 5) (the region of the current plateau in the $j,E$-curves), the shape of $Z''$, $Z'$ plots is independent of $c_{base.el.}$ and the very high $R_p$ and $|Z''|$ have been obtained in comparison with $Z''$, $Z'$ plots at $E = -1.6$ V. The characteristic relaxation time decreases weakly with increasing $c_{base.el.}$ and phase angle is nearly equal to $-45°$ at $f < 10$ Hz, pointing to the mainly diffusion limited charge transfer mechanism. The same tendencies are valid in the case of moderate reactant concentrations, except at very high reactant concentrations ($c_{S_2O_8^{2-}} > 1 \times 10^{-3}$ M) where the surface blocking (adsorption of $S_2O_8^{2-}$ or intermediates) takes place. Thus, $\tau_{max}$ has higher values at the potentials corresponding to the diffusion-limited process, compared with those for the potential region near $E = -1.3$ V corresponding to the mixed adsorption and charge transfer limited cathodic reaction.

### 3.2. Analysis of fitting data

The data presented in Figs. 1–5 have been used for analysis of the reaction mechanism by various equivalent circuits (Fig. 8) based on the models discussed before in introduction chapter and in [10–23,30]. Results of the nonlinear regression analysis of the Nyquist as well as Bode plots for $c_{S_2O_8^{2-}} \leqslant 5 \times 10^{-4}$ M show that, to a first very rough approximation, these plots can be simulated by using the classical Randles circuit (presented in Fig. 8(a)), which represents the mechanism of mixed kinetics, where both charge transfer and diffusion determine the rate of the whole electroreduction process. According to the fitting data, the $\chi^2$ function has comparatively low values ($\chi^2 < 4 \times 10^{-3}$) and the weighted sum of squares $\Delta^2$ is less than $1 \times 10^{-1}$. Only in the potential region corresponding
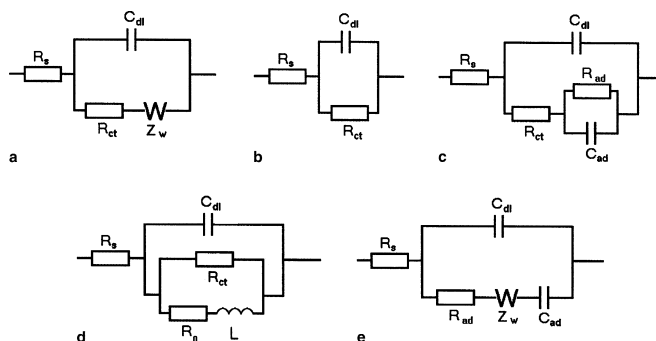
Fig. 8. Equivalent circuits of an electrode in $Na_2SO_4$ aqueous solution with addition of $Na_2S_2O_8$: (a,b) Randles; (c,d) models taking into account adsorption of one intermediate particle corresponding to the different adsorption capacitance, adsorption resistance and inductance values [23]; (c) for $B > 0$ in Eq. (17b) and (d) for $B < 0$ in Eq. (17b) [23,31,32]; (e) Ershler; ($C_{ad}$ – adsorption capacitance; $C_{dl}$ – double layer capacitance; $L$ – inductance; $R_{ad}$ – adsorption or partial charge transfer resistance; $R_{ct}$ – charge transfer resistance; $R_s$ – electrolyte solution resistance; $R_0$ – adsorption resistance [23,31,32]; $Z_W$ – Warburg-like diffusion impedance).

to the diffusion limited step ($E \geqslant -1.1$ V), there arise small problems with fitting the Nyquist plots, and higher $\chi^2$ values ($\chi^2 \geqslant 5 \times 10^{-3}$) have been obtained for more concentrated $S_2O_8^{2-}$ solutions in the base electrolyte.

It should be noted that a better fit of the experimental results has been observed when the equivalent circuit (c) has been used (i.e., the adsorption of the reaction intermediate particle $SO_4^{-\bullet}$ is assumed) [1–8,23,26,31,32]. It was found that the values of $R_{ct}$ and $C_{dl}$ established are in a good agreement with those obtained by using the classical Randles circuit. Errors in the individual parameters are comparatively small and the parameters obtained are given in Figs. 9–12. According to the data in Fig. 9, in the case of fixed solution composition, the charge transfer resistance increases with decreasing the negative potential in the region $-1.6 < E < -1.2$ V. At potentials more negative than $-1.2$ V, $R_{ct}$ decreases with rising $c_{S_2O_8^{2-}}$ (Fig. 9(a)). At $E \geqslant -1.1$ V, the values of $R_{ct}$ increase with $c_{S_2O_8^{2-}}$. At fixed $c_{S_2O_8^{2-}}$, $R_{ct}$ is inversely proportional to the base electrolyte concentration (Fig. 9(b)) and $R_{ct}$ decreases with increasing the negative electrode potential. Thus, $R_{ct}$ depends on thickness of the diffuse layer at the Cd(0 0 0 1) electrode surface. The "true" electrical double layer capacitance $C_{dl}$ [10–23] (given in Fig. 10(a)) obtained for solutions with different additions of $S_2O_8^{2-}$ has the reasonable values, being in a good agreement with the data for the base electrolyte at $-1.6 < E < -1.4$ V. At less negative potentials ($E > -1.4$ V), the values of $C_{dl}$ for $S_2O_8^{2-}$ containing solutions are systematically lower than for the pure base electrolyte, which points to the surface blocking effect for the Cd(0 0 0 1) electrode [26–28]. The data at fixed $c_{S_2O_8^{2-}}$ ($4 \times 10^{-5}$ M) show (Fig. 10(b)) that $C_{dl}$ increases with the base electrolyte concentration in the region of the potential of the diffuse layer minimum, $E_{min}$, but at $E < -1.2$ V, $C_{dl}$ decreases weakly with increasing $c_{base.el.}$. According to the data in [3] and $C, E$ curves measured at given ac frequen-
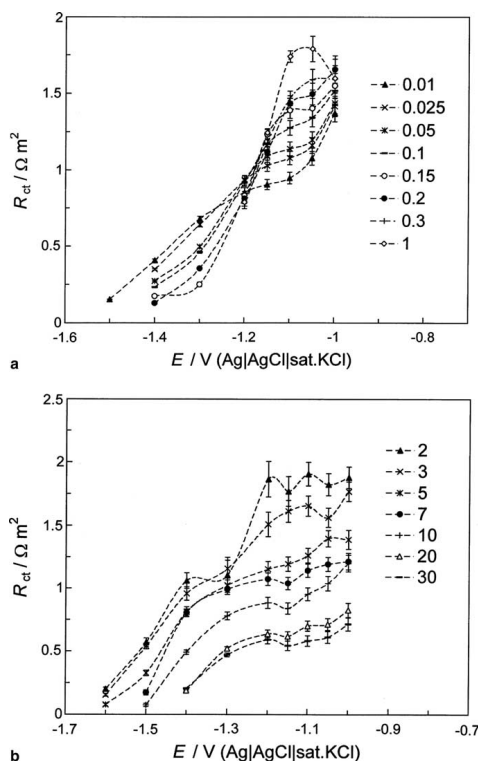


Fig. 9. Dependence of charge transfer resistance ($R_{ct}$) (circuit c) on the electrode potential in 0.01 M $Na_2SO_4$ solution with different addition of $Na_2S_2O_8$ (mM), noted in figure (a) and in $4 \times 10^{-5}$ M $Na_2S_2O_8$ solutions with different addition of $Na_2SO_4$ (mM), noted in (b).
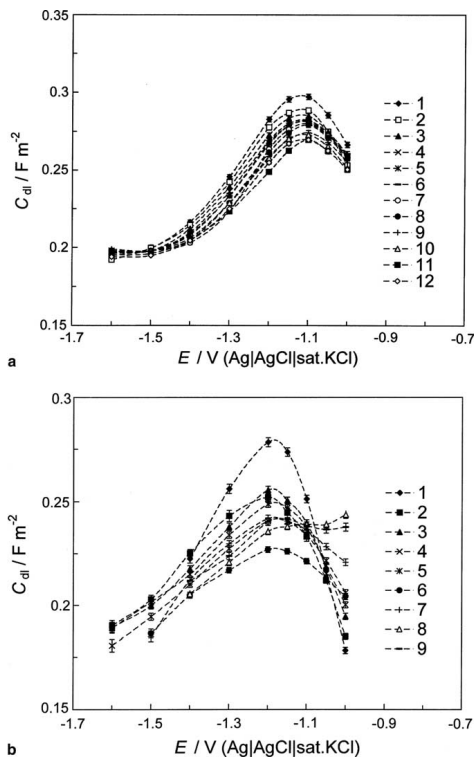
Fig. 10. Dependences of double layer capacitance ($C_{dl}$) (circuit c) on the electrode potential (a) in 0.01 M $Na_2SO_4$ aqueous solution (1) and with addition of $Na_2S_2O_8$: 0.005 mM (2); 0.01 mM (3); 0.025 mM (4); 0.05 mM (5); 0.1 mM (6); 0.15 mM (7); 0.2 mM (8); 0.3 mM (9); 0.5 mM (10); 0.7 mM (11); 1 mM (12) and (b) in 1 mM $Na_2SO_4$ aqueous solution (1); $4 \times 10^{-5}$ M $Na_2S_2O_8$ solutions with different additions of $Na_2SO_4$: 1 mM (2); 2 mM (3); 3 mM (4); 5 mM (5); 7 mM (6); 10 mM (7); 20 mM (8); 30 mM (9).

cies $E_{min}$ shifts weakly toward the negative direction with increasing $c_{S_2O_8^{2-}}$ as well as $c_{base.el.}$ at fixed another solution component concentration. This effect is more pronounced in the case of higher values of $c_{base.el.}$. Thus, the very weak adsorption of the $SO_4^{2-}$ and $S_2O_8^{2-}$ ions is probable (see discussion later).

The adsorption resistance $R_{ad}$ (Fig. 11) and adsorption capacitance $C_{ad}$ (Fig. 12) depend noticeably on the base electrolyte and reactant concentrations as well as on the electrode potential. At $E < -1.5$ V, the very low adsorption resistance ($R_{ad} \leqslant 1 \times 10^{-1}$ Ω m²) has been established, which corresponds to the very quick and reversible adsorption of the $Na^+$ cations as well as $Na^+$–$S_2O_8^{2-}$ ion pairs at the Cd(0001) electrode.

In the region of current pits the noticeable increase of $R_{ad}$ has been observed, rising with the reactant concentra-
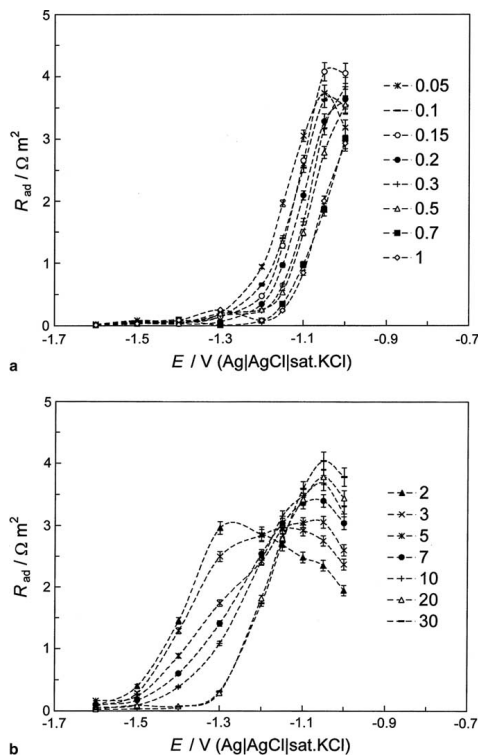


Fig. 11. Adsorption resistance $R_{ad}$, $E$ – dependences (Randles circuit) on the electrode potential in 0.01 M $Na_2SO_4$ solution with different additions of $Na_2S_2O_8$ (mM), noted in figure (a) and in $4 \times 10^{-5}$ M $Na_2S_2O_8$ solution with different additions of $Na_2SO_4$ (mM), noted in (b).

tion (Fig. 11(a)) but $R_{ad}$ is nearly independent of $c_{S_2O_8^{2-}}$ at $E = -1.1$ V. $R_{ad}$ has maximum values within the region of diffusion current plateaus. For systems with given $c_{S_2O_8^{2-}}$, $R_{ad}$ decreases with the base electrolyte concentration in the region of potentials between $-1.4$ and $-1.2$ V, but at $E \geqslant -1.1$ V $R_{ad}$ increases with $c_{base.el.}$.

Adsorption capacitance $C_{ad}$ (Fig. 12) has somewhat higher values at $E < -1.5$ V than $C_{dl}$, thus, the weak adsorption of the cations is possible. In the region of potentials from $-1.4$ to $-1.2$ V, $C_{ad}$ has 0.5 to 1.5 orders higher values than those for the pure base electrolyte solution, which indicates the weak adsorption of the $S_2O_8^{2-}$ ions or ($Na^+$–$S_2O_8^{2-}$) ion-pairs [3,4,7–9], caused by the squeezing out effect from the bulk solution by the $SO_4^{2-}$ anions. Thus, the results in Fig. 12 demonstrate that, for the more concentrated base electrolyte solutions, $C_{ad}$ has maximum values within the potential region from $-1.5$ to $-1.2$ V, where inhibition of the $S_2O_8^{2-}$ reduction reaction takes place. The
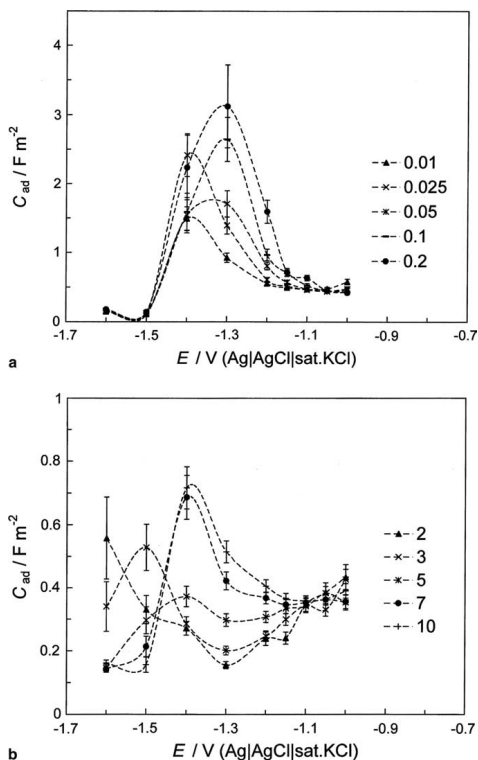
Fig. 12. Dependence of adsorption capacitance (adsorption of one intermediate particle model (c) [23]) on the electrode potential in 0.01 M $Na_2SO_4$ solution with different additions of $Na_2S_2O_8$ (mM), noted in (a) and in $4 \times 10^{-5}$ M $Na_2S_2O_8$ solution with different additions of $Na_2SO_4$ (mM), noted in (b).

very high values of $C_{ad}$ can be observed in the case of comparatively high reactant concentration ($C_{ad} \geqslant 3.5$ F m$^{-2}$ for $c_{S_2O_8^{2-}}$ from 0.3 to 0.7 mM). In the case of higher $c_{S_2O_8^{2-}}$ and less negative potentials than $-1.2$ V, the surface blocking is probable as the very low values of $C_{ad}$ have been obtained compared with $C_{ad}$ at $-1.4 < E < -1.2$ V. The decrease in $C_{ad}$ at $E > -1.1$ V has been established for other anions (I$^-$, Br$^-$) adsorbing at Cd(0001) plane from solutions with constant ionic strength [29].

It should be noted that a good fit of the experimental data has been established by using the classical Ershler circuit (1 e) (usually called as a combined Frumkin–Melik–Gaikazyan and Randles circuit) [26,33]. The values of $\chi^2$ function less than $1 \times 10^{-4}$ at more negative potentials than $-1.4$ V, and $\chi^2 \leqslant 5 \times 10^{-4}$ at $-1.4 \leqslant E - 1.0$ V for the solutions with $c_{base.el.}$ less than $1 \times 10^{-2}$ M have been obtained. The somewhat higher values of $\chi^2$ ($\chi^2 \leqslant 8 \times 10^{-4}$) for

solutions with higher base electrolyte concentration were observed only within the potential region where the acceleration of $S_2O_8^{2-}$ electroreduction with increasing $c_{base.el.}$ takes place (i.e., at $E < -1.55$ V). Under these conditions, the values of the adsorption resistance are in a good agreement with the values of charge transfer resistance, obtained using classical Randles or adsorption of one reactant model (Fig. 9), and the values of $C_{dl}$ are in agreement with the data given in Figs. 9 and 10.

However, it should be noted that the Randles (a) as well as Ershler (e) circuits (Fig. 8) contain the semi-infinite Warburg impedance, which causes the increase of the low frequency impedance to infinity. According to the data in Figs. 1–5 a constant dc current is passing through the electrode (i.e., $Z'$ has finite values). The analysis of the fitting data demonstrates that mathematically it is possible to fit the $Z''$, $Z'$-spectra (given in Figs. 1–5) by using the circuit 'a' or 'e' in Fig. 8. The same result has been obtained by Campbell and Peter [18] and Pajkossy et al. [33]. The probable physical explanation of this result is that diffusion is not the rate-determining step in the region of mixed kinetics studied in this work. The finite $Z'$ values can be explained by the fractal structure of the electrode surface [33] (in contradiction with the result that for the base electrolyte solution the very low fractality has been established) or by the linear diffusion to the disc electrode [34] as well as by the anomalous diffusion model with adsorbing boundary conditions [35–37]. Thus, the more detailed discussion about the finite $Z'$ component at $f \to 0$ is possible only after obtaining SNIFTIR spectroscopy data and impedance data in the case of rough Cd electrodes. However, from the mathematical point of view the Ershler model is too complicated as there is no noticeable decrease in the $\chi^2$ values with addition of the Warburg diffusion impedance into the equivalent circuit [23,30].

The results obtained indicate that the adsorption of $S_2O_8^{2-}$, $SO_4^{2-}$ or reaction intermediates of electroreduction and base electrolyte anions is possible. The SNIFTIR spectroscopy data can give the more reliable direct information about the surface state of Cd(0001) electrode in the case of $S_2O_8^{2-}$ electroreduction.

## 4. Conclusions

According to analysis of the experimental data, it can be concluded that the slow adsorption or co-adsorption processes of the cations and ion-pairs or anions in parallel to the "true" charge transfer process are the rate determining steps at $-1.4 < E < -1.2$ V, where the current pits have been observed in the current density vs. electrode potential plots for the rotating Cd(0001) electrode. At $E > -1.2$ V there prevails mixed kinetics in the case of more concentrated electrolyte solutions. The dependence of the fitted parameters on concentration of the $S_2O_8^{2-}$ ions and base electrolyte solution is a clear indication for the mixed kinetic process.

## Acknowledgement

## References

[1] E. Lust, R. Truu, K. Lust, Russ. J. Electrochem. 36 (2000) 1195.
[2] T. Thomberg, E. Lust, J. Electroanal. Chem. 485 (2000) 89.
[3] T. Thomberg, J. Nerut, E. Lust, Electrochim. Acta 49 (2004) 1271.
[4] T. Thomberg, J. Nerut, R. Jäger, P. Möller, K. Lust, E. Lust, J. Electroanal. Chem. 582 (2005) 130.
[5] A.N. Frumkin, Z. Elektrochem. 59 (1955) 807.
[6] O.A. Petrii, A.N. Frumkin, Dokl. Akad. Nauk SSSR 146 (1962) 1121.
[7] A.N. Frumkin, O.A. Petrii, Dokl. Akad. Nauk SSSR 147 (1962) 418.
[8] A.N. Frumkin, Elektrodnye Protsessy (The Electrode Processes), Nauka, Moscow, 1987.
[9] A.N. Frumkin, N.V. Nikolaeva-Fedorovich, N.P. Berezina, Kh.E. Keis, J. Electroanal. Chem. 58 (1975) 189.
[10] M. Sluyters-Rehbach, in: A. Bard (Ed.), Electroanalytical Chemistry, vol. 4, Marcel Dekker, New York, 1970, p. 1.
[11] R.D. Armstrong, M. Henderson, J. Electroanal. Chem. 39 (1972) 81.
[12] M. Sluyters-Rehbach, J.H. Sluyters, in: E. Yeager, J.O'M. Bockris, B.E. Conway, S. Sarangapani (Eds.), Comprehensive Treatise of Electrochem, vol. 9, Plenum Press, New York, 1984.
[13] I.D. Raistrick, J.R. MacDonald, D.R. Franceschetti, in: J.R. Mac-Donald (Ed.), Impedance Spectroscopy, Wiley, New York, 1987.
[14] M. Sluyters-Rehbach, Pure Appl. Chem. 66 (1994) 1831.
[15] G.J. Brug, A.L.G. van den Eeden, M. Sluyters-Rehbach, J.H. Sluyters, J. Electroanal. Chem. 176 (1984) 275.
[16] G.J. Brug, M. Sluyters-Rehbach, J.H. Sluyters, A. Hamelin, J. Electroanal. Chem. 181 (1984) 245.
[17] L.M. Peter, W. Dürr, P. Bindra, H. Gerischer, J. Electroanal. Chem. 71 (1976) 31.
[18] S.A. Campbell, L.M. Peter, J. Electroanal. Chem. 364 (1994) 257.
[19] J. Barber, S. Morin, B.E. Conway, J. Electroanal. Chem. 446 (1998) 125.
[20] C. Deslouis, I. Epelboin, M. Keddam, J.C. Lestrade, J. Electroanal. Chem. 28 (1970) 57.
[21] J.S. Chen, J.-P. Diard, R. Durand, C. Montella, J. Electroanal. Chem. 406 (1996) 1.
[22] L. Bai, D.A. Harrington, B.E. Conway, Electrochim. Acta 32 (1987) 1713.
[23] A. Lasia, in: B.E. Conway, J.O'M. Bockris, R.E. White (Eds.), Modern Aspects of Electrochemistry, vol. 32, Kluwer Academic/Plenum Publishers, New York, 1999, p. 143.
[24] B. Breyer, H.H. Bauer, Alternating Current Polarography and Tensammetry, Wiley Interscience, New York, 1963.
[25] E. Lust, K. Lust, A. Jänes, J. Electroanal. Chem. 413 (1996) 111.
[26] Z. Samec, K. Doblhofer, J. Electroanal. Chem. 432 (1997) 205.
[27] E. Lust, A. Jänes, K. Lust, M. Väärtnõu, Electrochim. Acta 42 (1997) 771.
[28] E. Lust, in: A.J. Bard, M. Stratman (Eds.), Encyclopedia of Electrochemistry, vol. 1, Wiley, New York, 2002, p. 188.
[29] R.R. Nazmutdinov, T.T. Zinkicheva, M. Probst, K. Lust, E. Lust, Surf. Sci. 577 (2005) 112–126.
[30] Z View for Windows (ver. 2.7), Scribner, Southern Pines, NC, USA.
[31] C.-N. Cao, Electrochim. Acta 35 (1993) 831.
[32] L. Bai, B.E. Conway, Electrochim. Acta 35 (1993) 1803.
[33] T. Pajkossy, T. Wandlowski, D.M. Kolb, J. Electroanal. Chem. 414 (1996) 209.
[34] M. Fleischmann, S. Pons, J. Daschbach, J. Electroanal. Chem. 317 (1991) 1.
[35] A. Compte, R. Metzlek, J. Phys. A 30 (1997) 7277.
[36] J. Bisquert, G. Garcia-belmonte, P.R. Bueno, E. Longo, L.O.S. Bulhões, J. Electroanal. Chem. 452 (1998) 229.
[37] J. Bisquert, A. Compte, J. Electroanal. Chem. 499 (2001) 112.

**IV**

# Electroreduction of Complex Ions at Bismuth and Cadmium Single Crystal Plane Electrodes

E. Lust, J. Nerut, E. Härk, S. Kallip, V. Grozovski,
T. Thomberg, R. Jäger, K. Lust, K. Tähnas

University of Tartu
2 Jakobi Str., 51013 Tartu, Estonia

The electrical double layer structure and kinetics of electroreduction of the $[Co(NH_3)_6]^{3+}$, $[Fe(CN)_6]^{3-}$ and $S_2O_8^{2-}$ ions on the electrochemically polished Cd(0001) and Bi(hkl) single crystals have been studied using *in situ* STM, impedance and rotating disc electrode methods. The large atomically flat surface areas have been observed on the electrochemically polished and cut Bi(111) electrode. The electroreduction data for $[Co(NH_3)_6]^{3+}$ show that rate constant of the heterogeneous reaction depends on the crystallographic structure of the plane as well as on the base electrolyte used. The apparent transfer coefficient slightly higher than 0.5 indicates that there are only small deviations from the Frumkin slow discharge theory. The electroreduction of $[Fe(CN)_6]^{3-}$ is limited mainly by the slow charge transfer step complicated by the adsorption of the reactants or reaction intermediates at the electrode in the region of current pits observed in the cyclic voltammograms obtained using the rotating disk electrode method.

## Introduction

The phase boundary structure, adsorption properties and electrochemical kinetics of various interfacial charge transfer reactions at solid surfaces depend significantly on the chemical composition but also on the morphology of the surface studied (1-8). Thus, the surface morphology and electrochemical roughness are very important properties as most electrochemical characteristics (exhange current density, rate constant of an heterogeneous reaction, surface coverage etc.) are the extensive quantities (9-10).

Electroreduction of the $[Co(NH_3)_6]^{3+}$, $S_2O_8^{2-}$ and $[Fe(CN)_6]^{3-}$ ions has been suggested as the model reactions to study the influence of the electric double layer characteristics on the charge transfer mechanism from the metal to the complex ion (1,2). Comparison of the results obtained by Hamelin and Weaver (1) with those obtained by Hromadova and Fawcett (2) shows that the rate constant values of the heterogeneous reactions of ions depend on the crystallographic structure of Au(hkl) surface, as well as on the chemical composition of the base electrolyte. The data obtained by Samec et al. (3,4) show that the electroreduction of $S_2O_8^{2-}$ on Au(hkl) has a very complicated mechanism and it depends on the electrode potential applied. Based on ac impedance spectroscopy, it was found that the apparent rate constant $k_{het}$ for the redox couple $[Fe(CN)_6]^{3-}/ [Fe(CN)_6]^{4-}$ largely depends on the surface structure of Pt(hkl) and $k_{het}$ increases in the order of planes (110) < (100) < (111) (11). The *in situ* spectroscopy data indicate the presence of the adsorbates ascribe to the cyanide group on every Pt(hkl) (11). The same conclusion has been made by Peter et al. (12,13). The strong influence of the surface structure and chemical nature of Bi(hkl) and Cd(hklf) electrodes on the $S_2O_8^{2-}$ electroreduction kinetics

has been established using the cyclic voltammetry and rotating disk electrode methods (5-8,14).

## Experimental details and surface structure characterisation

The surface of the basal Bi(111) plane has been prepared by cleaving a Bi single crystal at the temperature of liquid nitrogen (mentioned as Bi(111)$^C$) inside the glove box (Ar 99,999 % atmosphere) and submerged under cathodic polarisation ($E$ = -0.5 V vs. Ag | AgCl in saturated KCl aqueous solution) into the 0.05 M $Na_2SO_4$ + 0.0005 M $H_2SO_4$ aqueous solution (previously saturated with Ar (92%) + $H_2$ (8%) mixture). The self-made hermetic three-electrode cell with large Pt counter electrode and Ag | AgCl reference electrode, connected to the *in situ* STM cell through Luggin capillary, has been used. The region of ideal polarizability has been obtained using cyclic voltammetry and a good agreement with the results discussed in (6-10,14) has been established. The Molecular Imaging PicoSPM$^{TM}$ measurement system and the insulted Pt|Ir (70|30) STM tips from Molecular Imaging company have been used. The STM-tips and measurement system have been tested and calibrated using the highly oriented pyrolytic graphite basal plane C(0001)$^C$ (SPI$^{TM}$) cut inside the glove box. All STM images have been recorded in constant current mode with tunnelling currents ranging between 1.0 and 4.0 nA. The Nanotec Electronica WSxM$^{TM}$ free software has been used for image processing and roughness calculations (9,10).
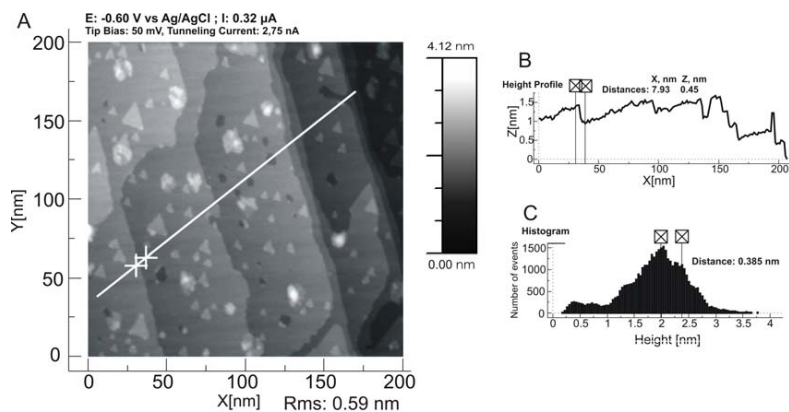


Fig. 1. *In situ* STM image (a), selected surface profile (b) and histogram of the height distribution (c) for the cleaved Bi(111)$^C$ plane in 5*10$^{-2}$ M $Na_2SO_4$ + 5*10$^{-4}$ M $H_2SO_4$ aqueous electrolyte.

The surface of the cleaved at temperature of liquid nitrogen Bi(111)$^C$ consists of atomically smooth terraces with steps of the height of 4.0±0.2 Å (Fig. 1) or of multiple heights. The boundaries of some terraces are close to the straight lines of the atomic rows on the Bi surface along the (110) direction. However, there are some terraces having considerably curved boundaries, and rounded islands of the triangular shape as well as

hollows of nanometric dimension, usually of the monatomic depth. It is very interesting to mention that the position of the two-dimensional crystal, i.e. the nanometric scale triangles (islands as well as hollows) is very stable during hours under the cathodic polarisation from $-0.7 \leq E \leq -0.1$ V (vs. Ag|AgCl) as well as under the various potentials applied during hours. The root mean square roughness (RMS) vs cathodic polarisation dependence affirmed these data. Thus, in a good agreement with the cyclic voltammetry and impedance data (6-10,14), there is no quick surface reconstruction process as it has been established for Au(hkl) (1,15,16).
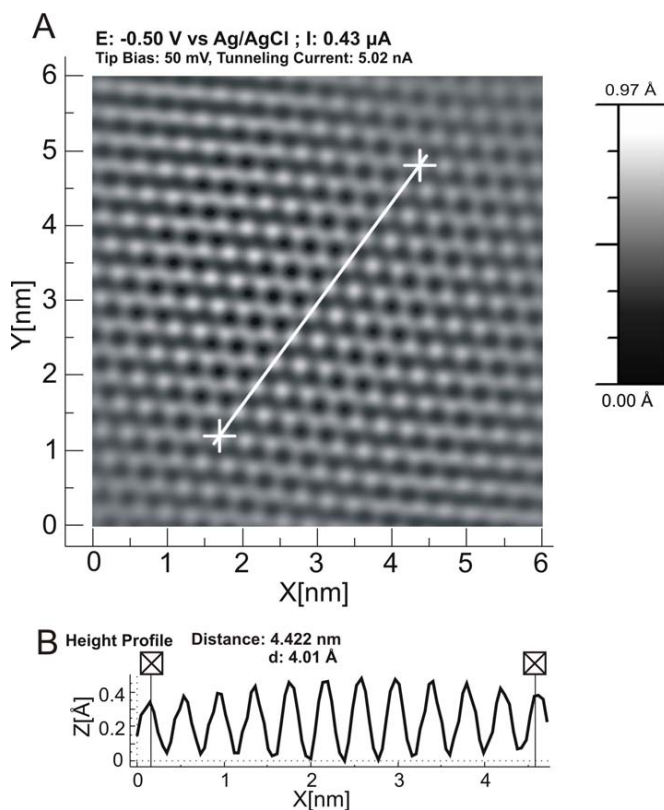


Fig. 2. *In situ* atomic resolution STM image(a) and height profile(b) for Bi(111)[C] electrode at $E = -0.5$ V in $5 \times 10^{-2}$ M $Na_2SO_4$ + $5 \times 10^{-4}$ M $H_2SO_4$ aqueous solution.

The data in Fig. 2 show that the quite regular atomic structure can be observed with interatomic distances $d = 4.0 \pm 0.1$ Å. The data in histogram show that the height fluctuations in the region of $(6 \times 6)$ nm$^2$ Bi(111)[C] surface are very small and this regular structure does not change noticeably under polarisation from $-0.7$ to $-0.1$ V (Ag|AgCl). According to the data in Fig. 2, the triangular structure of atoms prevails at the Bi(111)[C] surface.

According to the data given in Fig. 3, the surface of the Bi(111) electrode

electrochemically polished in the saturated KI + HCl aqueous solution at anodic current density $i$ =1.25 A cm$^{-2}$ is quite smooth and only some monatomic steps and hollows can be observed. The atomic resolution STM data demonstrate the same structure as shown in Fig. 3.
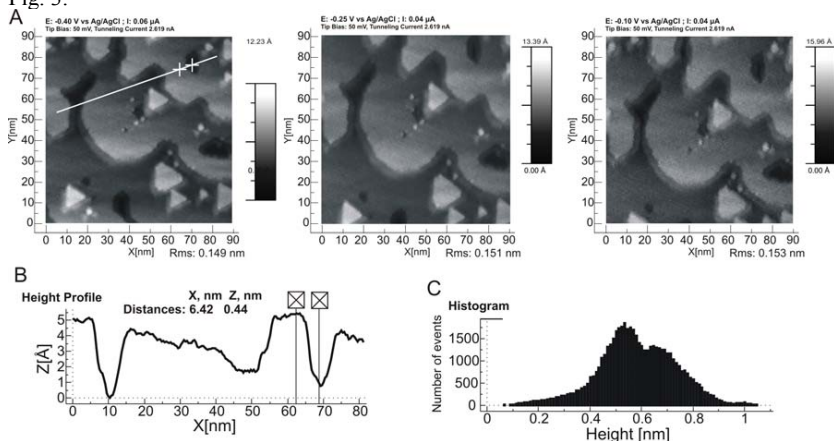


Fig. 3. *In situ* STM images at various electrode potentials (shown in figure)(a), selected surface profile(b), histogram of the height distribution(c) for electrochemically polished Bi(111)$^{EP}$ electrode in 0.0001 M HClO$_4$ + 0.0099 M LiClO$_4$ aqueous solution.

**Electroreduction data**

The another aim of this work was to obtain the electric double layer parameters in the LiClO$_4$ + HClO$_4$, Na$_2$SO$_4$ + Na$_2$S$_2$O$_8$, and KF + K$_3$[Fe(CN)$_6$] aqueous solutions and to use these data for analysis of the influence of the electrical double layer structure on the electroreduction kinetics of the complex ions at the electrochemically polished bismuth (111), (001), (011) and Cd(0001) planes (5-8,14). The ac impedance and rotating disk electrode methods have been used. The electroreduction rate of the [Co(NH$_3$)$_6$]$^{3+}$ cation depends on the electrode potential and electrolyte concentration, i.e. on thickness of the diffuse layer. The influence of the solution pH on the rate of reduction is not very remarkable at pH $\geq$ 2. The values of the apparent rate constant $k_{het}$ have been calculated using the kinetic current densities, $j_k$, obtained from the linear parts of the Koutecky-Levich plots (5-8). The values of corrected rate constant, $k_{het}^0$, at the zero charge potential $E_{\sigma=0}$ depend very weakly on the base electrolyte solution (14). The values of $k_{het}^0$ in the case of Bi planes are of the same order as those for Hg, but noticeably higher in comparison of those for Au(111) and somewhat lower for Au(210) and Au(110) planes (1,2,14) (Table 1).

The value of the apparent charge transfer coefficient $\alpha_{app} \geq 0.56$ for Bi(001) is somewhat higher than that for Bi($01\overline{1}$) plane in HClO$_4$ + LiClO$_4$ aqueous solution. Thus, there are only small deviations from the Frumkin slow discharge theory. However, the effective charge density values, obtained using the new method proposed by Fawcett et al. (17,18) i.e. by using the slope values of the [dln$k_{het}$ / d($\phi_m - \psi_d$)] vs. ($\phi_m - \psi_d$) dependences, are very slow ($z_{eff} \leq 0.6$), depending slightly on the Bi plane studied. The corrected Tafel plots are nearly linear in the wide electrode potential region studied and

coincide for the all base electrolyte concentrations studied, if the $z_{eff}$ values have been used.

Table 1 Kinetic data for $[Co(NH_3)_6]^{3+}$ ion electroreduction on various electrodes.

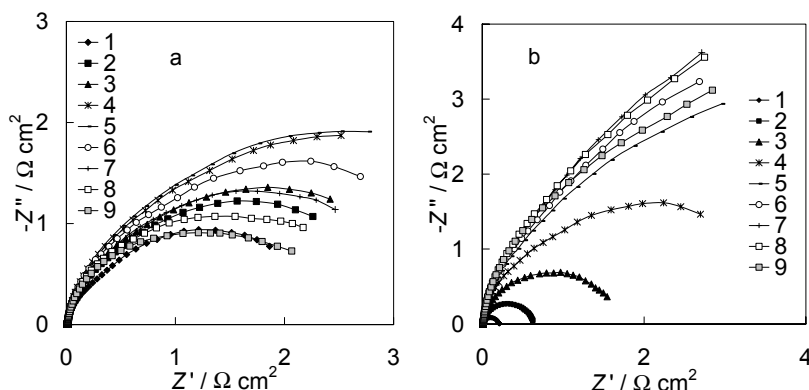| Electrolyte | Electrode | | $z_{eff}$ | $\alpha_{app}$ | $k^0_{het}$ /cm s$^{-1}$ |
|---|---|---|---|---|---|
| 0.06 M LiClO$_4$ + 0.001 M HClO$_4$ | Bi(001) | | 0,56±0.03 | 0.56±0.02 | $7.1 \times 10^{-3}$ ($\pm$ 0.3) |
| | Bi(01$\bar{1}$) | | 0,53±0.03 | 0.54±0.02 | $6.2 \times 10^{-3}$ ($\pm$ 0.3) |
| 0.06 M HClO$_4$ | Bi(001) | | 0,54±0.03 | 0.55±0.02 | $5.5 \times 10^{-3}$ ($\pm$ 0.3) |
| | Bi(111) | | - | 0.56 | $4.5 \times 10^{-3}$ ($\pm$ 0.3) |
| | Bi(01$\bar{1}$) | | - | 0.58 | $2.1 \times 10^{-3}$ ($\pm$ 0.3) |
| 0.1 M LiClO$_4$ | Hg | (4) | - | 0.67 | $2.0 \times 10^{-4}$ |
| 0.093 M HClO$_4$ | Au(111) | (7) | - | 1.05 | 8.1×10-7 |
| | Au(110) | (7) | - | 1.05 | 2.2×10-2 |
| | Au(210) | (7) | - | 1.10 | 4.3×10-1 |



Fig. 4. Nyquist plots at $E$ = -1.3 V (Ag/AgCl/sat. KCl) for the electrochemically polished Cd(0001) electrode (a) in 0.01 M KF aqueous solution with different additions of $K_3[Fe(CN)_6]$ (mM): 0 (1); 0.005 (2); 0.01 (3); 0.05 (4); 0.15 (5); 0.3 (6); 0.5 (7); 0.7 (8) and 1 (9); and (b) in 0.01 M KF + 0.0002 M $K_3[Fe(CN)_6]$ solution at electrode potentials (V): -1.6 (1), -1.5 (2), -1.4 (3), -1.3 (4), -1.2 (5), -1.15 (6), -1.1 (7), -1.05 (8) and -1.0 (9).

The complex impedance plane plots and differential capacitance vs. electrode potential dependences for the Na$_2$SO$_4$, KF and NaF aqueous solutions ($1 \times 10^{-3}$…$3 \times 10^{-2}$ M) as a base electrolyte and with the different additions of Na$_2$S$_2$O$_8$ or $[Fe(CN)_6]^{3-}$ ($5 \times 10^{-6}$…$2 \times 10^{-3}$ M) have been measured using the Autolab PGSTAT 30 with a FRA 2 system at Cd(0001) within the potential region $-1.60 \le E \le$ -1.0 V vs. (vs. Ag|AgCl|sat. KCl) and at Bi(hkl) from $-1.60$ to $-0.5$ V. It was found that for Cd(0001) the potential of the diffuse layer minimum in the $C,E$ curves does not shift noticeably in the case of small additions of Na$_2$S$_2$O$_8$ into the base electrolyte solution. However, a noticeable shift of $E_{\sigma=0}$ for Cd(0001) and Bi(hkl) electrodes takes place in the case of $[Fe(CN)_6]^{3-}$ and with increasing the concentration of S$_2$O$_8^{2-}$. Near $E_{\sigma=0}$, the differential capacitance decreases with increasing concentration of Na$_2$S$_2$O$_8$ as well as $[Fe(CN)_6]^{3-}$.
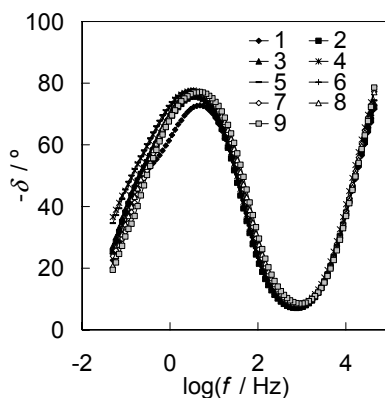
Fig. 5. Dependence of the phase angle ($\delta$) on ac frequency for the electrochemically polished Cd(0001) electrode in 0.01 M KF aqueous solution with different additions of $K_3[Fe(CN)_6]$ (mM): 0 (1); 0.005 (2); 0.01 (3); 0.05 (4); 0.15 (5); 0.3 (6); 0.5 (7); 0.7 (8) and 1 (9).
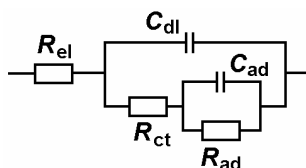


Fig. 6. Equivalent circuit used for fitting the $Z''$,$Z'$ plots at f < 2000 Hz. $R_{el}$ – high-frequency resistance, $C_{dl}$ – electrical double layer capacitance, $R_{ct}$ – charge transfer resistance, $C_{ad}$ and $R_{ad}$ – adsorption capacitance and resistance, respectively (19).

The impedance spectra were measured at ac frequencies $f$ from 0.05 to $1 \times 10^5$ Hz within the same potential region as the rotating disk electrode measurements. The $Z''$,$Z'$-plots for Bi(111) electrode in $1 \times 10^{-2}$ M $Na_2SO_4$ + $x$ M $Na_2S_2O_8$ solution at $E = -1.2$ V (vs. SCE), where the maximal depression (so called current pit) of the current density vs. electrode potential curves has been established, have anomalous shape (negative $Z'$ values at low $f$) in comparison with Nyquist plots at $E > -1.2$ and $E < -1.4$ V. The anomalous shape of $Z''$,$Z'$-plots can be explained by the adsorption of $S_2O_8^{2-}$ anion or $SO_4^{-\bullet}$ radical anion at the Bi(111) electrode surface. It should be noted that in this region of electrode potential the current density vs. electrode potential curves do not depend on the rotation speed of the disk electrode, indicating that the limiting rate determining step is the charge transfer process. The phase angle vs. log $f$ plots indicate that $\delta \le -80°$ in the medium ac frequency region, which is characteristic of the adsorption-limited charge transfer process. Only at very low ac frequency ($f < 1$ Hz) the values of $\delta$ increase and $\delta \ge -15°$ has been established, characteristic of the charge transfer limited reaction mechanism of the faradaic reactions. Only in the very dilute $Na_2S_2O_8$ solutions ($c < 5 \times 10^{-5}$M) at $f < 0.1$ Hz the phase angle is nearly equal to -45°, characteristic of the diffusion-limited electroreduction reaction mechanism of the $S_2O_8^{2-}$ ions at Cd(0001) and Bi(111) planes. Thus, according to the experimental data obtained the current pits in the

*j,E*-curves are mainly caused by adsorption of the reaction intermediates at the Bi(hkl) and Cd(0001) electrodes.

The data in Figs. 4 and 5 indicate that the same mechanism is valid in the case of electroreduction of $[Fe(CN)_6]^{3-}$ at the electropolished Cd(0001) plane. The data in Figs. 4 and 5 as well as for Bi(hkl) | $S_2O_8^{2-}$ and Cd(0001) | $S_2O_8^{2-}$ systems can be simulated by the equivalent circuit (Fig. 6), where the adsorption of reacting species or intermediates has been taking into account (19). The detailed analysis of the fitting data shows that the adsorption capacitance for Cd(0001) | $S_2O_8^{2-}$ system is maximal in the region of potentials from -1.4 to -1.2 V (SCE) and increases with concentration of the $S_2O_8^{2-}$ anions in bulk solution. The same effect has been observed for the systems with addition of the $[Fe(CN)_6]^{3-}$ complex anions at $E <$ -1.1 V. Thus, the adsorption of the reaction intermediates seems to be possible.
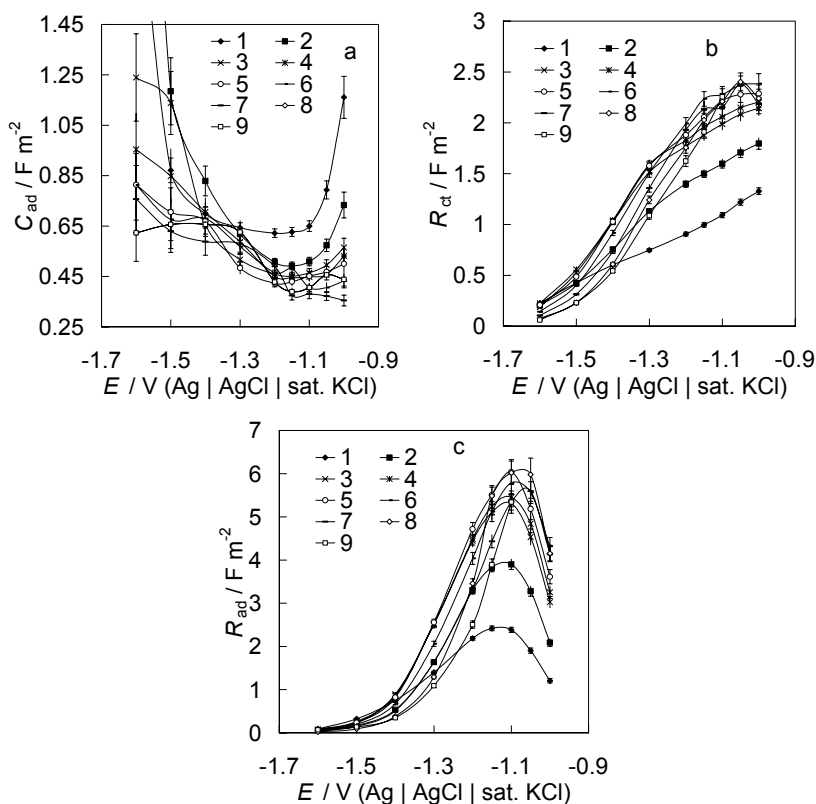


Fig. 7. Dependences of the adsorption capacitance (a), charge transfer resistance (b) and adsorption resistance (c) on the electrode potential for the electrochemically polished Cd(0001) electrode in 0.01 M KF aqueous solution with different additions of $K_3[Fe(CN)_6]$ (mM): 0 (1); 0.005 (2); 0.025 (3); 0.05 (4); 0.1 (5); 0.2 (6); 0.3 (7); 0.5 (8) and 0.7 (9).

According to the fitting data the adsorption capacitance values obtained for Cd(0001) (Fig. 7a) are higher than the electrical double layer capacitance values and $C_{ad}$ weakly increases with the rise of negative polarization of Cd(0001), indicating the adsorption of ion-pairs or intermediates at Cd(0001) surface. Differently from the Cd(0001) | $S_2O_8^{2-}$ + base electrolyte system the values of $C_{ad}$ only very weakly depend on concentration of $[Fe(CN)_6]^{3-}$ in the base electrolyte solution indicating the limiting adsorption at very slow $c_{[Fe(CN)_6]^{3-}}$. The same effect has been discussed by Damaskin et al. (20) for Hg | $S_2O_8^{2-}$ and Hg | $[Fe(CN)_6]^{3-}$ systems. The adsorption resistance (Fig. 7c) is maximal in the region of $E_{\sigma=0}$, where the limiting diffusion currents for rotating Cd(0001) or Bi(hkl) disk electrode have been established. At $E = -1.6$ V, $R_{ad}$ is very low (Fig. 9) and independent of $c_{[Fe(CN)_6]^{3-}}$ in solution but at $E_{\sigma=0}$ the values of $R_{ad}$ increase with $c_{[Fe(CN)_6]^{3-}}$. The charge transfer resistance $R_{ct}$ (Fig. 7b) is nearly independent of $c_{[Fe(CN)_6]^{3-}}$ at $E_{\sigma=0}$ and decreases nearly exponentially with increasing the cathodic polarization. In comparison with $R_{ad}$, the values of $R_{ct}$ are only 2…3 times lower, indicating the mixed kinetic mechanism of the $[Fe(CN)_6]^{3-}$ as well as $S_2O_8^{2-}$ electroreduction at Cd(0001) and Bi(hkl) planes.

The values of electric double layer capacitance calculated are in an agreement with the values of equilibrium capacitance for the pure base electrolyte solution (obtained by extrapolating to the condition $f = 0$). However, small decrease of $C_{dl}$ with increasing $c_{[Fe(CN)_6]^{3-}}$ indicates the adsorption of the reactant or reaction intermediate particles at the Bi(hkl) and Cd(0001) surfaces.

A satisfactory fit was achieved with a classical Randles equivalent circuit, where in parallel with charge transfer branch, i.e. the charge transfer resistance and diffusional impedance are connected in series. Near $E_{\sigma=0}$ the inhibition of the charge transfer step occurs as concentration of $Na_2S_2O_8$ increases, while the charge transfer resistance $R_{ct}$ increases. At more negative potentials the reduction rate rises and $R_{ct}$ starts to decrease with increasing the concentration of $Na_2S_2O_8$ or $K_3[Fe(CN)_6]$. At fixed concentration of $Na_2S_2O_8$, $R_{ct}$ decreases with increasing the base electrolyte concentration. The dependences of charge transfer resistance and diffusion resistance on the electrode potential are similar for Bi(001) and Cd(0001). However, near $E_{\sigma=0}$ at low $c_{[Fe(CN)_6]^{3-}}$, $R_{ct}$ increases with increasing the reactant concentration in solution, but at reactant concentration more than mM the decrease in $R_{ct}$ takes place. Thus, the inhibition of electroreduction takes place in the potential region, where the adsorption of the $[Fe(CN)_6]^{3-}$ ions is possible.

However, the shapes of the $Z''$,$Z$ and phase angle vs. ac frequency dependences show that there is no slow semi infinite diffusion at Bi(hkl) and Cd(0001) electrodes in the wide region of the electrode potentials.

## Conclusions

The mechanism of electroreduction of the complex cations very weakly depends on the surface structure of the Bi(hkl) electrode, and only very weak decrease of the rate constant of the heterogeneous reaction, corrected for the double layer effect, and apparent transfer coefficient values has been established, differently from Au(hkl) planes. The electroreduction of complex anions goes probably thrue the adsorption step and in the limited region of ac frequencies (from 0.1 to 100 Hz) the adsorption is the rate limiting

step. At lower frequencies the charge transfer stage is the rate limiting step. In the region of electrode potentials, where the current pit in the cyclic voltammograms for the rotating disk electrode has been established for $S_2O_8^{2}$ and $[Fe(CN)_6]^{3-}$ electroreduction reaction at Cd(0001) and Bi(hkl) electrode, the slow adsorption of reactant or reaction intermediates is possible.

## Acknowledgements

## References

1.  A. Hamelin, M.J. Weaver, *J. Electroanal. Chem*., **209**, 109 (1986).
2.  M. Hromadova, W.R. Fawcett, *J. Phys. Chem*. A, **104**, 4356 (2000).
3.  Z. Samec, K. Doblhofer, *J. Electroanal. Chem*., **367**. 141 (1994).
4.  Z. Samec, K. Kirscher, K. Doblhofer, *J. Electroanal. Chem*., **499**, 129 (2001).
5.  T. Thomberg, E. Lust, *J. Electroanal. Chem*., **485**, 89 (2000).
6.  E. Lust, R. Truu, K. Lust, *J. Russ. Electrochem*., **36**, 1195 (2000).
7.  T. Thomberg, J. Nerut, K. Lust, E. Lust, *Electrochim. Acta*, **49**, 1271 (2004).
8.  T. Thomberg, J. Nerut, R. Jäger, P. Möller, K. Lust, E. Lust, *J. Electroanal. Chem*., **586**, 237 (2006).
9.  E. Lust, S. Kallip, P. Möller, A. Jänes, V. Sammelselg, P. Miidla, M. Väärtnõu and K. Lust, *J. Electrochem. Soc*., **150**, E175 (2003).
10. S. Kallip, E. Lust, *Electrochem. Comm*., **7**, 863 (2005).
11. F. Kitamura, K. Nanbu, T. Ohsaka, K. Tokuda, *J. Electroanal. Chem*., **456**, 113 (1998).
12. L.M. Peter, W. Dürr, P. Bindra, H. Gerisher, *J. Electroanal. Chem*., **71**, 31 (1976).
13. S.A. Campbell, L.M. Peter, *J. Electroanal. Chem*., **364**, 257 (1994).
14. R. Jäger, E. Härk, P. Möller, J. Nerut, K. Lust, E. Lust, *J. Electroanal. Chem*., **566**, 217 (2004).
15. D.M. Kolb, *Prog. Surf. Sci*., **51**, 109 (1996).
16. Th. Wandlowski, in *Encyclopedia of Electrochemistry* 1, A.J. Bard, M. Stratmann, Editors, p. 383, Wiley-VCH, Weinheim (2002).
17. M. Hromadova, W.R. Fawcett, *J. Phys. Chem. B*, **108**, 3277 (2004).
18. W.R. Fawcett, T.G. Smagala, *J. Phys. Chem. B*, **109**, 1930 (2005).
19. A. Lasia, in *Modern Aspects of Electrochem*. 32, B.E. Conway, J.O'M. Bockris, H.E. White, Editors, p. 188, Kluwer Academic / Plenum Publishers, New York (1999).
20. B.B. Damaskin, J.V. Stenina, O.A. Baturina, L.N. Sviridova, *Elektrokhimiya*, **34**, 1083 (1998).

**V**

**J. Nerut**, K. Lust, E. Lust,
Adsorption of hexacyanoferrate(II) and hexacyanoferrate(III) anions on
electrochemically polished Cd(0001) plane,
J. Electroanal. Chem. Submitted (JELECHEM-D-06–00250R2).

**VI**

**J. Nerut**, K. Lust, E. Lust,
Impedance spectroscopy study of hexacyanoferrate(III) anion electroreduction
kinetics at electrochemically polished Cd(0001) plane,
J. Electrochem. Soc. Submitted (JES-07–0695).

# CURRICULUM VITAE

## Jaak Nerut

Born:            28.03.1980, Kohtla-Järve, Estonia
Citizenship:     Estonian
Martial status:  single
Address:         Institute of Physical Chenistry
                 University of Tartu
                 2 Jakobi St., Tartu 51014, Estonia
Phone:           +372 737 5165
Fax:             +372 737 5160
E-mail:          jaak.nerut@ut.ee

## Education

2003    University of Tartu, *Ph.D.* student (physical and electro-chemistry)
2003    University of Tartu, *M. Sc.* in physical and electrochemistry
2002    University of Tartu, chemistry teacher
2002    University of Tartu, *B. Sc.* in chemistry cum laude
1998    Hugo Treffner Gymnasium

## Professional employment

2005–...     University of Tartu, Institute of Physical Chemistry, researcher (0.6)
2004–2005    University of Tartu, Institute of Physical Chemistry, researcher (0.5)
2002–2004    University of Tartu, Institute of Physical Chemistry, chemist (0.5)

44

## Main scientific publications

1. J. Nerut, P. Möller and E. Lust, Electroreduction of hexacyanoferrate(III) anions on electrochemically polished Cd(0001) plane, Electrochim. Acta 49 (2004) 1597.
2. R. Jäger, E. Härk, P. Möller, J. Nerut, K. Lust and E. Lust, The kinetics of eletroreduction of hexaamminecobalt(III) cation on Bi planes in aqueous $HClO_4$ solutions, J. Electroanal. Chem. 566 (2004) 217.
3. T. Thomberg, J. Nerut, K. Lust and E. Lust, The kinetics of eletroreduction of peroxodisulfate anion on electrochemically polished Cd(0001) plane, Electrochim. Acta 49 (2004) 1271.
4. T. Thomberg, J. Nerut, R. Jäger, P. Möller, K. Lust, E. Lust, The kinetics of electroreduction of peroxodisulfate ions on single crystal cadmium and bismuth electrodes, J. Electroanal. Chem. 582 (2005) 130.
5. T. Thomberg, J. Nerut, E. Lust, Impedance spectroscopy data for $S_2O_8^{2-}$ anions electroreduction kinetics at Cd(0001) plane electrode, J. Electroanal. Chem. 586 (2006) 237.
6. Enn Lust, Jaak Nerut, Eneli Härk, Rutha Jäger, Karmen Lust, Kadri Tähnas, Electroreduction of Complex Ions at Bismuth and Cadmium Single Crystal Plane Electrodes, ECS Trans. 1 (17) (2006) 9.
7. J. Nerut, E. Lust, Impedance Spectroscopy Data for $[Fe(CN)_6]^{3-}$ Anions Electroreduciton at Cd(0001) Electrode, 209th ECS Meeting, USA, Denver/Colorado, 7–12 May 2006, Meet. Abstr. - Electrochem. Soc. 601 (2006) 1195 (Oral presentation).
8. J. Nerut, E. Lust, Impedance measurements of Cd(0001) electrode in aqueous potassium perchlorate, 7th International Symposium on Electrochemical Impedance Spectroscopy, France, 3–8 june 2007, abstract ID 178 (Oral presentation).
9. J. Nerut, K. Lust, E. Lust, Adsorption of hexacyanoferrate(II) and hexacyanoferrate(III) anions on electrochemically polished Cd(0001) plane, J. Electroanal. Chem. Submitted (JELECHEM-D-06–00250R2).
10. J. Nerut, E. Lust, Impedance spectroscopy study of hexacyanoferrate(III) anion electroreduction kinetics at electrochemically polished Cd(0001) plane, J. Electrochem. Soc. Submitted (JES-07–0695).

# ELULOOKIRJELDUS

## Jaak Nerut

Sündinud: 28.03.1980, Kohtla-Järve, Estonia
Kodakondsus: eesti
Perekonnaseis: vallaline
Aadress: Füüsikalise keemia instituut
Tartu Ülikool
Jakobi 2., Tartu 51014, Eesti
Telefon: +372 737 5165
Faks: +372 737 5160
E-mail: jaak.nerut@ut.ee

## Haridus

| | |
|---|---|
| 2003 | Tartu Ülikool, füüsika-keemiateaduskond, doktorant füüsikalise ja elektrokeemia erialal |
| 2003 | Tartu Ülikool, füüsika-keemiateaduskond, *M. Sc.* füüsikalise ja elektrokeemia erialal |
| 2002 | Tartu Ülikool, füüsika-keemiateaduskond, keemiaõpetaja |
| 2002 | Tartu Ülikool, füüsika-keemiateaduskond, *B. Sc.* kraad keemias *cum laude* |
| 1998 | Hugo Treffneri Gümnaasium |

## Teenistuskäik

| | |
|---|---|
| 2005–... | Tartu Ülikool, Füüsikalise keemia instituut, füüsikalise ja elektrokeemia teadur (0.6 koormust) |
| 2004–2005 | Tartu Ülikool, Füüsikalise keemia instituut, füüsikalise ja elektrokeemia teadur (0.5 koormust) |
| 2002–2004 | Tartu Ülikool, Füüsikalise keemia instituut, keemik (0.5 koormust) |

# Tähtsamad teaduspublikatsioonid

1. J. Nerut, P. Möller and E. Lust, Electroreduction of hexacyanoferrate(III) anions on electrochemically polished Cd(0001) plane, Electrochim. Acta 49 (2004) 1597.
2. R. Jäger, E. Härk, P. Möller, J. Nerut, K. Lust and E. Lust, The kinetics of eletroreduction of hexaamminecobalt(III) cation on Bi planes in aqueous $HClO_4$ solutions, J. Electroanal. Chem. 566 (2004) 217.
3. T. Thomberg, J. Nerut, K. Lust and E. Lust, The kinetics of eletroreduction of peroxodisulfate anion on electrochemically polished Cd(0001) plane, Electrochim. Acta 49 (2004) 1271.
4. T. Thomberg, J. Nerut, R. Jäger, P. Möller, K. Lust, E. Lust, The kinetics of electroreduction of peroxodisulfate ions on single crystal cadmium and bismuth electrodes, J. Electroanal. Chem. 582 (2005) 130.
5. T. Thomberg, J. Nerut, E. Lust, Impedance spectroscopy data for $S_2O_8^{2-}$ anions electroreduction kinetics at Cd(0001) plane electrode, J. Electroanal. Chem. 586 (2006) 237.
6. Enn Lust, Jaak Nerut, Eneli Härk, Rutha Jäger, Karmen Lust, Kadri Tähnas, Electroreduction of Complex Ions at Bismuth and Cadmium Single Crystal Plane Electrodes, ECS Trans. 1 (17) (2006) 9.
7. J. Nerut, E. Lust, Impedance Spectroscopy Data for $[Fe(CN)_6]^{3-}$ Anions Electroreduciton at Cd(0001) Electrode, 209th ECS Meeting, USA, Denver/ Colorado, 7–12 May 2006, Meet. Abstr. — Electrochem. Soc. 601 (2006) 1195 (Suuline ettekanne).
8. J. Nerut, E. Lust, Impedance measurements of Cd(0001) electrode in aqueous potassium perchlorate, 7th International Symposium on Electrochemical Impedance Spectroscopy, France, 3–8 june 2007, abstract ID 178 (Suuline ettekanne).
9. J. Nerut, K. Lust, E. Lust, Adsorption of hexacyanoferrate(II) and hexacyanoferrate(III) anions on electrochemically polished Cd(0001) plane, J. Electroanal. Chem. Submitted (JELECHEM-D-06–00250R2).
10. J. Nerut, E. Lust, Impedance spectroscopy study of hexacyanoferrate(III) anion electroreduction kinetics at electrochemically polished Cd(0001) plane, J. Electrochem. Soc. Submitted (JES-07–0695).

# DISSERTATIONES CHIMICAE
# UNIVERSITATIS TARTUENSIS

1. **Toomas Tamm.** Quantum-chemical simulation of solvent effects. Tartu, 1993, 110 p.
2. **Peeter Burk.** Theoretical study of gas-phase acid-base equilibria. Tartu, 1994, 96 p.
3. **Victor Lobanov.** Quantitative structure-property relationships in large descriptor spaces. Tartu, 1995, 135 p.
4. **Vahur Mäemets.** The $^{17}O$ and $^{1}H$ nuclear magnetic resonance study of $H_2O$ in individual solvents and its charged clusters in aqueous solutions of electrolytes. Tartu, 1997, 140 p.
5. **Andrus Metsala.** Microcanonical rate constant in nonequilibrium distribution of vibrational energy and in restricted intramolecular vibrational energy redistribution on the basis of slater's theory of unimolecular reactions. Tartu, 1997, 150 p.
6. **Uko Maran.** Quantum-mechanical study of potential energy surfaces in different environments. Tartu, 1997, 137 p.
7. **Alar Jänes.** Adsorption of organic compounds on antimony, bismuth and cadmium electrodes. Tartu, 1998, 219 p.
8. **Kaido Tammeveski.** Oxygen electroreduction on thin platinum films and the electrochemical detection of superoxide anion. Tartu, 1998, 139 p.
9. **Ivo Leito.** Studies of Brønsted acid-base equilibria in water and non-aqueous media. Tartu, 1998, 101 p.
10. **Jaan Leis.** Conformational dynamics and equilibria in amides. Tartu, 1998, 131 p.
11. **Toonika Rinken.** The modelling of amperometric biosensors based on oxidoreductases. Tartu, 2000, 108 p.
12. **Dmitri Panov.** Partially solvated Grignard reagents. Tartu, 2000, 64 p.
13. **Kaja Orupõld.** Treatment and analysis of phenolic wastewater with microorganisms. Tartu, 2000, 123 p.
14. **Jüri Ivask.** Ion Chromatographic determination of major anions and cations in polar ice core. Tartu, 2000, 85 p.
15. **Lauri Vares.** Stereoselective Synthesis of Tetrahydrofuran and Tetra-hydropyran Derivatives by Use of Asymmetric Horner-Wadsworth-Emmons and Ring Closure Reactions. Tartu, 2000, 184 p.
16. **Martin Lepiku.** Kinetic aspects of dopamine $D_2$ receptor interactions with specific ligands. Tartu, 2000, 81 p.
17. **Katrin Sak.** Some aspects of ligand specificity of P2Y receptors. Tartu, 2000, 106 p.
18. **Vello Pällin.** The role of solvation in the formation of iotsitch complexes. Tartu, 2001, 95 p.

45

19. **Katrin Kollist.** Interactions between polycyclic aromatic compounds and humic substances. Tartu, 2001, 93 p.
20. **Ivar Koppel.** Quantum chemical study of acidity of strong and superstrong Brønsted acids. Tartu, 2001, 104 p.
21. **Viljar Pihl.** The study of the substituent and solvent effects on the acidity of OH and CH acids. Tartu, 2001, 132 p.
22. **Natalia Palm.** Specification of the minimum, sufficient and significant set of descriptors for general description of solvent effects. Tartu, 2001, 134 p.
23. **Sulev Sild.** QSPR/QSAR approaches for complex molecular systems. Tartu, 2001, 134 p.
24. **Ruslan Petrukhin.** Industrial applications of the quantitative structure-property relationships. Tartu, 2001, 162 p.
25. **Boris V. Rogovoy.** Synthesis of (benzotriazolyl)carboximidamides and their application in relations with *N*- and *S*-nucleophyles. Tartu, 2002, 84 p.
26. **Koit Herodes.** Solvent effects on UV-vis absorption spectra of some solvatochromic substances in binary solvent mixtures: the preferential solvation model. Tartu, 2002, 102 p.
27. **Anti Perkson.** Synthesis and characterisation of nanostructured carbon. Tartu, 2002, 152 p.
28. **Ivari Kaljurand.** Self-consistent acidity scales of neutral and cationic Brønsted acids in acetonitrile and tetrahydrofuran. Tartu, 2003, 108 p.
29. **Karmen Lust.** Adsorption of anions on bismuth single crystal electrodes. Tartu, 2003, 128 p.
30. **Mare Piirsalu.** Substituent, temperature and solvent effects on the alkaline hydrolysis of substituted phenyl and alkyl esters of benzoic acid. Tartu, 2003, 156 p.
31. **Meeri Sassian.** Reactions of partially solvated Grignard reagents. Tartu, 2003, 78 p.
32. **Tarmo Tamm.** Quantum chemical modelling of polypyrrole. Tartu, 2003. 100 p.
33. **Erik Teinemaa.** The environmental fate of the particulate matter and organic pollutants from an oil shale power plant. Tartu, 2003. 102 p.
34. **Jaana Tammiku-Taul.** Quantum chemical study of the properties of Grignard reagents. Tartu, 2003. 120 p.
35. **Andre Lomaka.** Biomedical applications of predictive computational chemistry. Tartu, 2003. 132 p.
36. **Kostyantyn Kirichenko.** Benzotriazole — Mediated Carbon–Carbon Bond Formation. Tartu, 2003. 132 p.
37. **Gunnar Nurk.** Adsorption kinetics of some organic compounds on bismuth single crystal electrodes. Tartu, 2003, 170 p.
38. **Mati Arulepp.** Electrochemical characteristics of porous carbon materials and electrical double layer capacitors. Tartu, 2003, 196 p.

39. **Dan Cornel Fara.** QSPR modeling of complexation and distribution of organic compounds. Tartu, 2004, 126 p.

40. **Riina Mahlapuu.** Signalling of galanin and amyloid precursor protein through adenylate cyclase. Tartu, 2004, 124 p.

41. **Mihkel Kerikmäe.** Some luminescent materials for dosimetric applications and physical research. Tartu, 2004, 143 p.

42. **Jaanus Kruusma.** Determination of some important trace metal ions in human blood. Tartu, 2004, 115 p.

43. **Urmas Johanson.** Investigations of the electrochemical properties of polypyrrole modified electrodes. Tartu, 2004, 91 p.

44. **Kaido Sillar.** Computational study of the acid sites in zeolite ZSM-5. Tartu, 2004, 80 p.

45. **Aldo Oras.** Kinetic aspects of $dATP\alpha S$ interaction with $P2Y_1$ receptor. Tartu, 2004, 75 p.

46. **Erik Mölder.** Measurement of the oxygen mass transfer through the air-water interface. Tartu, 2005, 73 p.

47. **Thomas Thomberg.** The kinetics of electroreduction of peroxodisulfate anion on cadmium (0001) single crystal electrode. Tartu, 2005, 95 p.

48. **Olavi Loog.** Aspects of condensations of carbonyl compounds and their imine analogues. Tartu, 2005, 83 p.

49. **Siim Salmar.** Effect of ultrasound on ester hydrolysis in aqueous ethanol. Tartu, 2006, 73 p.

50. **Ain Uustare.** Modulation of signal transduction of heptahelical receptors by other receptors and G proteins. Tartu, 2006, 121 p.

51. **Sergei Yurchenko.** Determination of some carcinogenic contaminants in food. Tartu, 2006, 143 p.

52. **Kaido Tämm.** QSPR modeling of some properties of organic compounds. Tartu, 2006, 67 p.

53. **Olga Tšubrik.** New methods in the synthesis of multisubstituted hydrazines. Tartu. 2006, 183 p.

54. **Lilli Sooväli.** Spectrophotometric measurements and their uncertainty in chemical analysis and dissociation constant measurements. Tartu, 2006, 125 p.

55. **Eve Koort.** Uncertainty estimation of potentiometrically measured ph and $pK_a$ values. Tartu, 2006, 139 p.

56. **Sergei Kopanchuk.** Regulation of ligand binding to melanocortin receptor subtypes. Tartu, 2006, 119 p.

57. **Silvar Kallip.** Surface structure of some bismuth and antimony single crystal electrodes. Tartu, 2006, 107 p.

58. **Kristjan Saal.** Surface silanization and its application in biomolecule coupling. Tartu, 2006, 77 p.

59. **Tanel Tätte.** High viscosity $Sn(OBu)_4$ oligomeric concentrates and their applications in technology. Tartu, 2006, 91 p.

60. **Dimitar Atanasov Dobchev**. Robust QSAR methods for the prediction of properties from molecular structure. Tartu, 2006, 118 p.

61. **Hannes Hagu**. Impact of ultrasound on hydrophobic interactions in solutions. Tartu, 2007, 81 p.

62. **Rutha Jäger.** Electroreduction of peroxodisulfate anion on bismuth electrodes. Tartu, 2007, 142 p.

63. **Kaido Viht.** Immobilizable bisubstrate-analogue inhibitors of basophilic protein kinases: development and application in biosensors. Tartu, 2007, 88 p.

64. **Eva-Ingrid Rõõm.** Acid-base equilibria in nonpolar media. Tartu, 2007, 156 p.

65. **Sven Tamp.** DFT study of the cesium cation containing complexes relevant to the cesium cation binding by the humic acids. Tartu, 2007, 102 p.